5-2021

Synthesis of Bulky and Polar Galactonoamidines for the Inhibition of the Human α-Galactosidase

Ifedi Orizu
University of Arkansas, Fayetteville

Synthesis of Bulky and Polar Galactonoamidines for the Inhibition of the Human α-Galactosidase

A thesis submitted in partial fulfillment
of the requirements for the degree of
Master of Science in Chemistry

by

Ifedi Orizu
University of Ontario Institute of Technology
Bachelor of Science in Chemistry, 2016

May 2021
University of Arkansas

This thesis is approved for recommendation to the Graduate Council.

_____

Matt McIntosh, PhD.
Thesis Director

_____

Mahmoud Moradi, PhD.
Committee Member

_____

Chenguang Fan, PhD.
Committee Member

Abstract

Glycosidases are amongst the most abundant enzymes in nature. This is due to their role in the degradation of carbohydrates which are the major source of carbon or earth. The absence or malfunction of glycosidases is implicated in numerous diseases such as cancers, diabetes, and lysosomal storage disorders, which make them important drug targets for study in medicinal chemistry. The seminal work by Pauling and Wolfenden showed that enzymes bind to their substrate at the transition state with very strong affinity. Wolfenden estimated the dissociation constant to be around 10^{-22}M. This encouraged the design of glycosidase inhibitors which mimicked one or more features of the transition state. The notable features of the transition state of glycosidases include the development of a positive charge on the anomeric carbon atom, and the distortion of the sugar ring into one of a boat, an envelope, or a half-chair conformation to accommodate the formed positive charge.

The glyconoamidine family of inhibitors emerged as a class of compounds to mimic both the positive charge and distorted chair conformation of the transition state of glycosidases. Research in the Striegler group identified a library of galactonoamidines as highly potent competitive inhibitors of several β-galactosidases, with inhibition constants in the low nanomolar to picomolar range. The work described here summarizes an effort towards the synthesis of polar and bulky galactonoamidines for the inhibition of the human α-galactosidase. Following a protocol previously established in the group, the precursor galactothionolactam was synthesized and coupled with several amines to yield a library of perbenzylated galactonoamidines. Hydrogenation of the perbenzylated galactonoamidines in the presence of palladium on carbon afforded some of the desired compounds, whereas the others were unsuccessful.

Acknowledgements

I am thankful to Dr. Susanne Striegler for her enormous support and encouragement throughout the past 4 years of my graduate studies at the University of Arkansas. I appreciate the time, effort, and resources that she invested in me to become a better scientist. I thank the members of my Committee Dr. Matt McIntosh, Dr. Chenguang Fan and Dr. Mahmoud Moradi for their guidance and commitment to my success in the past 4 years. I also thank the present and past members of the Striegler group especially Dr. Jessica Pickens for taking a lot of time in training me on the setup and analysis of the molecular docking studies, I am also grateful for numerous discussions on her project which helped me gain a better insight into the biochemistry of galactonoamidines. I thank Dr. Qiu-Hua Fan who provided some of the perbenzylated galactonolactam used for this project. I thank Dr. Babloo Sharma for his friendship, support, and constant words of encouragement over the years. I thank Ms. Carlie Clem for being an amazing lab mate. Support for this research to Dr. Susanne Striegler by the National Science Foundation under grants No. CHE-1305543 and CHE-1854304, Arkansas Biosciences Institute (ABI) and University of Arkansas Chancellor's commercialization fund are gratefully acknowledged.

I am grateful to the Department of Chemistry and Biochemistry at the University of Arkansas for the support and for giving me the opportunity to engage in research. I am thankful to Kz Shein and Zay Lynn for always ensuring that the instruments were always functional.

I am most grateful to my family for their unwavering support and encouragement. To my parents Eugene and Chinelo Orizu. I cannot thank you enough for your sacrifices that has gotten me this far. To my siblings Chisom, Chekwube, Chidiogo and Chinwendu, thank you all for your love, support, and encouragement. Lastly, I thank my uncle and aunt Emmanuel and Geraldine Orizu who have cheered me on as I embarked on this journey.

Table of Contents

Table of Schemes

Table of Figures

1: Carbohydrates and Carbohydrate Processing Enzymes

1.1: Introduction

Carbohydrates along with their corresponding glycoconjugates are the most abundant class of biomolecules exiting in nature, and account for a significant portion of the carbon atoms on earth.[1] These biomolecules play very crucial roles that are responsible for the sustainability of life in living organisms. Some of the established roles of carbohydrates in biological systems include but are not limited to energy production and metabolism,[2] provision of structure and support,[3] protein quality check,[4] cell recognition,[5] and cell signalling. Moreover, overexpression of certain carbohydrates in cells serve as biomarkers for the onset or progression of diseases.[6] For example, an increase in serum levels of CA242 antigen is clinically used as a diagnostic biomarker for colorectal, pancreatic, and other cancers.[7, 8] Glycosyl transferases and glycoside hydrolases are the enzymes responsible for the build-up and breakdown of complex carbohydrates in cells. These enzymes regulate the amounts of carbohydrates and glycoconjugates in biological systems and are therefore crucial for cell regulation and function. The absence or malfunction of carbohydrate processing enzymes are well known to result in diseases such as cancers, diabetes, and lysosomal storage disorders. Therefore, these enzymes are interesting targets for drug discovery in medicinal chemistry.[6, 9] While both enzymes play very critical roles and are important targets for drug discovery, the discussion here is limited to glycoside hydrolases for brevity. Glycoside hydrolases (GH) also known as glycosidases are currently classified into 168 families based on the similarity of their amino acid sequence. The GH families are also grouped into 18 clans based on the conservation of the overall three-dimensional topology and amino acid sequence around the enzyme active site.[10-12] Enzymes

belonging in the same family typically employ a similar mechanism for the hydrolysis of their substrates.

1.2: Mechanisms of Glycoside Hydrolases

The mechanism for the hydrolysis of glycosides proposed by Koshland in 1953 involves the retention or inversion of stereochemistry at the anomeric carbon atom, with an oxocarbenium ion-like transition state.[13, 14] There is ample experimental evidence in support of the existence of an oxocarbenium ion-like transition state during the hydrolysis of glycosides using techniques as nuclear magnetic resonance spectroscopy (NMR),[15, 16] mass spectrometry,[17, 18] ^{13}C kinetic isotope effect studies,[19] and infrared ion spectroscopy.[20, 21] The transition state is characterized by a build-up of positive charge between atoms C1-O5, which is accommodated by the distortion of the sugar ring away from the typical chair conformation **Figure 1.1**.[13, 22]

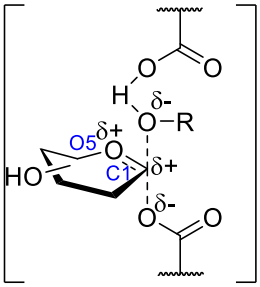

Figure 1.1: A general structure of the transition state of glycoside hydrolases.

The glycosidases that utilize the inversion or retention mechanism for the hydrolysis of their substrate employ either an aspartate or a glutamate amino acid as the catalytic residue.[23] In the inversion mechanism, one of the catalytic residues acting as an acid protonates the exocyclic oxygen **Figure 1.2A**. Next a water molecule deprotonated by the other catalytic residue attacks the anomeric carbon atom, resulting in the cleavage of the C-O bond.[13, 24] The retention mechanism is a double displacement process, which occurs in two steps **Figure 1.2B**. In the first step, the exocyclic oxygen is protonated by a catalytic residue, followed by a nucleophilic attack

of the second catalytic residue on the anomeric carbon atom, forming a glycosyl-enzyme intermediate, with the cleavage of the C-O bond, and one face of the sugar blocked from nucleophilic attack. In the next step, a catalytic residue deprotonates a water molecule which attacks the anomeric carbon atom from the exposed face, resulting in a product with a retained configuration at the anomeric carbon atom.[13, 24]

Figure 1.2A
Inversion mechanism

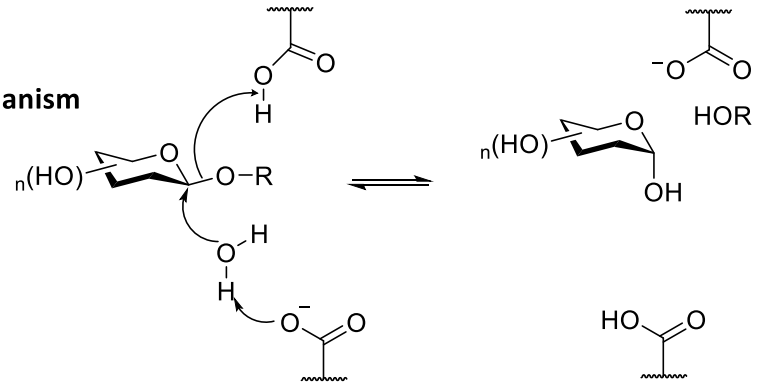

Figure 1.2B
Retention mechanism

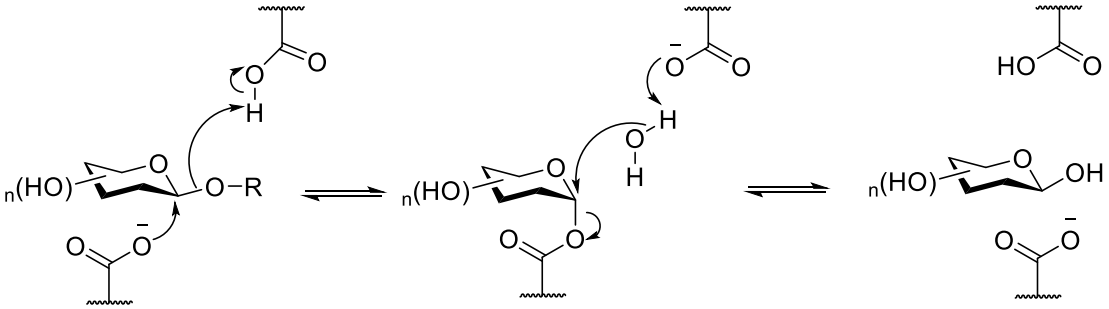

Figure 1.2: The Koshland inversion and retention mechanism for the hydrolysis of glycosides.

Over the years, more in-depth mechanistic studies of several glycoside hydrolase families have revealed several variants of the Koshland mechanism. For example, some *N*-acetylhexosoaminidases (NAGases) from families 18 and 20 which cleave *N*-acetyl-β-hexosaminidines during glycoprotein biosynthesis have be shown to operate through a substrate assisted mechanism.[25] In this mechanism, the exocyclic oxygen of the glycoside is protonated by a catalytic residue, followed by a nucleophilic attack of the anomeric carbon atom by the

carbonyl oxygen atom of the *N*-acetamido group, forming an oxazoline intermediate **Figure 1.3A**. In the next step, a water molecule deprotonated by a catalytic residue attacks the anomeric carbon atom to form the hydrolysis product with a retention of configuration.[25, 26] Several glycosidases such as sialidases and trans-sialidase belonging to glycoside hydrolase families 33, 34 and 143 are known to utilize an unusual nucleophile for the hydrolysis of their substrate. Enzymes in these glycoside hydrolase family use a tyrosine residue as the nucleophile instead of the commonly utilized aspartate or glutamate residue.[26] In this mechanism the exocyclic oxygen of the sialic acid is first protonated by an acidic catalytic residue **Figure 1.3B**. Subsequently, a nearby glutamate residue deprotonates a tyrosine residue which then attacks the anomeric carbon atom. Hydration of the formed intermediate by a deprotonated water molecule then affords the hydrolyzed product with a retention of configuration at the anomeric carbon atom.[27, 28] Also, α-mannosidase from glycoside hydrolase family 99 was found to catalyze its substrate via an epoxide intermediate formed between the C2-hydroxyl group and the anomeric carbon atom **Figure 1.3C**.[29] Here, the exocyclic oxygen is first protonated by a catalytic residue, subsequently, a nearby glutamate residue deprotonates the hydroxyl group on carbon 2, resulting in a nucleophilic attack at the anomeric carbon atom and the departure of the leaving group, and forming an epoxide intermediate. Next the epoxide oxygen is protonated by a carboxylate residue and the epoxide ring is opened by an attack of a deprotonated water molecule, yielding the hydrolyzed product with a retention of configuration at the anomeric carbon atom.[29, 30]

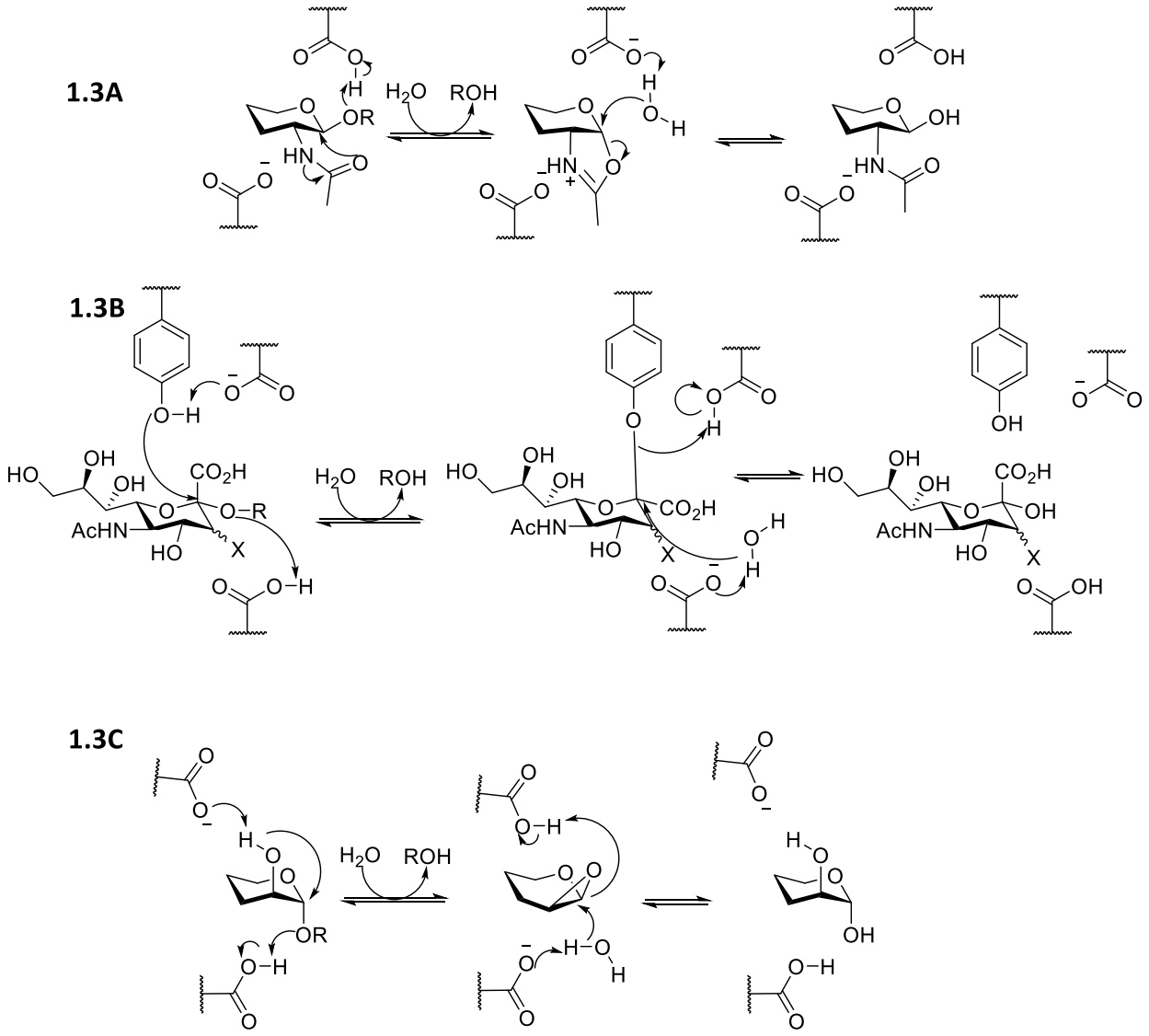

Figure 1.3: Non-Koshland mechanisms for the hydrolysis of glycosides.

It is now well established in the field that the hydrolysis of glycosides proceeds through a transition state with strong oxocarbenium ion-like character, with a delocalization of the positive charge between atoms C1-O5.[15, 31] The development of the positive charge is accommodated by conformational changes of the sugar ring away from the typical chair ($^4C_1$) conformation into a more planar or distorted conformation as it approaches the transition state.[23, 32] The reaction itineraries of numerous glycoside hydrolase families have been mapped out, by using a

combination of enzyme inhibition studies,[33] computational analysis,[26] and X-ray diffraction analysis.[34] A combination of these studies can be used to decipher the mechanism as well as predict the conformation of the enzyme bound substrate as it goes from the Michaelis-complex to the transition state and finally to the covalent intermediate.[35, 36] Since the transition state cannot be trapped, it can be predicted from the obtained conformations of the Michaleis-complex and the covalent intermediate by analysis of the Cremer-Pople coordinate,[37] which outlines the pathways for sugar puckering in combination with metadynamics simulations.[35] Mechanistic studies of numerous glycoside hydrolases have revealed the most common transition state conformations to be a half-chair (H), boat (B) or envelope (E) conformation.[22] The knowledge and understanding of glycoside hydrolase mechanism and reaction conformational itinerary have proved useful for the development of potent and selective glycosidase inhibitors.[38]

1.3: Mechanism based Inhibitors of Glycoside Hydrolases

Pauling postulated that the highest affinity inhibitors were those which mimicked the features of the transition state of the enzyme.[39] The seminal work by Wolfenden revealed glycosidases hydrolyzed their substrates with a rate enhancement of over 10^{17} -fold over the non-catalyzed reaction.[40] This translates to a binding constant of the transition state to be around 10^{-22}M.[41] This propelled the design of glycosidase inhibitors mimicking the features of the transition state of glycoside hydrolases. The design of glycosidase inhibitors was primarily focused on the two key features (i) inhibitors mimicking the positive charge of the transition state and (ii) inhibitors mimicking the shape or conformation of the transition state. Azasugar inhibitors such as nojirimycin **1** become protonated under physiological conditions to mimic the positive charge of the transition state of glycoside hydrolase **Figure 1.4**. Other inhibitors nitrogen containing

inhibitors such as, deoxynojirimycin **2**, isofagomine **3**, noeuromycin **4**, azafagomine **5**, castanospermine **6** and calystegine B_2 **7** have also been demonstrated to have modest to good inhibitory activities towards glycosidases with IC_{50} or inhibition constant (K_i) values in the low micromolar range. Their activity is attributed to their ability to become protonated under physiological conditions hence mimicking the positive charge of the transition state.

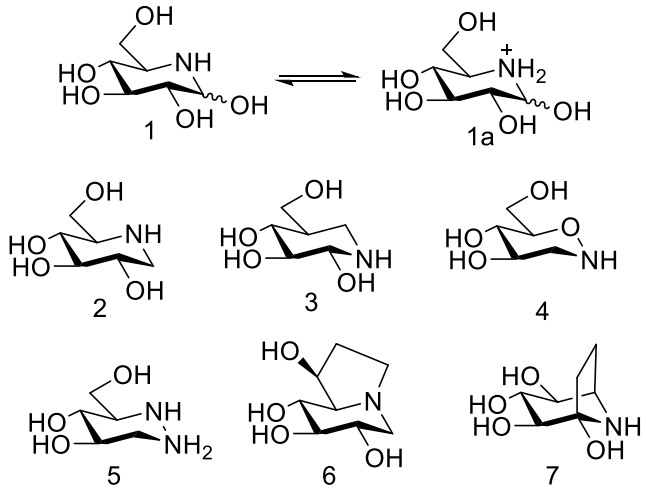

Figure 1.4: Glycosidase inhibitors mimicking the positive charge of the transition state.

Likewise, compounds mimicking the distorted chair conformation of the transition state such as gluconolactone **8**, gluconolactam **9**, isofagomine lactam **10**, glucotetrazole **11**, mannotetrazole **12** and glucoimidazole **13** have also been demonstrated to be potent inhibitors of glycosidases with IC_{50} and or K_i values in the micromolar to nanomolar range **Figure 1.5**. Indeed mannotetrazole **12** with a $B_{2,5}$ conformation has been experimentally proven to be a true transition state mimic of β-mannosidase from *Bacteroides thetaiotaomicron*, through linear free energy relationship analysis.[42] Early discussions in the literature focussed on establishing which feature was most essential for the binding of the inhibitors to the enzyme and was also the subject of several reviews.[43-45] While there is no definite conclusion as to whether the shape or the charge

contribution is more important for the binding of the inhibitors to the enzyme, studies now show that the preference for either the shape or charge contribution was enzyme dependent.[30] Moreover, recent studies are showing that the potency of glycosidase inhibitors goes beyond the shape and charge contribution but also includes other factors such as the ability of the inhibitor to have favorable interactions with the enzyme.[46, 47]

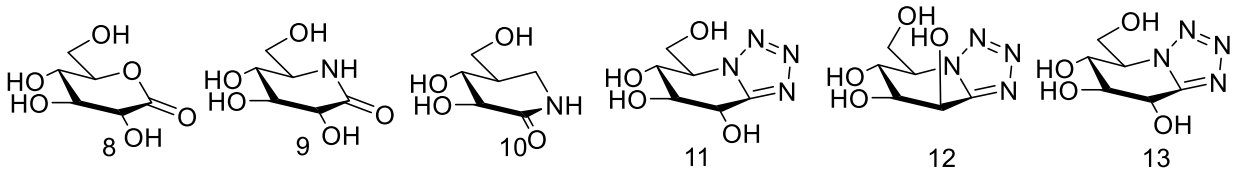

Figure 1.5: Glycosidase inhibitors mimicking the distorted chair conformation of the transition state.

To harness more binding affinity by transition state mimicry, Ganem and co-workers pioneered the synthesis of the glyconoamidine family of inhibitors which possesses a distorted chair conformation, and is protonated under physiological conditions to developing a positive charge to mimic the features of the transition state of glycoside hydrolase.[48-50] that combine the shape and charge mimicry of the transition state. Synthesis and evaluation of gluconoamidines **14 a-d**. against a panel of glycosidases revealed them to be potent broad-spectrum inhibitors with inhibition constant in the low micromolar to high nanomolar range **Figure 1.6** [48, 50] The potency of the inhibitors is attributed to their close mimicry of the features of the transition state of glycoside hydrolases. Moreover, the gluconoamidines displayed higher selectivity for the inhibition of glucosidase and a slightly weaker inhibition of mannosidase whereas the inhibition of the galactosidase was significantly lower, indicating configuration of the inhibitor contributes to the selectivity of the inhibitors.

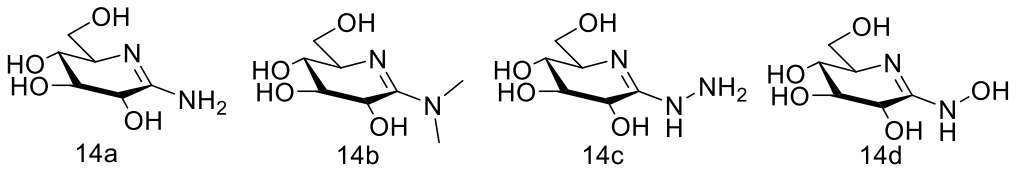

Figure 1.6: Structures of gluconoamidine inhibitors synthesized by Ganem and co-workers.

However, Tellier and coworkers noted that the gluconoamidines **14a-d** synthesized by Ganem did not take advantage of an aglycon interaction with the active site residues. Mannoamidine **15a** without a benzyl aglycon and mannoamidine **15b** with a sugar aglycon were synthesized and evaluated as inhibitors of several glycosidases **Figure 1.7**.[51, 52] Compound **15a** was shown to be a potent inhibitor of both α-mannosidase (jack bean) and β-mannosidase (snail) with inhibition constants of 0.55 μM and 6.0 μM respectively. On the other hand, **15b** was found to be a potent inhibitor of α-mannosidase (jack bean) with an inhibition constant of 2.6 μM and poor inhibitor of β-mannosidase (snail) with K_i of 120 μM. Compound **15a** was also a potent inhibitor of β-glucosidase (sweet almond), with K_i of 5 μM, whereas **15b** was a less potent inhibitor of β-glucosidase (sweet almond) with K_i of 100 μM. The result obtained from this study revealed a contribution of the aglycon towards the potency and selectivity of the inhibitors towards the investigated glycosidases.

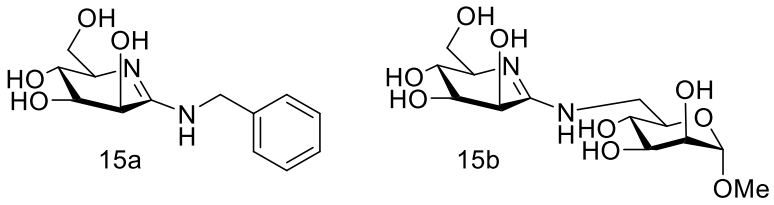

Figure 1.7: Structures of mannoamidine inhibitors synthesized by Tellier and co-workers.

Heck and coworkers also synthesized a small library of *N*-substituted gluconoamidines **14e-h** and mannoamidines **15c-f** with polar aliphatic side chains with varying lengths **Figure 1.8**.[53]

gluconoamidines **14 e-h** were potent inhibitors of both α- and β- glucosidase with inhibition constants of 32 μM, 14 μM, 39 μM and 31 μM for the inhibition of α-glucosidase (yeast) and 34 μM, 71 μM, 50 μM and 20 μM for the inhibition of β-glucosidase (sweet almond). The evaluated gluconoamidines showed no clear selectivity for either the α- or β-glucosidase. Interestingly, the gluconoamidines showed stronger inhibition of α- and β-mannosidase. Compound **14e** inhibited the enzymes with K_i values of 0.06 μM for the α-mannosidase (jack bean) and 1.3 μM for β-mannosidase (snail). Mannoamidines **15c-f** were much stronger inhibitors of the α- and β-mannosidases with inhibition constants of 6 nM, 19 nM, 12 nM and 80 nM for the inhibition of α-mannosidase (jack bean) and 9 nM, 150 nM, 60 nM and 150 nM for the inhibition of β-mannosidase (snail). Despite being a strong inhibitor of both mannosidases, compound **15c**, only showed modest or weak inhibition of other glycosidases, making it selective for the inhibition of mannosidases. The inhibition constants of **15c** obtained for the inhibition of other enzymes are as follow; 81 μM (α-glucosidase yeast), 6600 μM (β-glucosidase almond), 218 μM (α-galactosidase green coffee bean), 82 μM (β-galactosidase *Aspergillus oryzae*).

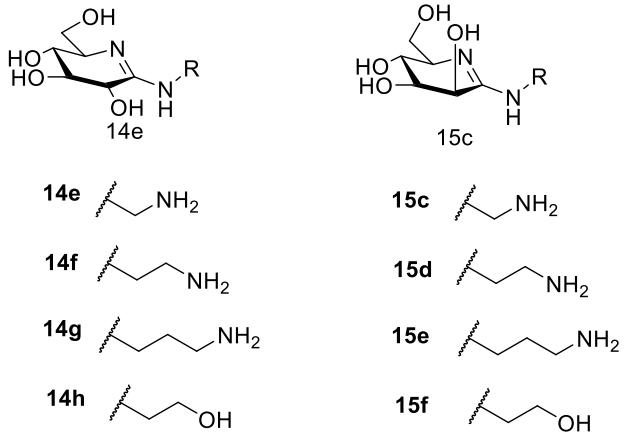

Figure 1.8: *N*-alkyl gluco- and manno-amidines.

1.4: Galactonoamidines as putative transition state analog inhibitors of β-galactosidases

A major research focus in the Striegler lab aims to develop macromolecular catalysts for the efficient transformations of carbohydrates. Along these lines, a series of binuclear copper (II) complex were designed and shown to discriminate between related sugars including epimers and anomers.[54-56] These catalysts were also shown to catalyze the oxidation of sugars,[57] as well as for the hydrolysis of glycosides.[58] The immobilization of the binuclear copper complexes into a polyacrylate microgel was shown to significantly enhance their catalytic properties, due to the stabilizing contributions of the matrix.[59, 60] moreover, templating the microgels with a ground state sugar also resulted in an improved catalytic efficiency. To further improve the efficiency of the polyacrylate microgels, it was envisaged that templating them with a transition state analog instead of a ground state analog would facilitate the distortion of the substrate into a transition state geometry, hence accelerating the hydrolysis of the glycosides. This ultimately led the group to search for transition state analog of glycosidases, with β-galactosidase being the model enzyme. In addition, the deficiency of functional lysosomal β-galactosidase results in a lysosomal storage disorder known as GM1-gangliosidosis.[61] Therefore, the development of a potent transition state analog inhibitor of β-galactosidase would serve a dual purpose, as both a potential therapeutic for the treatment of GM1-gangliosidosis,[61] and as a template for the development of carbohydrate transforming microgels.[62] As a result, research in the Striegler group in past decade has focussed on the synthesis and evaluation of galactonoamidines **16** as inhibitors of β-galactosidases. The evaluated compounds were shown to be highly potent inhibitors of several β-galactosidases. An initial evaluation of a small library of *N*-aryl galactonoamidines revealed these compounds to be highly potent and competitive inhibitors of β-galactosidase (*A. oryzae*) with inhibition constants ranging from 12-48 nM.[63] The result obtained

from this study prompted a more in-depth evaluation of the compounds as transition state analogs for the hydrolysis of glycosides by a β-galactosidase.[58] Strongly binding inhibitors are not necessarily true transition state analogs.[41, 64] Experimental methods must be provided in support of true transition state mimicry. Some of the methods which have been used to examine transition state mimicry include: X-ray diffraction analysis of enzymes complexed with inhibitors locked in a specific configuration,[65] evaluating the binding of a substrate to an enzyme with a mutated active site,[66] and spectroscopic analysis.[67] The spectroscopic analysis, the linear free energy relationship analysis method established by Bartlett measures the effect of equivalent structural perturbations on the affinity of the true transition state and on the affinity of the transition state analog.[67, 68] Therefore, a plot of (k_{cat}/K_M) versus K_i should give a straight line with a slope and correlation (R^2) of 1.[67] The galactonoamidines synthesized by the Striegler group were evaluated as transition state analogs for the hydrolysis of aryl-galactopyranosides **17** by β-galactosidase (*A. oryzae*).[58] Despite all compounds bearing a benzyl aglycon, only **16a** with a para-methyl substituent on the aglycon was determined to be a true transition state analog.[58] The result indicates that subtle differences in the structures of the inhibitor results in different interactions between the inhibitor and the amino acid residues in the enzyme active site. Compound **16a** with a *p*-methyl substituent had an inhibition constant of 8 nM and was also experimentally determined to be a true transition state analog for the enzyme. Whereas **16b** and **16c** with *m*-methyl and *o*-methyl substituent had inhibition constants of 29 nM and 23 nM respectively but were not true transition state analogs but fortuitous binders. All compounds are potent competitive inhibitors of the β-galactosidase (*A. oryzae*), however, the positioning of the methyl group on the inhibitor allows for the appropriate hydrophobic interaction which makes **16a** a true transition state analog. The compound library was further expanded to include

compounds possessing linear aliphatic aglycons such as **16d**, and cyclic aliphatic aglycon such as **16e Figure 1.9**.[69] All compounds in the 22-compound library were determined to be competitive inhibitors of β-galactosidase (*A. oryzae*) with K_i values ranging from 8-600 nM. As expected, the variation in the aglycons resulted in slight differences in the observed inhibition constant values, revealing an interplay between steric, electronic, hydrophobic, and π-π stacking interactions between the inhibitors and the amino acid residues of the enzyme.

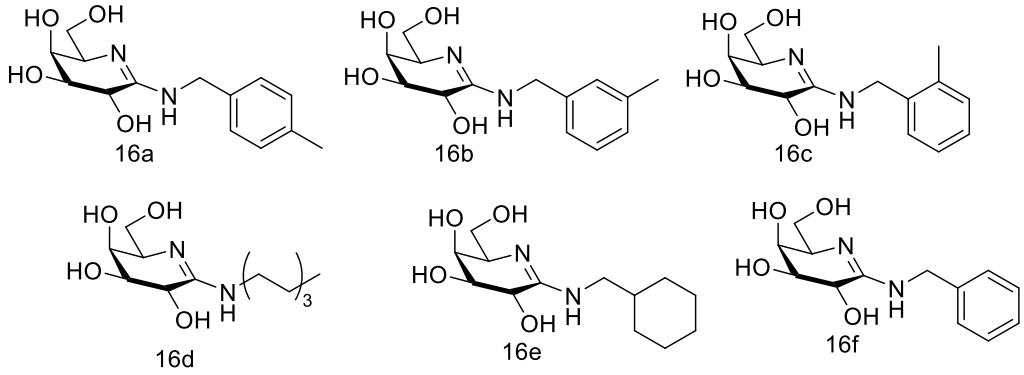

Figure 1.9: Structures of some previously evaluated N-aryl and N-alkyl Galactonoamidines.

The same library of compounds was found to be excellent inhibitors of β-galactosidase (*E. coli*) with K_i values ranging from 0.03 – 2.6 nM, with slight variations depending on the nature of the aglycon.[70] Compound **16a** was a strong inhibitor of the enzyme with a K_i value of 0.06 nM.[71] Derivation of the glycon of **16a** afforded compounds **16g-i** with either a methoxy substituent or a deoxy sugar derivative **Figure 1.10**.[71] The absence of the C2-OH group in **16g** resulted in a K_i value of 1.3 nM, a 21-fold increase from the parent compound. This agrees with the work done by others which shows the importance of the C2-OH for transitions state stabilization.[72-74] When the hydroxyl group at C2 or C4 is replaced with a methoxy substituent, K_i of 42 nM and 32 nM are obtained, which are 700- and 530- fold increase respectively from the parent compound **16a** Molecular docking analysis revealed the sterically hindering methoxy groups repelled the

inhibitors away from the active site of the enzyme.[71] Although compounds **16g-i** are still competitive inhibitors, the study reveals a strong contribution of hydrogen bonding interaction towards the inhibition of the enzyme.

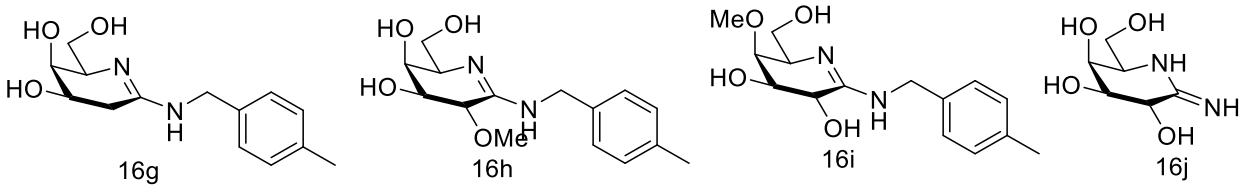

Figure 1.10: Structures of galactonoamidines with derivations in the glycon.

Next, the galactonoamidines were evaluated as inhibitors of β-galactosidase (bovine liver) and also found to be highly potent inhibitors of the enzyme with K_i values ranging from 0.05 – 2.34 nM.[75] To understand how the galactonoamidines achieved such high potency, molecular dynamics simulations were performed with a few of the inhibitors and the enzyme.[75] Compounds 16g (K_i = 0.05 nM), 16i (K_i = 1500 nM) and 16k (K_i = 2000 nM) were chosen for the study. Compound (16f) was found to reside within the active site of the enzyme, had significant hydrogen bonding interaction with the amino acid residues of the enzyme active site, and interacted with both catalytic residues of the enzyme: proton donor (Glu-187) and nucleophile (Glu-267) throughout the simulation. Moreover, a loop closure event supported by π-π stacking interaction of the aromatic aglycon and Trp-272 and Tyr-484 was observed, which stabilized the protein upon binding of the inhibitor. The simulation reveals compound 16h is pushed out of the enzyme active site due to steric repulsion by the methoxy group at C2, only interacts with the nucleophile (Glu-267) and has slightly fewer hydrogen bonding interactions with the amino acid residues of the active site. On the other hand, compound (16j) without an aglycon was unable to induce the loop closure movement, and ultimately resulted in significantly lower hydrogen

bonding interactions. The structure activity relationship study and the computational analyses of galactonoamidines with several β-galactosidases reveal the exceptional potency to be due to a synergy of interactions between the inhibitors and the enzymes.

2: Designing galactonoamidines for the inhibition of the human α-galactosidase.

2.1: Introduction

The exceptional potency of galactonoamidines towards the inhibition of β-galactosidases encouraged us to explore their activity towards α-galactosidases. The human α-galactosidase is a lysosomal glycosidase responsible for the cleavage of the α-galactosyl moiety of globotriaosylceramide in the lysosome, hence enabling its degradation **Figure 2.1**.[76, 77] The α-galactosidase is synthesized in the endoplasmic reticulum and then transported to the lysosome where it performs it functions.[78] However, several mutations in the gene encoding the α-galactosidase are known to result in an improper folding of the protein, which leads to a failed protein quality check and prevents transportation to the lysosome. The absence of lysosomal α-galactosidase results in the accumulation globotriaosylceramide in plasma and tissue.[79, 80] This eventually reaches a toxic level resulting in organ damage such as heart failure, kidney malfunction and stroke.[81] This is a condition known as Fabry disease.[82] Enzyme replacement therapy is common method for the treatment of lysosomal storage disorders such as Fabry disease, where the patients are intravenously supplied with the enzyme.[83]

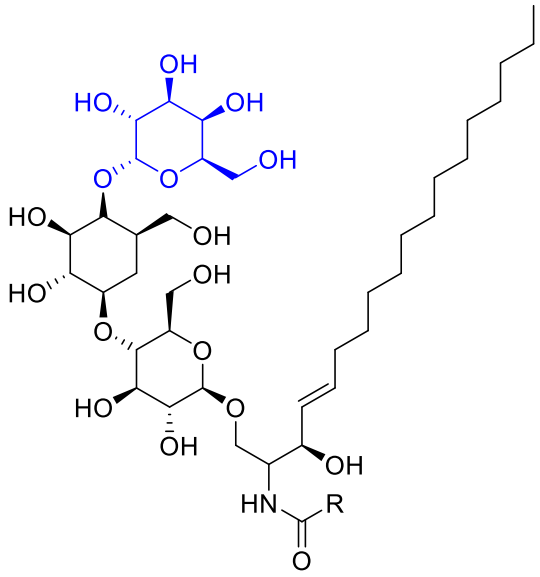

Figure 2.1: Structure of globotriaosylceramide responsible for Fabry disease.

This method of treatment is expensive and prompted the search for other viable treatment methods such as substrate reduction therapy,[84, 85] and pharmacological chaperone.[86, 87] The substrate reduction therapy uses a small molecule inhibitor to reduce the synthesis of the glycosphingolipid, whereas the pharmacological chaperone therapy uses an inhibitor to stabilize the unfolded protein and allow its transportation to the lysosome.[6, 9] Competitive inhibitors of α-galactosidase such as 1-deoxygalactonojirimycin **17a**[88] and several of its derivatives; α-homogalactonojirimycin **17b**,[89] α-homoallonojirimycin **17c**,[90] and β-1-C-butly-deoxygalactonojirimycin **17d**,[91] **Figure 2.2** with IC_{50} values of 0.04 μM, 0.21 μM, 4.3 μM and 16 μM respectively have been shown to increase the α-galactosidase activity in Fabry lymphoblast.[92] In 2018, compound **17a** was approved by the FDA as a pharmacological chaperone for the treatment of Fabry disease.[93] This makes the evaluation of galactonoamidines as inhibitors of the human α-galactosidase very appealing. We expect the galactonoamidines to be stronger inhibitors of the human α-galactosidase than the 1-deoxygalactonojirimycin **17a**

because, they mimic the positive charge and distorted chair ($^4H_3$) conformation of the transition state,[62] whereas compound **17a** only mimics the positive charge of the transition state.

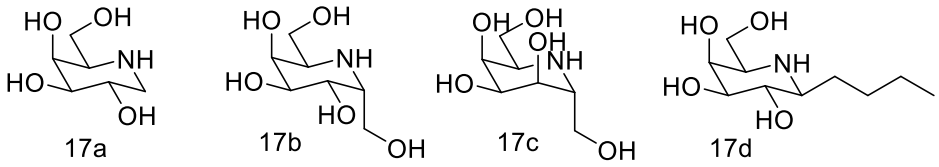

Figure 2.2: Structures of competitive inhibitors shown to improve the α-galactosidase activity in Fabry lymphoblast.

Results obtained from the computational simulation of galactonoamidines with β-galactosidase reveal a necessity for hydrogen bonding interaction between the inhibitors and the proton donor and nucleophile of the enzyme active site. In this regard, the previously synthesized galactonoamidines could not be used as is for the inhibition of the human α-galactosidase. This is because compared to the previously evaluated β-galactosidases which had distances of around 5.0Å between the catalytic residues **Figures 2.3a,b**,[94, 95] the human alpha galactosidase has a distance of 8.2Å between its catalytic residues **Figure 2.3c**,[77] which would prevent optimal hydrogen bonding interaction between the inhibitor and the catalytic residues of the active site. *We therefore hypothesized that galactonoamidines with polar or bulky aglycons will be potent inhibitors of the human α-galactosidase*. The installation of a polar functional group on the aglycon will increase the chances of hydrogen bonding interaction between the inhibitor the catalytic residues of the enzyme, whereas the installation of bulky aglycons will promote other favorable interactions such as π-π stacking, electrostatic or hydrophobic interactions between the inhibitor and the amino acid residues of the enzyme.

a) b) c)

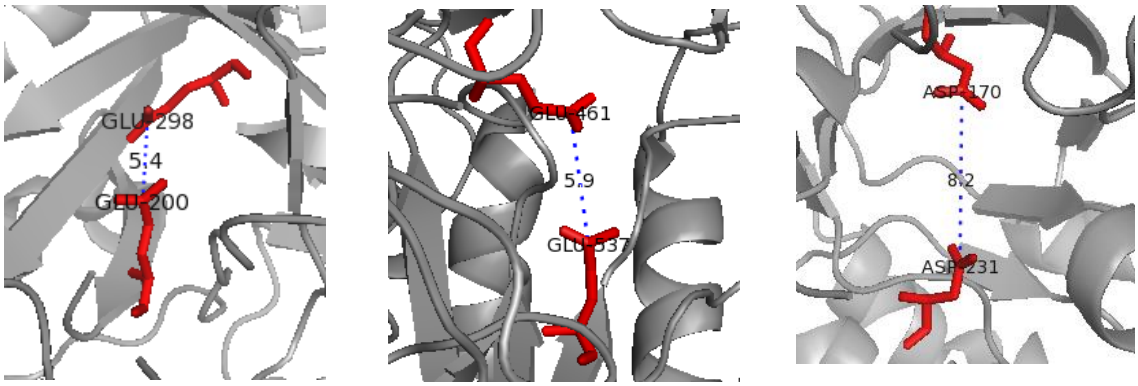

Figure 2.3: Distances between the catalytic residues of galactosidases; a) β-galactosidase (*A. oryzae*), b) β-galactosidase (*E. coli*), c) α-galactosidase (Human).

2.3: Synthesis of galactothionolactam

The galactothionolactam was synthesized in 10 steps from commercially available galactose following procedures which were previously described by our group and others (**Scheme 2.1)**. D-Galactose was treated with sodium acetate and acetic anhydride to afford the peracetylated galactose **18** in 74% yield.[96] To protect the anomeric hydroxyl group, the resulting peracetylated galactose **18** was treated with *p*-thiocresol in the pesence of boron trifluoride to afford the peracetylated thiogalactoside **19** in 91% yield.[97] A Zemplén deacetylation of **19** using a catalytic amount of sodium methoxide in methanol afforded thiogalactoside **20** in 98% yield.[97] A global benzylation of **20** in the presence of benzyl chloride, sodium hydride and a catalytic amount of potassium iodide afforded the perbenzylated thiogalactoside **21** in 83% yield.[97] Removal of the thiocresol group was achieved by treatment of **21** with *N*-bromosuccinimide in a 9:1 v/v mixture of acetone and water to afford the perbenzylated galactopyranose **22** in 87% yield.[98] A Swern oxidation of **22** with dimethyl sulfoxide and acetic anhydride afforded the perbenzylated galactonolactone **23**. The endocyclic nitrogen is installed by the treatment of **23** with a 7 M solution of ammonia in methanol to afford the hydroxy amide **24** in 68% yield after two steps.[99] A Swern oxidation of **24** afforded the keto amide **25** in 84% yield. Reductive

amination of **25** using sodium cyanoborohydride and formic acid afforded a mixture of the D-galactonolactam **26a** and L-altronolactam **26b** in 88% yield.[100] The mixture of compounds can be separated by repetitive column chromatography or can be used as is for the next step. Treatment of **26** with Lawesson's reagent affords a mixture of D-galactothionolactam (**27a**) and L-altrothionolactam **27b** in 84% yield.[62] Similarly, the mixture of isomers can be separated by repetitive chromatography, albeit under the risk of partial compound decomposition on silica. Previous study from our group have also shown that when this mixture of isomers is used for the next step, only **27a** reacts to form the perbenzylated galactonoamidine **28**.[62] The overall yield for the synthesis from galactose is 20%

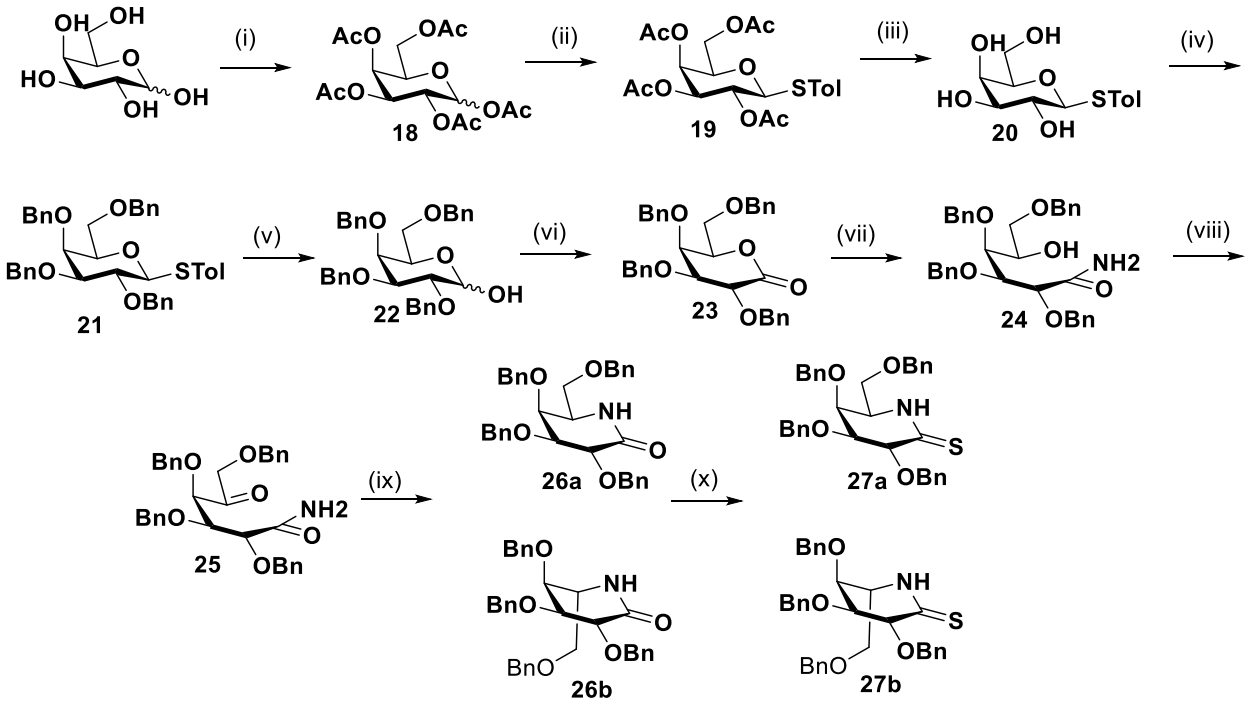

Scheme 2.1: Synthesis of galactothionolactam: Reagents and conditions: i) NaOAc, Ac_2O, 120 °C, 2 h, 94%; ii) p-thiocresol, $BF_3.Et_2O$, CH_2Cl_2, 0 °C to rt, 6 h, 91%; iii) NaOMe, MeOH, 1 h, 98%; iv) NaH, BnCl, DMF, rt, 18 h, 83%; v) NBS, acetone / water (9:1 v/v), rt, 5 h, 97%; vi) Ac_2O, DMSO, rt, 19 h; vii) conc NH_3 / MeOH, rt, 2 h, 68% after 2 steps; viii) Ac_2O, DMSO, rt, 12 h, 84%; ix) $NaCNBH_3$, HCOOH, reflux, 3 h, 88%; x) Lawesson's reagent, benzene, reflux, 84%.

2.4: Synthesis of amines

Despite the failure of the molecular docking analysis to provide reliable results, polar and bulky galactonoamidines still seemed like a viable option for the potent inhibition of the human α-galactosidase. The required amines **29a-j** were typically synthesized in 2-3 steps following literature procedures. The precursor nitriles **31a**-k were assembled via one of: a Williamson-ether synthesis **29a-f**,[101] cross-coupling reaction **29g-i**,[102] or a nucleophilic aromatic substitution **29j**.[103] The precursor for **29f and 29l** was obtained by successively benzylating and mesylating the hydroxyl groups of ethylene glycol.[104, 105] The obtained intermediate was treated with sodium azide to afford the precursor for **29f** or reacted with 4-hydroxybenzonitrile, under the conditions of a Williamson ether synthesis to obtain the precursor for **29l**.[104, 105] The corresponding amines were obtained in good yields by reduction of the nitrile or azide moiety using lithium aluminum hydride **Scheme 2.2**. [106]

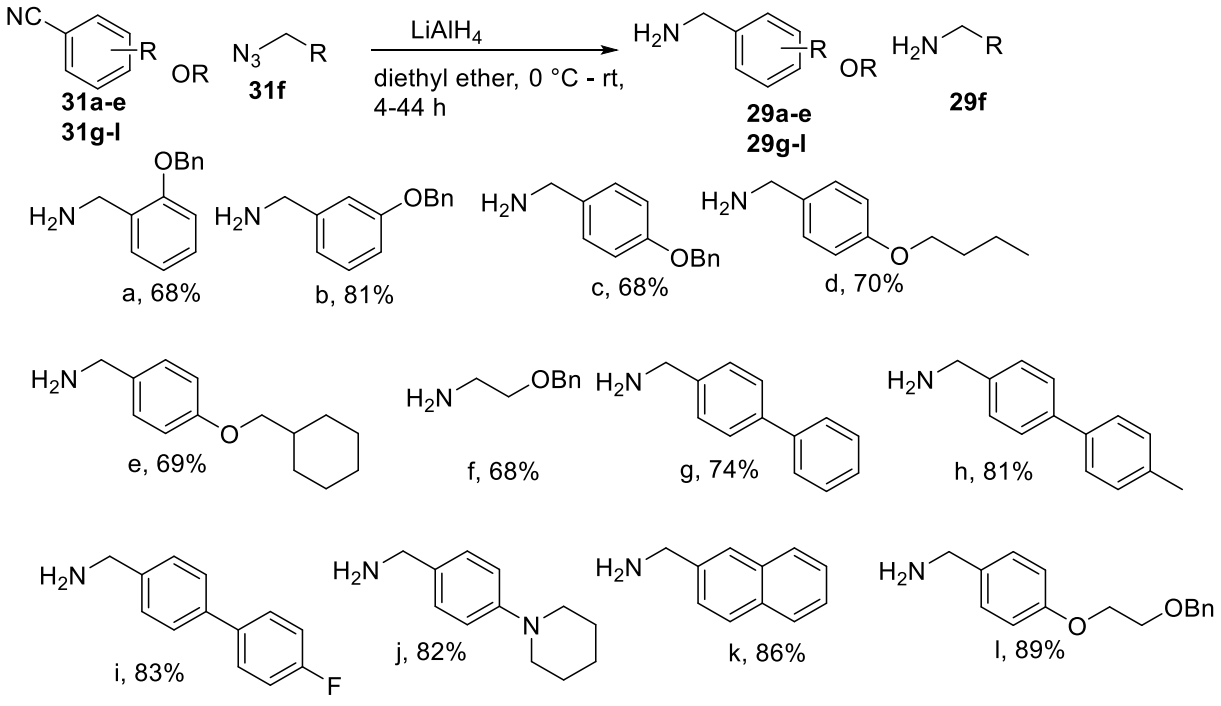

Scheme 2.2: Synthesis of bulky and polar amines.

2.5: Synthesis of perbenzylated galactonoamidines

Following a procedure previously elaborated in the group, perbenzylated galactothionolactam **27a** is activated by treatment with Meerwein's salt to obtain an intermediate galactoiminothioether **30** (**Scheme 2.3**).[62] Subsequently, the obtained intermediate **30** is reacted with freshly distilled amine to obtain the perbenzylated galactonoamidine **28** (**Scheme 2.3**).[62] The coupling of benzyloxybenzylamines, methoxybenzylamines and butoxybenzylamine proceeded as expected, yielding compounds **28a-f** in modest yields. These would potentially yield the desired polar galactonoamidines. The coupling of a few bulky amines afforded the corresponding bulky perbenzylated galactonoamidines perbenzylated galactonoamidines **28g-j** in modest yields as well (**Scheme 2.3**). Unfortunately, the same results could not be obtained for the other bulky amines which were attempted. For example, the coupling of the bipenylamines either yielded trace amount of the desired product or nothing at all. TLC analysis of the failed reactions indicated that all the galactothionolactam **27a** had been transformed to the intermediate galactoiminothioether **30**, but only very little or no transformation of **30** to the corresponding perbenzylated galactonoamidine **28**. Several attempts at increasing the reaction time or using 4-10 equivalents of the amine did not result in a significant improvement of the reaction outcome. The coupling reaction is set up under scrupulously anhydrous conditions, with amines that are distilled and stored under nitrogen atmosphere for no more than 24 hours prior to use, which rules out the possibility that the amine had been oxidized or protonated before being introduced to the reaction mixture. Moreover, ^{1}H-NMR analysis of the commercial and synthesized amines was used to ascertain the purity of the amines prior to use. Interestingly, on several occasions, when TLC analysis of an aliquot of the reaction mixture indicated no significant transformation of product formation after 8-14 days of stirring, a different amine, typically 4-

methylbenzylamine was added to the reaction flask, and after 16 hours of stirring, all unreacted intermediate **30** was transformed to the corresponding perbenzylated galactonoamidine **28q**. Since the failure of these coupling reactions could not be attributed to poor experimental set up or the use of bad reagents or moisture containing solvent, the other plausible explanation would be difference in the reactivity of the amines under the reaction conditions. The amines that had failed to couple under the previously established conditions even with increased reaction times and amine equivalents are bulky in nature. However, the poor reactivity cannot necessarily be attributed to steric effect. The successful coupling of 2-methoxybenzylamine and 2-benzyloxybenzylamine which have bulky substituents at the ortho position next to the amine moiety indicate the poor reactivity is possibly due to an electronic effect. Perhaps, the electron withdrawing phenyl rings at the para position of the biphenylamines render them less reactive towards the coupling with the galactoiminothioether **30**.

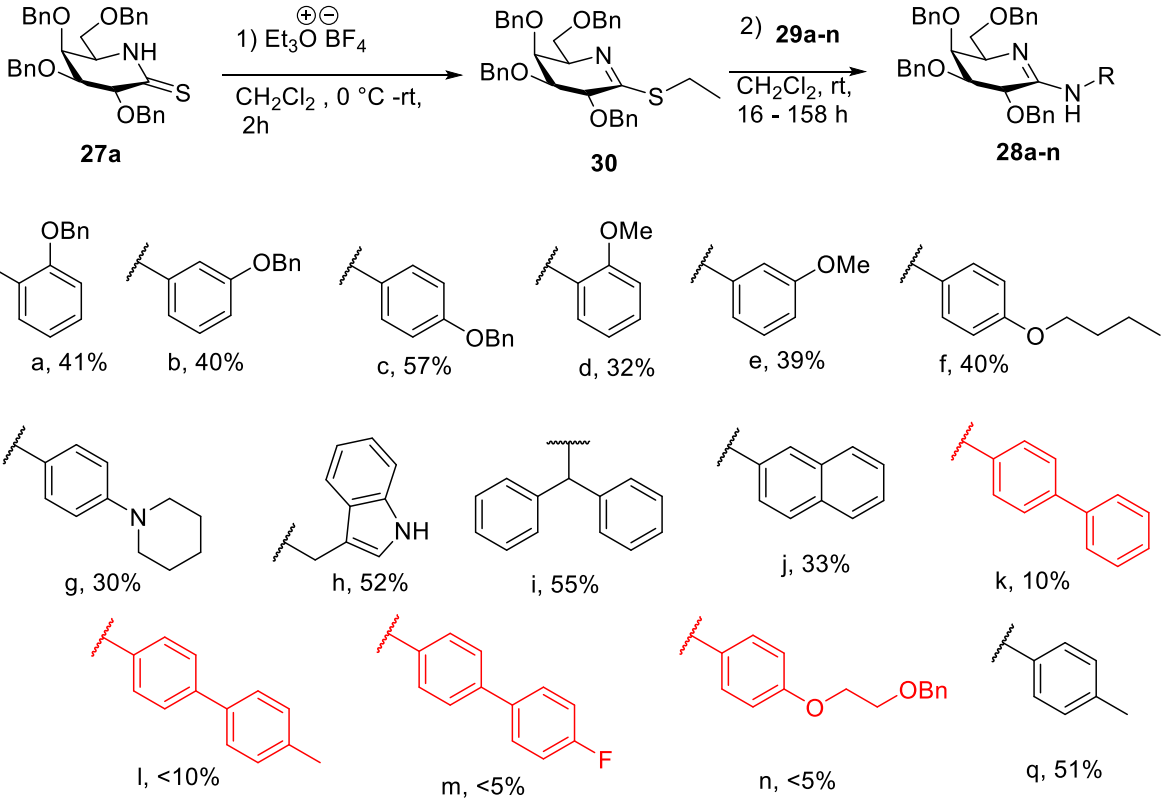

Scheme 2.3: Synthesis of perbenzylated galactonoamidines **28a-k** in dichloromethane.

Next, the failed coupling reactions were repeated using acetonitrile as the solvent. This resulted in an overall improvement in the yields of the isolated compounds. The yield of compound **28k** improved from a 10% in dichloromethane to a 30% when the reaction was done in acetonitrile. Compounds **28l-n** were also now accessible, albeit in low-modest yields, which was sufficient to move on to the next step. In addition, **28o-p** were added to the library (**Scheme 2.4**).

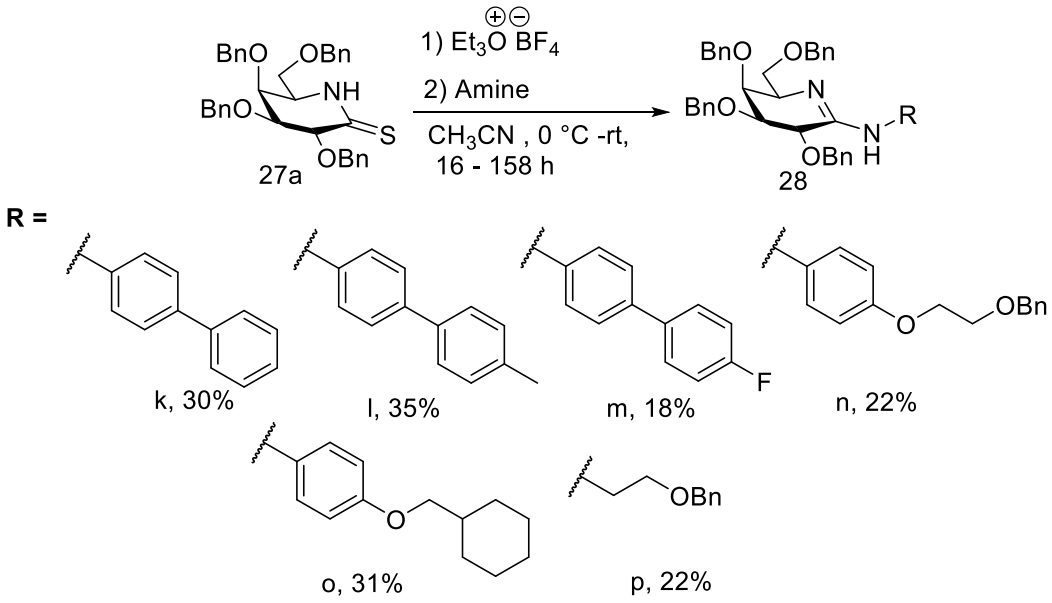

Scheme 2.4: Synthesis of perbenzylated galactonoamidines **28k-p** in acetonitrile.

2.6: Synthesis of galactonoamidines

Following a procedure previously described by the group, polar galactonoamidines **16k-q** were obtained readily in excellent yields from their precursor perbenzylated galactonoamidines by hydrogenation in the presence of palladium on carbon, ethanol and trifluoroacetic acid, **Scheme 2.5**.[62] The addition of the trifluoroacetic acid is necessary to prevent the coordination of palladium to the amidine site.[62] NMR and HRMS analysis of the obtained compounds indicated

complete debenzylation occurred, and the desired compounds were obtained. Following the same procedure, bulky galactonoamidines **16r-s** were also obtained in high yields. The hydrogenation of **28h**, yielded a mixture of compounds. NMR and LC-MS analysis of the obtained compound indicated the major product was **16t**, where the indole moiety of the aglycon had been completely reduced to the octahydrotryptophan. The indole moiety of tryptophan in a peptide was reduced to an octahydrotryptophan by hydrogenation in the presence of palladium and formic acid.[107] Unfortunately, attempts at synthesizing the other bulky galactonoamidines **16u-z** did not yield clean compounds. In all cases, the recovered compound weighed almost twice as much as expected, and moreover, the obtained ^{1}H-NMR spectrum for the compounds either had broad signals due to the presence of residual palladium or were messy due to incomplete hydrogenation. The compounds were re-suspended in the ethanol-trifluoroacetic (freshly distilled) acid mixture and the hydrogenation was repeated several times to hopefully prevent the coordination of the palladium to the amidine site and allow for complete debenzylation. Increasing the reaction time, palladium loading or the amount of trifluoroacetic acid did not result in an improvement in the hydrogenation. There is no clear explanation on why the hydrogenation worked for some of the compounds in the library and not for others. The galactonoamidines **16k-z** only vary in the structure of their aglycon, which doesn't seem like it would affect the progression of the hydrogenation reaction.

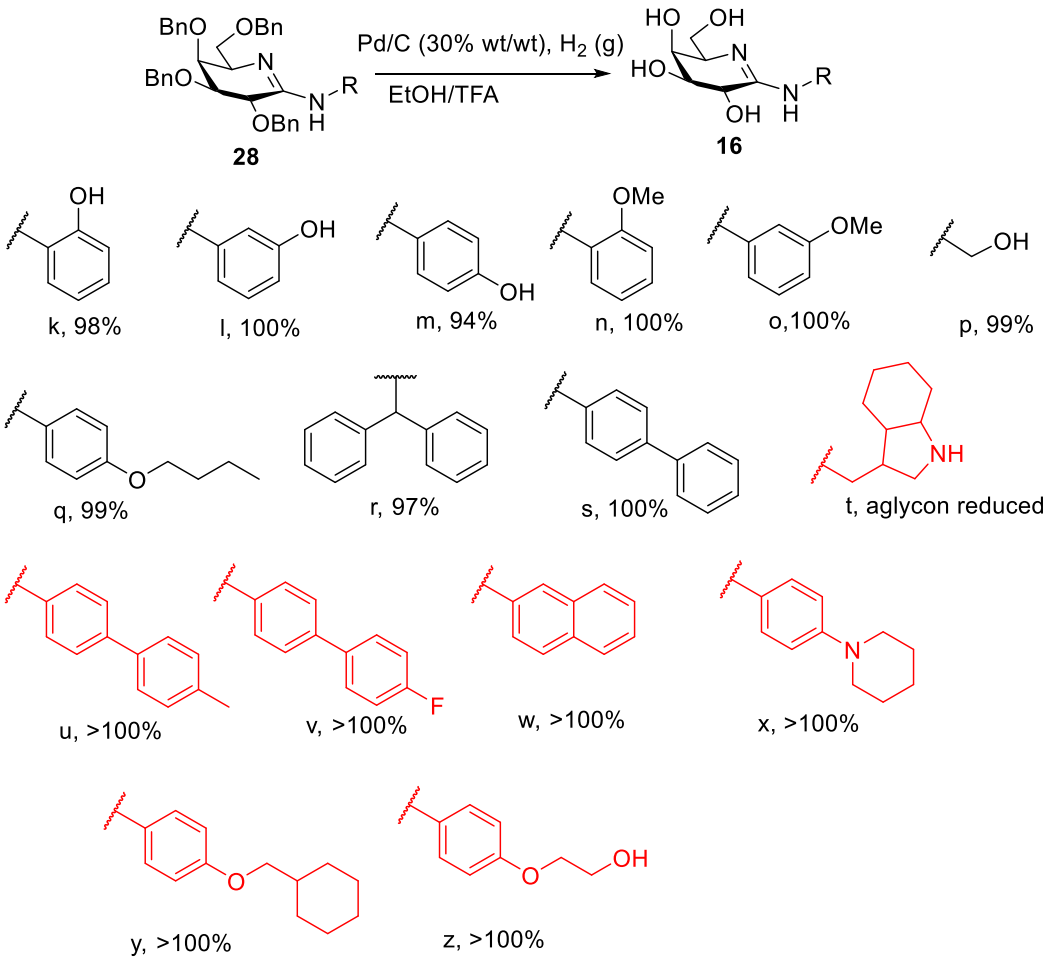

Scheme 2.5: Synthesis of polar galactonoamidines

3: Conclusion and outlook

The work described here aimed to synthesize a new library of galactonoamidines with polar and bulky aglycons in hopes of optimizing their interactions with the human α-galactosidase. Following a procedure previously described by the group a library of perbenzylated galactonoamidines were synthesized by either performing the reaction in dichloromethane or acetonitrile. With the perbenzylated galactonoamidines in hand, hydrogenation in the presence of palladium on carbon afforded nine of the desired galactonoamidines, while the other attempted 7 contained a significant amount of coordinated palladium. The purity and performance of the hydrogenation reaction could potentially be improved by increasing the ratio of trifluoroacetic acid to ethanol to prevent the coordination of the palladium. The compounds could also be potentially purified by high performance liquid chromatography (HPLC) on an appropriate stationary phase to avoid decomposition. Nonetheless, the development of galactonoamidine inhibitors for the human α-galactosidase has very good potential of yielding a competitive and highly potent competitive inhibitor which could eventually be evaluated as a pharmacological chaperone for the treatment of Fabry disease. 1-deoxygalactonojirimycin (migalastat) a competitive inhibitor of the human α-galactosidase was recently approved by the FDA as a treatment for Fabry diseases. It is important to note that this compound only mimics the positive charge of the transition state, whereas the galactonoamidines with a $^{4}H_{3}$ conformation mimics both the shape and charge of the transition state. Moreover, the aglycon moiety of the galactonoamidines can be derivatized to optimize the overall interactions between the inhibitor and the amino acid residues within the active site of the enzyme. Therefore, the polar and bulky galactonoamidines have the potential of becoming stronger inhibitors and becoming stronger pharmacological chaperones for the human α-galactosidase.

4: Experimental section

4.1: Instrumentation

NMR spectra of all compounds were measured on a Bruker 400 MHz spectrometer equipped with a Topspin 2.1 software. High resolution mass spectrometry data were obtained at the University of Arkansas statewide mass spectrometry facility. Elemental analyses were performed by Atlantic Micro lab, Inc. IR spectra were measured using a Shimadzu ATR-FTIR 8000 spectrophotometer, equipped with LabSolutions IR software version 2.15. Optical rotations were measured on an Autopol III Automatic polarimeter using a 1.0 dm cell. Amines were distilled using a Büchi GKR-51 Kugel Rohr apparatus, under vacuum. Freeze drying was performed on a FreeZone 1 L bench top freeze dry system from Labconco. Melting points were measured on a Mel-Temp melting point apparatus, and the values are uncorrected.

4.2: Materials and methods

NMR measurements were done using deuterated chloroform, deuterated dichloromethane, DMSO-d_6, acetone-d_6, MeOH-d_4, and deuterium oxide as solvents. The chemical shifts (δ) in the NMR data are expressed in parts per million (PPM) and coupling constants (J) in Hertz. The signal multiplicities are denoted as s (singlet), d (doublet), t (triplet), q (quartet), and m (multiplet). The chemical shift values are reported with respect to the residual solvents ($CDCl_3$ δ_H 7.29, δ_C 77.0; CD_2Cl_2 δ_H 5.32, δ_C 54.0; DMSO-d_6 δ_H 2.50, δ_C 39.5; acetone-d_6 δ_H 2.05, δ_C 29.8; MeOH-d_4 δ_H 4.80, δ_C 49.0; D_2O δ_H 4.80, δ_C 49.0 after the addition of a drop of MeOH-d_4). Column chromatography was performed on silica gel (40-63 μm, 230-450 mesh, Silicycle) or basic alumina (50-200 μm, 60 Å, ACROS). Thin layer chromatography (TLC) was performed on silica gel TLC plates from SORBENT Technologies, 200 μM, aluminum backed with

fluorescence indicator F254 and visualization by UV light or by charring with an ethanolic vanillin-sulfuric acid reagent and subsequent heating of the TLC plate.

4.3: Chemicals

All commercially obtained chemicals had reagent-grade quality or better and were used as received unless noted otherwise. 2-methoxybenzylamine, 3-methoxybenzylamine, 2-(3-indolylethyl) amine, 2,2'-diphenylethylamine were distilled prior to use. Dichloromethane and diethyl ether were dried by running over neutral aluminum oxide, under a positive flow of nitrogen. 2-benzyloxybenzonitrile,[101] 3-benzyloxybenzonitrile,[101] 4-benzyloxybenzonitrile,[108] 4-butoxybenzonitrile,[109] 4-phenylbenzonitrile,[102] p-(p-tolyl)lbenzonitrile,[102] 4-cyano-4'-fluorobiphenyl,[102] 4-(piperidin-1-yl)benzonitrile,[103] 4-cyclohexylmethoxybenzonitrile,[101] (2-azidoethoxy)methylbenzene,[104, 105, 110] and 4-[2-(benzyloxy)ethoxy]benzonitrile[104, 105] were synthesized following literature known procedures.

4.4: Molecular docking analysis

The PDB coordinates for the human α-galactosidase (PDB ID: 1R47) were obtained from the Protein Data Bank.[111] The file was opened in PyMOL, where the substrate, water and solvent molecules were removed.[112] The three-dimension coordinates of the protein were imported into PMV-1.5.6 software where the polar hydrogen atoms and Kollman charges were added to the atoms and converted into a pdbqt file. The galactonoamidine structures were energy minimized using MM2 force field and converted to pdbqt coordinate files with all non-ring bonds rotatable. A 30×30×30 $Å^3$ grid box was centred in the enzyme active site. The grid dimensions and positions were imputed into the command prompt of AutoDock Vina 1.1.2 software,[113] along with the pdbqt files of the galactonoamidines and the enzyme to compute the inhibitor-enzyme interactions with an exhaustiveness of 100. The software outputs and ranks nine inhibitor

conformations based on their energies. The inhibitor conformation with the lowest binding score was used to analyze the hydrogen bonding interactions.

4.5: General procedure for the synthesis of amines a-m

Lithium aluminum hydride (4.0 equiv) was transferred to a Schlenk flask and cooled in a 0 °C ice bath under nitrogen atmosphere for 15 minutes. Afterwards, 20-30 mL of dry diethyl ether or 1,2-dimethoxyethane was added, followed by the corresponding azide or nitrile (1.0 equiv). The reaction mixture was warmed to ambient temperature and stirred for 2-40 hours. The reaction mixture was cooled in a 0 °C ice bath, followed by the addition of water (0.5-1 mL), 15% wt/wt solution of sodium hydroxide (0.5-1 mL), water (1.5-3.0 mL) and stirred for an hour. The formed slurry was filtered off, and the resulting solution was concentrated under reduced pressure to afford the crude amines which were purified by distillation using a Kugel Rohr apparatus to afford the title amines in good to excellent yields.

2-Benzyloxybenzylamine (29a): Lithium aluminum hydride (0.94 g, 25 mmol) and 2-benzyloxybenzonitrile (1.30 g, 6.21 mmol, 1.0 equiv) in 30 mL diethyl ether; reaction time 5 h; compound **29a** (0.90 g, 68%) as a colorless oil; R_f = 0.12 (SiO_2; CH_2Cl_2/MeOH; 25/1 v/v). ^{1}H NMR (400.15 MHz, $CDCl_3$) δ 7.34 - 7.50 (m, 4H), 7.22 - 7.31 (m, 2H), 6.94 - 7.01 (m, 2H), 5.15 (s, 2H), 3.91 (s, 2H); ^{13}C NMR (100.6 MHz, $CDCl_3$) δ 156.6, 137.1, 132.3, 128.6, 128.0, 127.9, 127.1, 120.9, 111.6, 69.9, 42.7.

3-Benzyloxybenzylamine (29b): Lithium aluminum hydride (0.70 g, 19 mmol) and 3-benzyloxybenzonitrile (0.97 g, 4.6 mmol, 1.0 equiv) in 30 mL diethyl ether; reaction time 17 h; compound **29b** (0.80 g, 81%) as a colorless oil; ^{1}H NMR (400.15 MHz, $CDCl_3$) δ 7.32 - 7.49 (m,

5H), 7.24 - 7.28 (m, 1H), 6.81 - 7.04 (m, 3H), 5.09 (s, 2H), 3.86 (s, 2H); ^{13}C NMR (101 MHz, $CDCl_3$) δ 159.1, 145.1, 137.1, 129.6, 128.5, 127.9, 127.4, 119.6, 113.6, 113.1, 69.9, 46.5

4-Benzyloxybenzylamine (29c): Lithium aluminum hydride (0.40 g, 11 mmol) and 4-benzyloxybenzonitrile (0.55 g, 2.6 mmol, 1.0 equiv) in 20 mL 1,2-dimethoxyethane; reaction time 21 h; compound **29c** (0.90 g, 68%) as a colorless solid; m.p 110-112 °C; ^{1}H NMR (400 MHz, $CDCl_3$) δ 7.33 - 7.49 (m, 5H), 7.24 - 7.28 (m, 2H), 6.96 - 7.01 (m, 2H), 5.10 (s, 2H), 3.84 (s, 2H); ^{13}C NMR (101 MHz, $CDCl_3$) δ 157.7, 137.1, 135.9, 128.5, 128.2, 127.9, 127.4, 114.9, 70.0, 45.9

4-Butoxybenzylamine (29d): Lithium aluminum hydride (0.83 g, 22 mmol) and 4-butoxybenzonitrile (0.96 g, 5.5 mmol, 1.0 equiv) in 30 mL diethyl ether; reaction time 17 h; compound **29d** (0.69 g, 70%) as a colorless oil; ^{1}H NMR (400.15 MHz, Acetone) δ 7.20 - 7.25 (m, 2H), 6.82 - 6.88 (m, 2H), 4.34 (s, 1H), 3.94 - 3.99 (m, 2H), 1.69 - 1.77 (m, 2H), 1.44 - 1.55 (m, 2H), 0.94 - 0.99 (m, 3H); ^{13}C NMR (100.6 MHz, Acetone) δ 158.7, 134.0, 129.5, 114.9, 68.2, 55.0, 32.1, 19.9, 14.1

4-(Cyclohexylmethyoxy)benzylamine (29e): Lithium aluminum hydride (0.43 g, 11 mmol) and 4-cyclohexylmethoxybenzonitrile (0.61 g, 2.8 mmol, 1.0 equiv) in 40 mL diethyl ether; reaction time 4 h; compound **29e** (0.43 g, 69%) as a colorless solid; m.p 75-79 °C; ^{1}H NMR (400.15 MHz, Acetone) δ 7.19 - 7.25 (m, 2H), 6.82 - 6.87 (m, 2H), 4.34 (s, 1H), 3.74 - 3.79 (m, 2H), 3.71 (s, 1H), 1.82 - 1.91 (m, 2H), 1.65 - 1.82 (m, 4H), 1.15 - 1.37 (m, 3H), 1.00 - 1.14 (m, 2H); ^{13}C NMR (100.6 MHz, Acetone) δ 158.8, 134.0, 129.5, 128.9, 114.9, 73.9, 55.0, 38.6, 27.2, 26.5;

(FT-IR): 2933, 2850, 1508, 1241, 1029. Elemental analysis calculated for $C_{14}H_{21}NO$; C, 76.67; H, 9.65; N, 6.39, found C, 76.51; H, 9.57; N, 6.39.

***O*-Benzylethanolamine (29f):** Lithium aluminum hydride (0.14 g, 3.8 mmol) and 2-benzyloxyethylazide (0.75 g, 3.0 mmol, 1.0 equiv) in 10 mL diethyl ether; reaction time 2 h; compound **29f** (0.26 g, 68%) as a colorless oil; ^{1}H NMR (400.15 MHz, $CDCl_3$) δ 7.30 - 7.42 (m, 4H), 4.57 (s, 2H), 3.53 - 3.57 (m, 2H), 2.92 (t, *J* = 5.26 Hz, 2H); ^{13}C NMR (100.6 MHz, $CDCl_3$) δ 138.3, 128.4, 127.7, 127.6, 73.1, 72.6, 42.0

4-Phenylbenzylamine (29g): Lithium aluminum hydride (0.46 g, 12 mmol) and 4-phenylbenzonitrile (0.54 g, 3.0 mmol, 1.0 equiv) in 30 mL diethyl ether; reaction time 16 h; compound **29g** (0.41 g, 74%) as a colorless solid; m.p 54-56 °C; ^{1}H NMR (400.15 MHz, $CDCl_3$) δ 7.56 - 7.68 (m, 4H), 7.34 - 7.51 (m, 5H), 3.89 - 4.02 (m, 2H); ^{13}C NMR (100.6 MHz, $CDCl_3$) δ 142.4, 140.9, 139.8, 128.7, 127.5, 127.3, 127.2, 127.0, 46.2

4-(4'-Methylphenyl)benzylamine (29h): Lithium aluminum hydride (0.27 g, 7.2 mmol) and p-(p-tolyl)lbenzonitrile (0.35 g, 1.8 mmol, 1.0 equiv) in 30 mL diethyl ether; reaction time 22 h; compound **29h** (0.29 g, 81%) as a colorless solid; m.p 92-94 °C; ^{1}H NMR (400.15 MHz, $CDCl_3$) δ 7.57 - 7.62 (m, 2H), 7.50 - 7.55 (m, 2H), 7.41 (d, *J* = 8.31 Hz, 2H), 7.26 - 7.31 (m, 2H), 3.94 (s, 2H), 2.43 (s, 3H); ^{13}C NMR (100.6 MHz, $CDCl_3$) δ 142.1, 139.7, 138.0, 136.9, 129.4, 127.5, 127.1, 126.9, 46.2, 21.1

4-(4'-Fluorophenyl)benzylamine (29i): Lithium aluminum hydride (0.35 g, 9.3 mmol) and 4-cyano-4'-fluorobiphenyl (0.46 g, 2.3 mmol, 1.0 equiv) in 30 mL diethyl ether; reaction time 17 h; compound **29i** (0.39 g, 83%) as a colorless solid; m.p 63-64 °C; ^{1}H NMR (400.15 MHz, $CDCl_3$) δ 7.52 - 7.60 (m, 4H), 7.41 (d, *J* = 8.07 Hz, 2H), 7.10 - 7.19 (m, 2H), 3.95 (s, 2H); ^{13}C NMR (100.6 MHz, $CDCl_3$) δ 163.6, 161.2, 142.4, 138.8, 137.1, 128.6, 128.5, 127.6, 127.2, 115.7, 115.5, 46.2.

4-Piperidin-1-yl-benzylamine (29j): Lithium aluminum hydride (0.84 g, 22 mmol) and 4-(piperidin-1-yl)benzonitrile (1.03 g, 5.53 mmol, 1.0 equiv) in 42 mL diethyl ether; reaction time 40 h; compound **29j** (0.86 g, 82%) as a colorless wax; ^{1}H NMR (400.15 MHz, $CDCl_3$) δ 7.19 - 7.24 (m, 2H), 6.92 - 6.97 (m, 2H), 3.80 (s, 2H), 3.13 - 3.19 (m, 4H), 1.71 - 1.80 (m, 6H), 1.56 - 1.64 (m, 2H); ^{13}C NMR (100.6 MHz, $CDCl_3$) δ 151.2, 134.0, 127.8, 116.6, 50.8, 45.9, 25.8, 24.2.

2-Naphthylmethylamine (29k): Lithium aluminum hydride (0.47 g, 12 mmol) and 2-naphthalenecarbonitrile (0.43 g, 2.8 mmol, 1.0 equiv) in 30 mL diethyl ether; reaction time 40 h; compound **29k** (0.90 g, 68%) as a colorless solid; m.p 50-52 °C; ^{1}H NMR (400.15 MHz, $CDCl_3$) δ 7.82 - 7.91 (m, 3H), 7.76 - 7.81 (m, 1H), 7.44 - 7.53 (m, 3H), 4.07 (s, 2H); ^{13}C NMR (100.6 MHz, $CDCl_3$) δ 140.7, 133.5, 132.5, 128.2, 127.6, 127.6, 126.0, 125.7, 125.5, 125.0, 46.6.

4-(2-Phenylmethyoxy)benzylamine (29l): Lithium aluminum hydride (0.45 g, 11 mmol) and 4-[2-benzyloxyethoxy]benzonitrile (0.75 g, 3.0 mmol, 1.0 equiv) in 30 mL diethyl ether; reaction time 4 h; compound IO390 (0.68 g, 89%) as a colorless oil; ^{1}H NMR (400.15 MHz, METHANOL-d_4) δ 7.20 - 7.39 (m, 6H), 6.87 - 6.93 (m, 2H), 4.60 (s, 2H), 4.08 - 4.15 (m, 2H),

3.79 - 3.83 (m, 2H), 3.70 (s, 2H); ^{13}C NMR (100.6 MHz, METHANOL-d_4) δ 159.3, 139.5, 136.0, 129.7, 129.4, 128.9, 128.7, 115.7, 74.2, 69.9, 68.6, 46.1. Elemental analysis calculated for $C_{16}H_{19}NO_2$; C, 74.68; H, 7.44; N, 5.44, found C, 73.25; H, 7.42; N, 5.32.

4.6: Synthesis of 2,3,4,6-tetra-O-benzyl-D-galactothionolactam

Compound **26a** (1.66 g, 3.09 mmol, 1.0 equiv) was dissolved in 45 mL of dry benzene under nitrogen atmosphere. Lawesson's reagent (0.87 g, 2.2 mmol, 0.71 equiv) was added and the reaction mixture was refluxed for 2 hours. The reaction mixture was cooled to ambient temperature and diluted with 200 mL of ethyl acetate. The resulting solution was washed with a saturated solution of sodium bicarbonate (50 mL), water (50 mL), brine (50 mL) and dried over anhydrous sodium sulfate. The sodium sulfate was filtered off and the resulting solution was concentrated under reduced pressure to afford a yellow residue which was purified by column chromatography on silica gel (hexane-ethyl acetate; 1/0→6/1→4/1→2/1 v/v) to afford compound **27a** (1.30 g, 76%) as a yellow oil. ^{1}H NMR (400.15 MHz, DMSO-d_6) δ ppm 9.91 (br. s., 1 H) 7.20 - 7.45 (m, 22 H) 5.19 (d, *J*=11.00 Hz, 1 H) 4.81 (d, *J*=11.37 Hz, 1 H) 4.69 - 4.78 (m, 2 H) 4.61 (dd, *J*=18.98, 11.65 Hz, 2 H) 4.44 - 4.56 (m, 2 H) 4.29 (br. s., 1 H) 4.20 (d, *J*=8.62 Hz, 1 H) 3.98 (d, *J*=8.62 Hz, 1 H) 3.85 (br. s., 1 H) 3.69 - 3.77 (m, 1 H) 3.56 - 3.66 (m, 1 H); ^{13}C NMR (100 MHz, DMSO-d_6) δ ppm 200.7, 138.5, 138.4, 138.3, 137.9, 128.2, 128.2, 128.2, 128.0, 127.9, 127.7, 127.7, 127.6, 127.5, 127.4, 127.4, 127.3, 81.4, 79.2, 74.3, 73.6, 72.4, 72.0, 71.3, 67.1, 56.6

4.7: General procedure for the synthesis of perbenzylated galactonoamidines

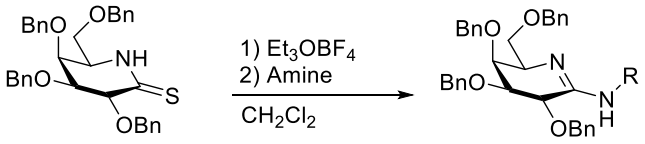

The syntheses were performed according to a general protocol described by Rami Kanso and Susanne Striegler in *Carbohydrate Research*, **2011**, 346, 897-904.

Meerwein's salt was added to a solution of 2,3,4,6-tetra-O-benzyl-D-galactothionolactam in dry dichloromethane under nitrogen atmosphere in a 0 °C ice bath and stirred for 2-4 hours. Freshly distilled amine was added, and the reaction mixture was warmed to ambient temperature and stirred for 16 h – 10 days. The reaction mixture was concentrated under reduced pressure and purified by flash column chromatography over deactivated silica gel or basic alumina to afford the desired compounds.

2-Benzyloxybenzyl-2,3,4,6-tetra-O-benzyl-D-galactonoamidine (28a): Meerwein's salt (0.09 g, 0.5 mmol, 1.5 equiv) and galactothionolactam (0.17 g, 0.31 mmol) in 6 mL of dichloromethane; 2-benzyloxybenzylamine (0.13 g, 0.61 mmol, 2.0 equiv); reaction time 42 h; silica gel chromatography (cyclohexane/ethyl acetate = 1/0-1/0-10/1-4/1, v/v), basic alumina chromatography cyclohexane/ethyl acetate = 8/1-4/1, v/v) compound **28a** (0.09 g, 0.1 mmol, 41%); yellow oil. R_f 0.21 (SiO_2, hexane/ethyl acetate = 1/1 v/v); $[\alpha]^{24}_D$ +14.9 (*c* 1.77, $CHCl_3$); ^{1}H NMR (400.15 MHz, CD_2Cl_2) δ 7.17 - 7.42 (m, 23H), 6.87 - 6.92 (m, 2H), 5.02 (s, 2H), 4.93 (d, *J* = 11.19 Hz, 1H), 4.65 (d, *J* = 11.19 Hz, 1H), 4.60 (dd, *J* = 3.12, 11.55 Hz, 2H), 4.56 (s, 2H), 4.42 - 4.54 (m, 2H), 4.24 - 4.34 (m, 2H), 3.96 (dd, *J* = 1.93, 9.63 Hz, 1H), 3.58 - 3.78 (m, 3H), 2.08 (s), 1.28 (s); ^{13}C NMR (100.6 MHz, CD_2Cl_2) δ 157.2, 156.3, 139.8, 139.4, 139.0, 138.8, 137.9, 129.8, 129.0, 129.0, 128.9, 128.7, 128.6, 128.5, 128.5, 128.4, 128.3, 128.3, 128.2, 128.1, 128.0, 127.7, 121.2, 112.2, 82.4, 76.2, 75.2, 74.7, 74.1, 73.8, 72.0, 71.6, 70.4, 60.0, 40.6; ν_{max} (FT-IR): 3436, 3024, 2869, 1618, 1491, 1456, 1354, 1228, 1080, 760, 702. HRMS (ESI) calculated for $C_{48}H_{48}N_2O_5$ $[M+H]^+$: 733.3636; found 733.3634.

3-Benzyloxybenzyl-2,3,4,6-tetra-O-benzyl-D-galactonoamidine (28b): Meerwein's salt (0.14 g, 0.73 mmol, 1.5 equiv) and galactothionolactam (0.27 g, 0.49 mmol) in 6 mL of dichloromethane; 3-benzyloxybenzylamine (0.21 g, 0.98 mmol, 2.0 equiv); reaction time 182 h; basic alumina chromatography (cyclohexane/ethyl acetate = 1/0-10/1-1/2, v/v) compound **28b** (0.14 g, 0.19 mmol, 40%); yellow oil. R_f 0.08 (SiO_2, hexane/ethyl acetate = 2/1 v/v); $[\alpha]^{23}_D$ +4.23 (*c* 1.37, CH_2Cl_2); ^{1}H NMR (400.15 MHz, CD_2Cl_2) δ 7.16 - 7.44 (m, 25H), 6.78 - 6.88 (m, 3H), 5.00 (s, 2H), 4.92 (d, *J* = 11.00 Hz, 1H), 4.87 (d, *J* = 11.37 Hz, 1H), 4.83 (d, *J* = 11.74 Hz, 1H), 4.60 - 4.68 (m, 3H), 4.50 - 4.57 (m, 3H), 4.20 - 4.35 (m, 3H), 3.98 (dd, *J* = 1.83, 9.54 Hz, 1H), 3.55 - 3.78 (m, 3H), 1.28 (s); ^{13}C NMR (100.6 MHz, CD_2Cl_2) δ 159.5, 156.4, 142.1, 139.7, 139.4, 138.9, 138.7, 137.8, 129.9, 129.1, 129.0, 129.0, 128.9, 128.8, 128.6, 128.5, 128.4, 128.3, 128.2, 128.1, 128.1, 128.0, 127.9, 127.4, 120.6, 114.4, 113.9, 82.5, 76.0, 75.3, 74.7, 74.3, 73.8, 72.0, 71.6, 70.4, 60.1, 45.2. ν_{max} (FT-IR): 3441, 3020, 2874, 1644, 1498, 1462, 1266, 1084, 1018, 741, 698. HRMS (ESI) calculated for $C_{48}H_{48}N_2O_5$ $[M+H]^+$: 733.3636; found 733.3640.

4-Benzyloxybenzyl-2,3,4,6-tetra-O-benzyl-D-galactonoamidine (28c): Meerwein's salt (0.10 g, 0.53 mmol, 1.5 equiv) and galactothionolactam (0.20 g, 0.36 mmol) in 5 mL of dichloromethane; 4-benzyloxybenzylamine (0.15 g, 0.722 mmol, 2.0 equiv); reaction time 34 h; silica gel chromatography cyclohexane/ethyl acetate = 10/1-6/1-2/1, v/v) compound **28c** (0.15 g, 0.21 mmol, 57%); yellow oil. R_f 0.23 (SiO_2, hexane/ethyl acetate = 1/1 v/v); $[\alpha]^{21}_D$ +14.0 (*c* 1.04, $CHCl_3$); ^{1}H NMR (400.15 MHz, CD_2Cl_2) δ 7.21 - 7.48 (m, 25H), 7.12 (d, *J* = 8.80 Hz, 2H), 6.85 - 6.92 (m, 2H), 5.05 (s, 2H), 4.93 (d, *J* = 11.00 Hz, 1H), 4.80 - 4.88 (m, 2H), 4.59 - 4.68 (m, 3H), 4.55 (s, 2H), 4.49 (d, *J* = 9.54 Hz, 1H), 4.28 - 4.34 (m, 1H), 4.12 - 4.25 (m, 2H), 3.97 (dd, *J* = 1.83, 9.72 Hz, 1H), 3.58 - 3.78 (m, 3H), 1.28 (s); ^{13}C NMR (100.6 MHz, CD_2Cl_2) δ 158.4, 156.3, 139.7, 139.4, 138.9, 138.7, 137.9, 132.7, 129.5, 129.1, 129.0, 128.9, 128.8, 128.6, 128.5,

128.4, 128.3, 128.2, 128.1, 128.0, 115.2, 82.4, 76.0, 75.2, 74.7, 74.2, 73.8, 72.0, 71.6, 70.5, 60.0, 44.8; ν_{max} (FT-IR) 3067, 3021, 2853, 2021, 1666, 1507, 1460, 1226, 1095, 1012, 740, 703. HRMS: calcd for $C_{48}H_{48}N_2O_5$ $[M+H]^+$: 733.3636; found: 733.3627.

2-Methoxybenzyl-2,3,4,6-tetra-O-benzyl-D-galactonoamidine (28d): Meerwein's salt (0.07 g, 0.4 mmol, 1.6 equiv) and galactothionolactam (0.13 g, 0.24 mmol) in 4 mL of dichloromethane; 2-methoxybenzylamine (0.13 g, 0.61 mmol, 2.0 equiv); reaction time 63 h; silica gel chromatography cyclohexane/ethyl acetate = 1/0-10/1-4/1, v/v) compound **28d** (0.05 g, 0.08 mmol, 32%); yellow oil. R_f 0.15 (SiO_2, hexane/ethyl acetate = 2/1 v/v); $[\alpha]^{24}_D$ +4.68 (*c* 1.40, CH_2Cl_2); ^{1}H NMR (400.15 MHz, CD_2Cl_2) δ 7.20 - 7.49 (m, 22H), 6.86 - 6.96 (m, 2H), 4.97 (d, *J* = 11.00 Hz, 1H), 4.91 (d, *J* = 11.37 Hz, 1H), 4.86 (d, *J* = 11.74 Hz, 1H), 4.68 - 4.72 (m, 1H), 4.63 - 4.68 (m, 2H), 4.61 (s, 2H), 4.33 - 4.38 (m, 2H), 4.01 (dd, *J* = 1.83, 9.72 Hz, 1H), 3.78 - 3.86 (m, 1H), 3.66 - 3.76 (m, 5H), 1.29 (s); ^{13}C NMR (100.6 MHz, CD_2Cl_2) δ 158.2, 156.4, 139.7, 139.4, 138.9, 138.8, 129.9, 129.0 (2), 128.9, 128.7, 128.5 (2), 128.4, 128.3 (2), 128.2, 128.1, 128.0, 120.8, 110.8, 82.3, 76.2, 75.2, 74.6, 74.2, 73.8, 72.0, 71.6, 60.0, 55.7, 41.0; ν_{max} (FT-IR): 3445, 3033, 2911, 2848, 1640, 1493, 1455, 1238, 1084, 1023, 737, 699. HRMS (ESI) calculated for $C_{42}H_{44}N_2O_5$ $[M+H]^+$: 657.3323; found 657.3325.

3-Methoxybenzyl-2,3,4,6-tetra-O-benzyl-D-galactonoamidine (28e): Meerwein's salt (0.15 g, 0.77 mmol, 1.5 equiv) and galactothionolactam (0.28 g, 0.51 mmol) in 6 mL of dichloromethane; 3-methoxybenzylamine (0.15 g, 1.1 mmol, 2.0 equiv); reaction time 14 h; basic alumina chromatography cyclohexane/ethyl acetate = 1/0-5/1-2/1, v/v) compound **28e** (0.13 g, 0.20 mmol, 39%); yellow oil. R_f 0.19 (SiO_2, hexane/ethyl acetate = 2/1 v/v); $[\alpha]^{24}_D$ +9.80 (*c* 2.05, $CHCl_3$) ^{1}H NMR (400.15 MHz, CD_2Cl_2) δ 7.24 - 7.45 (m, 21H), 7.15 - 7.24 (m, 1H), 6.71 - 6.84

(m, 3H), 4.94 (d, *J* = 11.00 Hz, 1H), 4.89 (d, *J* = 11.37 Hz, 1H), 4.84 (d, *J* = 11.55 Hz, 1H), 4.60 - 4.69 (m, 3H), 4.54 - 4.59 (m, 2H), 4.51 - 4.55 (m, 1H), 4.32 (s, 1H), 4.27 (d, *J* = 4.77 Hz, 2H), 3.99 (dd, *J* = 1.74, 9.63 Hz, 1H), 3.60 - 3.78 (m, 6H), 1.28 (s); ^{13}C NMR (100.6 MHz, CD_2Cl_2) δ 160.4, 156.4, 142.0, 139.7, 139.4, 138.9, 138.7, 129.9, 129.1, 129.0, 128.9, 128.8, 128.6, 128.5, 128.4, 128.4, 128.2, 128.1, 128.0, 120.3, 113.4, 113.1, 82.5, 76.1, 75.3, 74.7, 74.3, 73.8, 72.0, 71.7, 60.0, 55.6, 45.3. ν_{max} (FT-IR): 3427, 3018, 2857, 1695, 1628, 1477, 1444, 1268, 1076, 724, 691. HRMS (ESI) calcd for $C_{42}H_{44}N_2O_5$ $[M+H]^+$: 657.3323; found 657.3333.

4-Butoxybenzyl-2,3,4,6-tetra-O-benzyl-D-galactonoamidine (28f): Meerwein's salt (0.10 g, 0.53 mmol, 1.5 equiv) and galactothionolactam (0.20 g, 0.36 mmol) in 3 mL of dichloromethane; 4-butoxybenzylamine (0.13 g, 0.73 mmol, 2.0 equiv); reaction time 96 h; silica gel chromatography hexane/ethyl acetate = 10/1-4/1, v/v); compound **28f** (0.10 g, 0.14 mmol, 40%); yellow oil. R_f 0.17 (SiO_2, hexane/ethyl acetate = 2/1 v/v); $[\alpha]^{24}_D$ +10.8 (*c* 0.88, $CHCl_3$); ^{1}H NMR (400.15 MHz, CD_2Cl_2) δ 7.22 - 7.44 (m, 20H), 7.08 - 7.14 (m, 2H), 6.78 - 6.82 (m, 2H), 4.93 (d, *J* = 11.00 Hz, 1H), 4.84 (dd, *J* = 10.00, 11.46 Hz, 2H), 4.60 - 4.68 (m, 3H), 4.56 (s, 2H), 4.50 (d, *J* = 9.54 Hz, 1H), 4.31 (t, *J* = 1.93 Hz, 1H), 4.12 - 4.25 (m, 2H), 3.99 (d, *J* = 2.02 Hz, 1H), 3.91 - 3.97 (m, 3H), 3.60 - 3.77 (m, 3H), 1.70 - 1.80 (m, 2H), 1.44 - 1.55 (m, 2H), 0.95 - 1.01 (m, 3H), 1.28 (s); ^{13}C NMR (100.6 MHz, CD_2Cl_2) δ 158.9, 156.4, 139.7, 139.4, 138.9, 138.6, 132.0, 129.5, 129.1, 129.0, 128.9, 128.8, 128.6, 128.5, 128.4, 128.3, 128.2, 128.1, 128.0, 114.9, 82.3, 76.0, 75.2, 74.6, 74.2, 73.8, 71.9, 71.6, 68.3, 60.0, 44.9, 31.9, 19.8, 14.2. ν_{max} (FT-IR) 3430, 3037, 2872, 1652, 1502, 1455, 1235, 1092, 739, 675. HRMS: calcd for $C_{45}H_{50}N_2O_5$ $[M+H]^+$: 699.3792; found: 699.3785.

4-(Piperidin-1-yl)benzyl-2,3,4,6-tetra-O-benzyl-D-galactonoamidine (28g): Meerwein's salt (0.06 g, 0.3 mmol, 1.5 equiv) and galactothionolactam (0.12 g, 0.22 mmol) in 2 mL of dichloromethane; 4-(piperidin-1-yl)benzylamine (0.08 g, 0.4 mmol, 1.9 equiv); reaction time 136 h; silica gel column chromatography (hexane/ethyl acetate = 1/0-10/1-4/1-1/1, v/v) compound **28g** (0.0464 g, 0.0654 mmol, 30%); yellow oil. R_f 0.19 (SiO_2, hexane/ethyl acetate = 1/1 v/v); $[\alpha]^{21}_D$ +5.76 (*c* 0.63, $CHCl_3$); ^{1}H NMR (400.15 MHz, CD_2Cl_2) δ 7.16 - 7.44 (m, 19H), 6.99 - 7.12 (m, 2H), 6.74 - 6.89 (m, 2H), 4.92 (d, *J* = 11.19 Hz, 1H), 4.84 (d, *J* = 6.97 Hz, 1H), 4.81 (d, *J* = 7.34 Hz, 1H), 4.59 - 4.66 (m, 3H), 4.54 - 4.57 (m, 2H), 4.46 - 4.51 (m, 1H), 4.30 (t, *J* = 2.02 Hz, 1H), 4.08 - 4.22 (m, 2H), 3.97 (dd, *J* = 1.93, 9.63 Hz, 1H), 3.57 - 3.78 (m, 3H), 3.04 - 3.17 (m, 4H), 1.69 (td, *J* = 5.59, 11.19 Hz, 4H), 1.49 - 1.63 (m, 2H), 1.30 (s), 1.03 (s); ^{13}C NMR (100.6 MHz, CD_2Cl_2) δ 156.3, 152.1, 139.8, 139.4, 138.9, 138.7, 130.4, 129.0, 129.0, 128.9, 128.7, 128.6, 128.5, 128.4, 128.4, 128.3, 128.2, 128.1, 128.0, 116.9, 82.4, 76.1, 75.2, 74.7, 74.1, 73.8, 72.0, 71.6, 60.0, 51.3, 46.9, 45.0, 26.5, 24.9; ν_{max} (FT-IR): 3021, 2933, 2854, 1659, 1510, 1457, 1335, 1238, 1088, 737, 684. HRMS (ESI) calculated for $C_{46}H_{51}N_3O_4$ $[M+H]^+$: 710.3958; found 710.3964.

2-(3-Indolyl)ethyl-2,3,4,6-tetra-O-benzyl-D-galactonoamdine (28h): Meerwein's salt (0.15 g, 0.81 mmol, 1.5 equiv) and galactothionolactam (0.30 g, 0.54 mmol) in 4 mL of dichloromethane; 2-(3-indolyl)ethylamine (0.18 g, 1.1 mmol, 2.1 equiv); reaction time 35 h; silica gel column chromatography (cyclohexane/ethyl acetate = 1/0-10/1-4/1, v/v) compound **28h** (0.19 g, 0.28 mmol, 52%); colorless foam. R_f 0.09 (SiO_2, hexane/ethyl acetate = 2/1 v/v); $[\alpha]^{18}_D$ +35.6 (*c* 0.71, $CHCl_3$); ^{1}H NMR (400.15 MHz, CD_2Cl_2) δ 7.95 (br. s., 1H), 7.58 (d, *J* = 7.89 Hz, 1H), 7.21 - 7.45 (m, 18H), 7.09 - 7.18 (m, 3H), 7.01 - 7.07 (m, 1H), 6.86 (d, *J* = 2.02 Hz, 1H), 4.88 - 4.96

(m, 1H), 4.80 (dd, *J* = 5.78, 11.46 Hz, 2H), 4.62 - 4.66 (m, 1H), 4.57 - 4.62 (m, 1H), 4.56 (s, 2H), 4.51 (d, *J* = 11.19 Hz, 1H), 4.42 (d, *J* = 9.17 Hz, 1H), 4.24 - 4.33 (m, 1H), 3.93 (dd, *J* = 1.83, 9.72 Hz, 1H), 3.76 (dd, *J* = 3.94, 7.06 Hz, 1H), 3.59 - 3.72 (m, 2H), 3.43 (t, *J* = 6.69 Hz, 2H), 2.89 (t, *J* = 6.88 Hz, 2H) 1.28 (s, 1H); ^{13}C NMR (100.6 MHz, CD_2Cl_2) δ 156.6, 139.8, 139.3, 138.9, 138.7, 136.9, 129.0, 128.9, 128.9, 128.8, 128.6, 128.6, 128.4, 128.3, 128.2, 128.1, 128.0, 122.7, 122.3, 119.6, 119.3, 113.8, 111.6, 82.3, 76.2, 75.3, 74.6, 74.2, 73.8, 71.9, 71.6, 60.0, 41.4, 25.2. ν_{max} (FT-IR): 3062, 2923, 2838, 1630, 1506, 1444, 1367, 1090, 728, 697. HRMS (ESI) calculated for $C_{44}H_{45}N_3O_4$ $[M+H]^+$: 680.3483; found 680.3482.

2,2'Diphenylethyl-2,3,4,6-tetra-O-benzyl-D-galactonoamidine (28i): Meerwein's salt (0.08 g, 0.4 mmol, 1.6 equiv) and galactothionolactam (0.15 g, 0.27 mmol) in 3 mL of dichloromethane; 2,2'-diphenylethylamine (0.11 g, 0.56 mmol, 2.1 equiv); reaction time 87 h; silica gel chromatography (cyclohexane/ethyl acetate = 1/0-10/1- 4/1, v/v) compound **28i** (0.11 g, 0.15 mmol, 57%); yellow oil. R_f 0.39 (SiO_2, hexane/ethyl acetate = 1/1 v/v); $[\alpha]^{24}_D$ +22.9 (*c* 1.17, $CHCl_3$); ^{1}H NMR (400.15 MHz, CD_2Cl_2) δ 7.16 - 7.47 (m, 26H), 6.95 (dd, *J* = 1.56, 7.61 Hz, 2H), 4.91 (d, *J* = 11.00 Hz, 1H), 4.80 (d, *J* = 11.74 Hz, 1H), 4.70 (d, *J* = 11.00 Hz, 1H), 4.59 - 4.65 (m, 2H), 4.57 (s, 2H), 4.41 - 4.48 (m, 1H), 4.35 (d, *J* = 9.54 Hz, 1H), 4.29 (t, *J* = 1.93 Hz, 1H), 4.12 - 4.22 (m, 1H), 3.91 (dd, *J* = 1.83, 9.72 Hz, 1H), 3.59 - 3.82 (m, 4H), 1.28 (s); ^{13}C NMR (100.6 MHz, CD_2Cl_2) δ 156.3, 143.4, 143.2, 139.8, 139.4, 138.9, 138.4, 129.2, 129.1, 129.0, 128.9, 128.7 (2), 128.6, 128.5 (2), 128.4, 128.3 (2), 128.2, 128.1, 128.0, 127.1, 127.1, 82.4, 75.8, 75.2, 74.6, 74.2, 73.8, 72.0, 71.6, 60.0, 50.7, 45.6. ν_{max} (FT-IR): 3428, 3027, 2926, 2857, 1650, 1487, 1463, 1084, 1022, 728, 704. HRMS calcd for $C_{48}H_{48}N_2O_4$ $[M+H]^+$: 717.3687; found 717.3699.

2-Naphthylmethyl-2,3,4,6-tetra-O-benzyl-D-galactonoamidine (28j): Meerwein's salt (0.08 g, 0.4 mmol, 1.5 equiv) and galactothionolactam (0.16 g, 0.29 mmol) in 2 mL of dichloromethane; 2-napthalenemethanamine (0.09 g, 0.6 mmol, 2.0 equiv); reaction time 89 h; silica gel column chromatography (cyclohexane/ethyl acetate = 1/0-10/1-4/1, v/v) compound **28j** (0.0633 g, 0.0935 mmol, 32%); yellow oil. R_f 0.13 (SiO_2, hexane/ethyl acetate = 2/1 v/v); $[\alpha]^{24}_D$ +13.2 (*c* 1.03, $CHCl_3$) ^{1}H NMR (400.15 MHz, CD_2Cl_2) δ 7.72 - 7.87 (m, 4H), 7.65 (s, 1H), 7.40 - 7.50 (m, 5H), 7.20 - 7.40 (m, 19H), 4.95 (d, *J* = 11.19 Hz, 1H), 4.89 (d, *J* = 11.37 Hz, 1H), 4.84 (d, *J* = 11.74 Hz, 1H), 4.61 - 4.70 (m, 3H), 4.52 - 4.59 (m, 3H), 4.44 - 4.49 (m, 2H), 4.30 - 4.36 (m, 1H), 4.01 (dd, *J* = 1.83, 9.54 Hz, 1H), 3.70 - 3.78 (m, 2H), 3.61 - 3.68 (m, 1H), 1.28 (s); ^{13}C NMR (100.6 MHz, CD_2Cl_2) δ 156.5, 139.8, 139.4, 138.9, 134.0, 133.2, 129.1, 129.0, 128.9, 128.8, 128.6, 128.5, 128.5, 128.4, 128.4, 128.2, 128.1, 128.1, 128.0, 126.7, 126.5, 126.4, 126.1, 82.4, 76.1, 75.3, 74.7, 74.3, 73.8, 71.9, 71.7, 60.0, 45.5. ν_{max} (FT-IR): 3439, 3067, 3010, 2914, 2858, 1638, 1500, 1444, 1096, 732, 684. HRMS (ESI) calculated for $C_{45}H_{44}N_2O_5$ $[M+H]^+$: 677.3374; found 677.3372.

4-Phenylbenzyl-2,3,4,6-tetra-O-benzyl-D-galactonoamidine (28k): Meerwein's salt (0.11 g, 0.58 mmol, 1.5 equiv) and galactothionolactam (0.21 g, 0.38 mmol) in 3 mL of acetonitrile; 4-phenylbenzylamine (0.17 g, 0.93 mmol, 2.4 equiv); reaction time 115 h; basic alumina column chromatography (hexane/ethyl acetate = 1/0-4/1-1/1, v/v) compound **28k** (0.08 g, 0.1 mmol, 30%); yellow oil. R_f 0.10 (SiO_2, hexane/ethyl acetate = 2/1 v/v); $[\alpha]^{18}_D$ +13.4 (*c* 0.62, $CHCl_3$); ^{1}H NMR (400.15 MHz, CD_2Cl_2) δ 7.58 - 7.63 (m, 2H), 7.51 - 7.55 (m, 2H), 7.45 - 7.48 (m, 2H), 7.41 - 7.44 (m, 3H), 7.25 - 7.40 (m, 21H), 4.95 (d, *J* = 11.00 Hz, 1H), 4.90 (d, *J* = 11.37 Hz, 1H), 4.85 (d, *J* = 11.55 Hz, 1H), 4.68 (d, *J* = 2.57 Hz, 1H), 4.62 - 4.67 (m, 2H), 4.53 - 4.58 (m, 3H),

4.30 - 4.36 (m, 3H), 4.00 (dd, *J* = 1.83, 9.54 Hz, 1H), 3.69 - 3.78 (m, 2H), 3.61 - 3.68 (m, 1H), 1.28 (s); ^{13}C NMR (100.6 MHz, CD_2Cl_2) δ 156.4, 141.4, 140.3, 139.7, 139.5, 139.4, 138.9, 138.7, 129.3, 129.1, 129.0, 128.9, 128.8, 128.7, 128.6, 128.5, 128.5, 128.4, 128.4, 128.2, 128.1, 128.0, 127.8, 127.6, 127.5, 82.4, 76.0, 75.3, 74.6, 74.4, 73.8, 71.9, 71.7, 60.0, 45.0;. ν_{max} (FT-IR): 3449, 3011, 2869, 1658, 1490, 1335, 1090, 755, 716. HRMS (ESI) calculated for $C_{47}H_{47}N_2O_4$ $[M+H]^+$: 703.3536; found 703.3530.

4-(4'-Methylphenyl)benzyl-2,3,4,6-tetra-O-benzyl-D-galactonoamidine (28l): Meerwein's salt (0.11 g, 0.579 mmol, 1.5 equiv) and galactothionolactam (0.22 g, 0.40 mmol) in 3 mL of acetonitrile; 4-(4'-methylphenyl)benzylamine (0.17 g, 0.86 mmol, 2.2 equiv); reaction time 115 h; basic alumina column chromatography (hexane/ethyl acetate = 8/1-4/1, v/v) compound **28l** (0.10 g, 0.14 mmol, 35%); yellow oil. R_f 0.21 (SiO_2, hexane/ethyl acetate = 1/1 v/v); $[\alpha]^{20}_D$ +7.05 (*c* 0.55, $CHCl_3$) ^{1}H NMR (400.15 MHz, CD_2Cl_2) δ 7.46 - 7.52 (m, 4H), 7.23 - 7.43 (m, 24H), 4.94 (d, *J* = 11.00 Hz, 1H), 4.88 (d, *J* = 11.37 Hz, 1H), 4.84 (d, *J* = 11.74 Hz, 1H), 4.64 (dd, *J* = 9.26, 11.10 Hz, 3H), 4.51 - 4.57 (m, 3H), 4.28 - 4.35 (m, 2H), 3.99 (dd, *J* = 1.83, 9.72 Hz, 1H), 3.68 - 3.76 (m, 2H), 3.57 - 3.67 (m, 1H), 2.32 - 2.45 (m, 3H); ^{13}C NMR (100.6 MHz, CD_2Cl_2) δ 156.3, 140.2, 139.7, 139.4, 139.2, 138.9, 138.7, 138.5, 137.7, 130.0, 129.2, 129.1, 129.0, 128.9, 128.8, 128.7, 128.6, 128.5, 128.4, 128.4, 128.3, 128.3, 128.2, 128.1, 128.0, 127.3, 127.3, 82.5, 76.1, 75.3, 74.7, 74.3, 73.8, 72.0, 71.7, 60.1, 45.0, 21.4; ν_{max} (FT-IR): 3435, 3031, 2863, 2613, 1649, 1496, 1450, 1208, 1090, 728, 696, 639. HRMS (ESI) calculated for $C_{48}H_{49}N_2O_4$ $[M+H]^+$: 717.3692; found 717.3675.

4-(4'-Fluorophenyl)benzyl-2,3,4,6-tetra-O-benzyl-D-galactonoamidine (28m): Meerwein's salt (0.08 g, 0.4 mmol, 1.7 equiv) and galactothionolactam (0.14 g, 0.25 mmol) in 2 mL of acetonitrile; 4-(4'-fluorophenyl)benzylamine (0.10 g, 0.50 mmol, 2.0 equiv); reaction time 23 h; basic alumina column chromatography (hexane/ethyl acetate = 1/0-10/1-4/1, v/v) compound **28m** (0.0334 g, 0.0464 mmol, 18%); yellow oil. R_f 0.10 (SiO_2, hexane/ethyl acetate = 2/1 v/v); $[\alpha]^{20}_D$ +12.4 (*c* 0.75, $CHCl_3$); ^{1}H NMR (400.15 MHz,CD_2Cl_2) δ 7.55 - 7.60 (m, 2H), 7.46 - 7.50 (m, 2H), 7.41 - 7.45 (m, 2H), 7.26 - 7.40 (m, 20H), 7.12 - 7.19 (m, 2H), 4.95 (d, *J* = 11.00 Hz, 1H), 4.91 (d, *J* = 11.37 Hz, 1H), 4.85 (d, *J* = 11.74 Hz, 1H), 4.62 - 4.69 (m, 4H), 4.52 - 4.60 (m, 4H), 4.28 - 4.39 (m, 4H), 4.01 (dd, *J* = 1.83, 9.54 Hz, 1H), 3.68 - 3.77 (m, 2H), 3.61 - 3.68 (m, 1H); ^{13}C NMR (100.6 MHz, CD_2Cl_2) δ 163.0 (d, *J* = 245.4 Hz), 156.3, 139.7, 139.5, 139.4, 139.2, 138.9, 138.7, 137.7 (d, *J* = 3.2 Hz), 129.2, 129.1, 129.0, 128.9, 128.8, 128.7, 128.5, 128.4, 128.4, 128.3, 128.2, 128.2, 128.1 (d, *J* = 4.4 Hz), 127.4, 116.1 (d, *J* = 21.5 Hz), 82.5, 76.1, 75.3, 74.7, 74.4, 73.8, 71.9, 71.7, 60.0, 45.0. ν_{max} (FT-IR): 3420, 3034, 2859, 1646, 1498, 1222, 1084, 809, 735, 698. HRMS (ESI) calculated for $C_{47}H_{46}N_2O_4$ $[M+H]^+$: 721.3442; found 721.3443.

4-(2-Phenylmethoxy)benzyl-2,3,4,6-tetra-O-benzyl-D-galactonoamidine (28n) : Meerwein's salt (0.07 g, 0.4 mmol, 1.5 equiv) and galactothionolactam (0.14 g, 0.25 mmol) in 2 mL of acetonitrile; 4-(2-phenylmethyoxy)benzylamine (0.10 g, 0.39 mmol, 2.1 equiv); reaction time 94 h; silica gel column chromatography (hexane/ethyl acetate = 1/0-4/1-1/2, v/v) compound **28n** (0.0436 g, 0.0560 mmol, 22%); yellowish oil. R_f 0.07 (SiO_2, hexane/ethyl acetate = 2/1 v/v); $[\alpha]^{21}_D$ +6.80 (*c* 0.68, $CHCl_3$); ^{1}H NMR (400.15 MHz, CD_2Cl_2) δ 7.21 - 7.43 (m, 25H), 7.09 - 7.14 (m, 2H), 6.80 - 6.86 (m, 2H), 4.93 (d, *J* = 11.00 Hz, 1H), 4.80 - 4.88 (m, 2H), 4.63 - 4.67 (m, 2H), 4.59 - 4.62 (m, 3H), 4.56 (s, 2H), 4.50 (d, *J* = 9.72 Hz, 1H), 4.31 (t, *J* = 1.93 Hz, 1H),

4.16 - 4.25 (m, 2H), 4.10 - 4.15 (m, 2H), 3.97 (dd, *J* = 1.83, 9.72 Hz, 1H), 3.80 - 3.84 (m, 2H), 3.59 - 3.76 (m, 3H); ^{13}C NMR (100.6 MHz, CD_2Cl_2) δ 158.5, 156.3, 139.7, 139.4, 139.0, 138.9, 138.7, 132.6, 129.5, 129.1, 129.0, 128.9, 128.9, 128.8, 128.6, 128.5, 128.4, 128.3, 128.3, 128.2, 128.1, 128.1, 128.0, 115.0, 82.4, 76.0, 75.2, 74.7, 74.2, 73.8, 73.8, 72.0, 71.6, 69.3, 68.1, 60.0, 44.8. ν_{max} (FT-IR): 3439, 3043, 2915, 2838, 1645, 1503, 1461, 1240, 1091, 745, 697. HRMS (ESI) calculated for $C_{50}H_{53}N_2O_6$ $[M+H]^+$: 777.3904; found 777.3891.

4-(Cyclohexylmethoxy)benzyl-2,3,4,6-tetra-O-benzyl-D-galactonoamidine (28o):

Meerwein's salt (0.11 g, 0.60 mmol, 1.5 equiv) and galactothionolactam (0.22 g, 0.40 mmol) in 3 mL of acetonitrile; 4-(cyclohexyl methoxy)benzylamine (0.17 g, 0.78 mmol, 2.0 equiv); reaction time 23 h; basic alumina column chromatography (hexane/ethyl acetate = 1/0-10/1-4/1 v/v) compound **28o** (0.0912 g, 0.123 mmol, 31%); yellow oil. R_f 0.26 (SiO_2, hexane/ethyl acetate = 1/1 v/v); $[\alpha]^{20}_D$ +8.50 (*c* 0.66, $CHCl_3$); ^{1}H NMR (400.15 MHz, CD_2Cl_2) δ 7.20 - 7.46 (m, 24H), 7.08 - 7.16 (m, 2H), 6.73 - 6.86 (m, 2H), 4.94 (d, *J* = 11.00 Hz, 2H), 4.85 (dd, *J* = 8.71, 11.46 Hz, 2H), 4.60 - 4.68 (m, 4H), 4.54 - 4.60 (m, 3H), 4.48 - 4.53 (m, 1H), 4.32 (t, *J* = 1.93 Hz, 1H), 4.14 - 4.25 (m, 2H), 3.98 (dd, *J* = 1.83, 9.72 Hz, 1H), 3.59 - 3.79 (m, 7H), 1.83 - 1.94 (m, 3H), 1.66 - 1.82 (m, 6H), 1.19 - 1.40 (m, 5H), 1.00 - 1.14 (m, 3H); ^{13}C NMR (100.6 MHz, CD_2Cl_2) δ 159.0, 156.2, 139.8, 139.4, 138.9, 138.7, 132.1, 129.4, 129.1, 129.0, 128.9, 128.8, 128.6, 128.5, 128.4, 128.3, 128.2, 128.1, 128.0, 114.9, 82.4, 76.1, 75.2, 74.7, 74.2, 74.1, 73.8, 72.0, 71.6, 60.1, 44.9, 38.3, 30.5, 27.2, 26.4; ν_{max} (FT -IR): 3028, 2916, 2838, 1634, 1498, 1239, 1081, 733. HRMS (ESI) calculated for $C_{48}H_{55}N_2O_5$ $[M+H]^+$: 739.4111; found 739.4108.

***O*-Benzylethanol-2,3,4,6-tetra-O-benzyl-D-galactonoamidine (28p)**: Meerwein's salt (0.07 g, 0.4 mmol, 1.6 equiv) and galactothionolactam (0.13 g, 0.24 mmol) in 2 mL of acetonitrile; *O*-benzylethanolamine (0.07 g, 0.5 mmol, 2.0 equiv); reaction time 97 h; silica gel column chromatography (hexane/ethyl acetate = 4/1-1/1, v/v) compound **28p** (0.0436 g, 0.0650 mmol, 22%); yellow oil. R_f 0.21 (SiO_2, hexane/ethyl acetate = 1/1 v/v); $[\alpha]^{21}_D$ +32.1 (*c* 0.58, $CHCl_3$); ^{1}H NMR (400.15 MHz, CD_2Cl_2) δ 7.02 - 7.53 (m, 25H), 4.92 (d, *J* = 11.00 Hz, 1H), 4.87 (d, *J* = 11.19 Hz, 1H), 4.82 (d, *J* = 11.74 Hz, 1H), 4.63 (td, *J* = 5.43, 10.96 Hz, 3H), 4.53 - 4.57 (m, 2H), 4.45 - 4.51 (m, 3H), 4.29 (t, *J* = 2.02 Hz, 1H), 3.95 (dd, *J* = 1.93, 9.63 Hz, 1H), 3.58 - 3.73 (m, 3H), 3.46 - 3.57 (m, 2H), 3.20 - 3.43 (m, 2H); ^{13}C NMR (100.6 MHz, CD_2Cl_2) δ 156.5, 139.7, 139.4, 139.1, 138.9, 138.7, 129.0, 129.0, 128.9, 128.8, 128.7, 128.6, 128.5, 128.4, 128.3, 128.2, 128.1, 128.1, 128.0, 82.3, 76.0, 75.2, 74.7, 74.2, 73.8, 73.4, 71.9, 71.6, 69.4, 60.0, 41.1; . ν_{max} (FT-IR): 3024, 2947, 2862, 1646, 1499, 1464, 1361, 1087, 736, 703. HRMS (ESI) calculated for $C_{43}H_{47}N_2O_5$ $[M+H]^+$: 671.3485; found 671.3470.

4.8: General procedure for the synthesis of galactonoamidines

The perbenzylated galactonoamidines were suspended with palladium (30 wt % on activated carbon) and 5/1 v/v mixture of ethanol and trifluoroacetic acid and stirred under hydrogen atmosphere at ambient temperature. After 16-24 h, the mixture was filtered through a pad of Celite. The pad was rinsed with 2 mL of ethanol three times. The combined filtrated were concentrated under reduced pressure to about 2 mL. Centrifuged at 8500 rpm for 10-15 minutes, concentrated to form a residue which was lyophilized to obtain the desired amidines.

2-Hydroxybenzyl-D-galactonoamidine (16k): Compound **28a** (0.0588 g, 0.0802 mmol), Pd/C (0.05 g) in 0.8 mL of trifluoroacetic acid and 4 mL of ethanol; reaction time 40 h; ethanol amount for rinsing 2 mL each; compound **16k** (0.0221 g, 0.0783 mmol, 98%); yellow foam. R_f =

0.23 (SiO_2, ethyl acetate/methanol = 5/1 v/v); $[\alpha]^{23}_D$ +25.0 (*c* 0.68, H_2O) ^1H NMR (400.15 MHz, D_2O + MeOD) δ 7.27 - 7.37 (m, 2H), 6.94 - 7.04 (m, 2H), 4.52 - 4.62 (m, 3H), 4.29 (s, 1H), 3.94 (dd, *J* = 2.38, 10.09 Hz, 1H), 3.86 (d, *J* = 5.50 Hz, 1H), 3.74 - 3.82 (m, 2H); ^{13}C NMR (100.6 MHz, D_2O) δ 164.7, 154.5, 131.6, 131.4, 122.0, 121.7, 116.5, 71.6, 68.0, 67.3, 61.4, 58.4, 41.1. ν_{max} (FT-IR): 3241, 2951, 1668, 1457, 1185, 1141, 842, 807, 763, 720. HRMS (ESI) calculated for $C_{13}H_{18}N_2O_5$ $[M+H]^+$: 283.1288; found 283.1293.

3-Hydroxybenzyl-D-galactonoamidine (16l): Compound **28b** (0.0914 g, 0.125 mmol), Pd/C (0.10 g) in 1.5 mL of trifluoroacetic acid and 7.5 mL of ethanol; reaction time 60 h; ethanol amount for rinsing 2 mL each; compound **16l** (0.0351 g, 0.125 mmol, 100%); yellow foam. R_f = 0.15 (SiO_2, ethyl acetate/methanol = 10/1 v/v); $[\alpha]^{21}_D$ +21.4 (*c* 0.92, H_2O); ^1H NMR (400.15 MHz, D_2O) δ 7.33 (t, *J* = 7.89 Hz, 1H), 6.81 - 6.96 (m, 3H), 4.65 - 4.70 (m, 1H), 4.61 (d, *J* = 4.40 Hz, 2H), 4.31 (t, *J* = 2.20 Hz, 1H), 4.01 (dd, *J* = 2.29, 10.18 Hz, 1H), 3.69 - 3.88 (m, 3H); ^{13}C NMR (100.6 MHz, D_2O+MeOD) δ 165.0, 157.4, 136.6, 131.6, 120.4, 116.1, 115.1, 71.3, 68.0, 67.4, 61.0, 58.3, 45.9. ν_{max} (FT-IR): 3243, 2934, 1645, 1451, 1193, 1141, 858, 793, 716. HRMS (ESI) calculated for $C_{13}H_{18}N_2O_5$ $[M+H]^+$: 283.1288; found 283.1293.

4-Hydroxybenzyl-D-galactonoamidine (16m): Compound **28c** (0.1017 g, 0.1388 mmol), Pd/C (0.11 g) in 1 mL of trifluoroacetic acid and 5 mL of ethanol; reaction time 38 h; ethanol amount for rinsing 2 mL each; compound **16m** (0.0370 g, 0.131 mmol, 94%); colorless foam. R_f = 0.29 (SiO_2, ethyl acetate/methanol = 5/1 v/v); $[\alpha]^{24}_D$ +17.4 (*c* 1.00, H_2O); ^1H NMR (400.15 MHz, D_2O) δ 7.27 (d, *J* = 8.44 Hz, 2H), 6.79 - 7.05 (m, 2H), 4.64 (d, *J* = 10.27 Hz, 1H), 4.57 (d, *J* = 2.57 Hz, 1H), 4.32 (t, *J* = 2.20 Hz, 1H), 4.00 (dd, *J* = 2.38, 10.09 Hz, 1H), 3.71 - 3.88 (m, 3H);

^{13}C NMR (100.5 MHz, D_2O) δ 165.6, 157.2, 130.9, 127.2, 117.7, 72.2, 68.6, 68.0, 61.7, 58.9, 46.4. ν_{max} (FT-IR): 3255, 1655, 1130, 799, 722, 593. HRMS calcd for $C_{13}H_{18}N_2O_5$ $[M+H]^+$: 283.1288; found 283.1285.

Ethanol-D-galactonoamidine (16n): Compound **28p** (0.1008 g, 0.1736 mmol), Pd/C (0.11 g) in 2.5 mL of trifluoroacetic acid and 5 mL of ethanol; reaction time 24 h; ethanol amount for rinsing 2 mL each; compound **16n** (0.0386 g, 0.175 mmol, 99%); colorless foam. R_f = 0.61 (SiO_2, ethyl acetate/methanol = 5/1 v/v); $[\alpha]^{23}_D$ +19.1 (*c* 0.96, H_2O); ^{1}H NMR (400.15 MHz, D_2O) δ 4.63 (d, *J* = 10.27 Hz, 1H), 4.29 - 4.36 (m, 1H), 4.00 (dd, *J* = 2.38, 10.27 Hz, 1H), 3.78 - 3.90 (m, 6H), 3.53 - 3.61 (m, 2H); ^{13}C NMR (100.6 MHz, D_2O) δ 167.0, 72.2, 68.6, 68.1, 61.8, 61.3, 58.8, 46.2. ν_{max} (FT-IR): 3350, 1668, 1202, 1169. HRMS (ESI) calcd for $C_8H_{16}N_2O_5$ $[M+H]^+$: 221.1132; found 221.1128.

2-Methoxybenzyl-D-galactonoamidine (16o): Compound **28d** (0.0543 g, 0.0827 mmol), Pd/C (0.05 g) in 0.8 mL of trifluoroacetic acid and 4 mL of ethanol; reaction time 40 h; ethanol amount for rinsing 2 mL each; compound **16o** (0.0245 g, 0.0827 mmol, quantitative); yellow foam. R_f = 0.19 (SiO_2, ethyl acetate/methanol = 5/1 v/v); $[\alpha]^{25}_D$ +28.8 (*c* 0.54, H_2O); ^{1}H NMR (400.15 MHz, D_2O) δ 7.33 - 7.51 (m, 2H), 7.02 - 7.18 (m, 2H), 4.53 - 4.66 (m, 3H), 4.30 (br. s., 1H), 3.85 - 3.99 (m, 5H), 3.79 (br. s., 2H); ^{13}C NMR (100.6 MHz, D_2O) δ 164.2, 157.6, 131.3, 130.8, 122.7, 122.1, 112.4, 71.3, 67.8, 67.1, 61.2, 58.2, 56.6, 41.1; ν_{max} (FT-IR): 3286, 2921, 1662, 1446, 1197, 1139, 799, 790, 716, 509. HRMS (ESI) calculated for $C_{14}H_{20}N_2O_5$ $[M+H]^+$: 297.1445; found 297.1449.

3-Methoxybenzyl-D-galactonoamidine (16p): Compound **28e** (0.1434 g, 0.2183 mmol), Pd/C (0.15 g) in 1mL of trifluoroacetic acid and 5 mL of ethanol; reaction time 36 h; ethanol amount for rinsing 2 mL each; compound **16p** (0.0647 g, 0.218 mmol, quantitative); yellow foam. R_f = 0.16 (SiO_2, ethyl acetate/methanol = 10/1 v/v); $[\alpha]^{24}_D$ +21.8 (*c* 0.72, H_2O); ^{1}H NMR (400.15 MHz, D_2O) δ 7.41 (t, *J* = 7.89 Hz, 1H), 6.95 - 7.04 (m, 3H), 4.62 - 4.70 (m, 3H), 4.32 (br. s., 1H), 4.01 (dd, *J* = 1.93, 10.00 Hz, 1H), 3.67 - 3.88 (m, 6H); ^{13}C NMR (100.6 MHz, D_2O) δ 165.9, 161.0, 137.1, 132.1, 121.5, 115.5, 114.6, 72.2, 68.6, 68.1, 61.6, 59.0, 57.0, 46.7; ν_{max} (FT-IR): 3243,1666, 1438, 1200, 1151, 849, 800, 719. HRMS (ESI) calcd for $C_{14}H_{20}N_2O_5$ $[M+H]^+$: 297.1445; found 297.1452.

4-Butoxybenzyl-D-galactonoamidine (16q): Compound **28f** (0.0905 g, 0.129 mmol), Pd/C (0.05 g) in 0.5 mL of trifluoroacetic acid and 2.mL of ethanol; reaction time 15 h; ethanol amount for rinsing 2 mL each; compound **16q** (0.0437 g, 0.129 mmol, 99%); yellow foam. R_f = 0.38 (SiO_2, ethyl acetate/methanol = 5/1 v/v); $[\alpha]^{24}_D$ +26.7 (*c* 0.82, H_2O); ^{1}H NMR (400.15 MHz, D_2O) δ 7.31 (d, *J* = 8.25 Hz, 2H), 7.01 (d, *J* = 8.44 Hz, 2H), 4.64 (d, *J* = 10.09 Hz, 1H), 4.57 (br. s., 2H), 4.30 (br. s., 1H), 4.06 (t, *J* = 6.42 Hz, 2H), 3.99 (d, *J* = 9.35 Hz, 1H), 3.65 - 3.89 (m, 3H), 1.65 - 1.82 (m, 2H), 1.43 (qd, *J* = 7.31, 14.58 Hz, 2H), 0.93 (t, *J* = 7.34 Hz, 3H); ^{13}C NMR (100.6 MHz, D_2O+MeOD) δ 165.6, 159.9, 130.7, 127.9, 116.9, 72.2, 70.1, 68.6, 68.0, 61.6, 58.9, 46.3, 32.0, 20.2, 14.6. ν_{max} (FT-IR): 3350, 1660, 1210, 1113. HRMS (ESI) calcd for $C_{17}H_{26}N_2O_5$ $[M+H]^+$: 339.1914; found 339.1909.

2,2'-Diphenylethyl-D-galactonoamidine (16r): Compound **28i** (0.1006 g, 0.1403 mmol), Pd/C (0.10 g) in 1.4 mL of trifluoroacetic acid and 7.mL of ethanol; reaction time 18 h; ethanol

amount for rinsing 2 mL each; compound **16r** (0.0483 g, 0.136 mmol, 97%); yellow foam. R_f = 0.63 (SiO_2, ethyl acetate/methanol = 10/1 v/v); $[\alpha]^{24}_D$ +21.3 (*c* 0.88, MeOH); ^{1}H NMR (400.15 MHz, MeOD) δ 7.55 - 7.71 (m, 1H), 7.16 - 7.35 (m, 5H), 4.28 - 4.41 (m, 1H), 4.05 - 4.13 (m, 1H), 3.97 - 4.04 (m, 1H), 3.63 - 3.73 (m, 1H), 3.56 - 3.62 (m, 1H), 3.24 - 3.40 (m, 2H), 2.78 - 3.02 (m, 3H); ^{13}C NMR (100.6 MHz, MeOD) δ 166.4, 142.5, 142.3, 129.9, 129.8, 129.3, 129.0, 128.3, 128.2, 72.4, 68.5, 67.8, 61.4, 59.4, 50.9, 47.1. ν_{max} (FT-IR): 3363, 2863, 1663, 1438, 1196, 1116, 834, 801, 704. HRMS (ESI) calcd for $C_{20}H_{24}N_2O_4$ $[M+H]^+$: 357.1809; found 357.1801.

4-Phenylbenzyl-D-galactonoaomamidine (16s): Compound **28k** (0.08 g, 0.1 mmol), Pd/C (0.08 g) in 1 mL of trifluoroacetic acid and 5 mL of ethanol; reaction time 41 h; ethanol amount for rinsing 2 mL each; compound **16s** (0.0390 g, 0.114 mmol, quantitative); colorless foam. R_f = 0.07 (SiO_2, ethyl acetate/methanol = 5/1 v/v); $[\alpha]_D^{20}$+25.4 (c 0.528, MeOH); ^{1}H NMR (400.15 MHz, METHANOL-d_4) δ 7.66 (d, *J* = 8.25 Hz, 2H), 7.57 - 7.63 (m, 2H), 7.39 - 7.47 (m, 4H), 7.31 - 7.36 (m, 1H), 7.24 (s, 1H), 4.65 - 4.69 (m, 2H), 4.55 - 4.64 (m, 1H), 4.20 (t, *J* = 2.48 Hz, 1H), 3.86 (dd, *J* = 2.29, 9.63 Hz, 1H), 3.78 (t, *J* = 6.51 Hz, 2H), 3.69 (dd, *J* = 2.66, 6.33 Hz, 1H), 2.37 (s); ^{13}C NMR (100.6 MHz, METHANOL-d_4) δ 166.7, 142.6, 141.6, 134.8, 129.9, 128.9, 128.6, 128.6, 127.9, 72.7, 68.7, 68.4, 61.4, 59.5, 45.9. ν_{max} (FT-IR): 3256, 2921, 1670, 1438, 1206, 1128. HRMS (ESI) *m/z* calcd for $C_{19}H_{23}N_2O_4$ $[M+H]^+$: 343.1658 found 343.1657.

2-(Octahydro-1*H*-indol-3-yl)ethyl-D-galactonoamidine (16t) Compound **28h** (60.70 mg, 0.0893 mmol), Pd/C (0.06 g) in 2.0 mL of trifluoroacetic acid and 6.0 mL of ethanol; reaction time 61 h; ethanol amount for rinsing 2 mL each; compound **16t** (0.0446 g, 0.140 mmol, 156%);

colorless foam. R_f = 0.26 (SiO_2, dichloromethane/methanol = 25/1 v/v); ^{1}H NMR (400.15 MHz, D_2O) δ 4.63 (d, *J* = 10.09 Hz, 1H), 4.38 (br. s., 1H), 4.02 (d, *J* = 10.27 Hz, 1H), 3.79 - 3.94 (m, 3H), 3.47 (d, *J* = 6.60 Hz, 3H), 2.94 - 3.18 (m, 1H), 2.21 - 2.60 (m, 1H), 1.70 (d, *J* = 10.82 Hz, 8H), 1.11 - 1.53 (m, 4H); ^{13}C NMR (100.6 MHz, D_2O) δ 164.1, 163.2, 162.8, 117.9, 115.0, 70.6, 67.2, 66.4, 63.7, 60.1, 58.6, 58.5, 57.4, 47.2, 42.0, 40.5, 40.4, 39.2, 38.7, 38.5, 36.3, 36.1, 30.3, 29.2, 27.9, 25.0, 24.5, 24.0, 23.9, 22.8, 21.8, 20.5, 20.3, 19.1; LC-MS calculated for $C_{16}H_{29}N_3O_4$ $[M+H]^+$: 328.4; found 328.3 and 356.3

***N*-4(4'-Methylphenyl)benzyl-D-galactonoamidine (16u)**: Compound **28k** (0.05 g, 0.07 mmol); Pd/C (0.05 g) in 1 mL of trifluoroacetic acid and 5 mL ethanol; reaction time 72 h; ethanol amount for rinsing 2 mL each; compound **16u** (0.0532 g, 0.155 mmol, 222%); beige foam. R_f = 0.23 (SiO_2, ethyl acetate/methanol = 5/1 v/v).

***N*-4(4'-Fluorophenyl)benzyl-D-galactonoamidine (16v)**: Compound **28m** (0.0334 g, 0.0463 mmol); Pd/C (0.03 g) in 0.5 mL of trifluoroacetic acid and 2.5 mL ethanol; reaction time 37 h; ethanol amount for rinsing 2 mL each; compound **16v** (0.0349 g, 0.0968 mmol, 209%); yellowish foam.

***N*-2-Napthylmethyl-D-galactonoamidine (16w)**: Compound **28j** (0.05 g, 0.074 mmol); Pd/C (0.05 g) in 0.5 mL of trifluoroacetic acid and 5 mL ethanol; reaction time 69 h; ethanol amount for rinsing 2 mL each; compound IO406 (0.0381 g, 0.1216 mmol, 164%); yellowish foam. R_f = 0.13 (SiO_2, ethyl acetate).

***N*-4-(Piperidin-1-yl)benzyl-D-galactonoamidine (16x)**: Compound **28g** (0.0464 g, 0.0654 mmol); Pd/C (0.04 g) in 0.5 mL of trifluoroacetic acid and 5 mL ethanol; reaction time 40 h; ethanol amount for rinsing 2 mL each; compound **16x** (0.0398 g, 0.1139 mmol, 174%); brown foam. R_f = 0.13 (SiO_2, ethyl acetate/methanol = 5/1 v/v)

***N*-4-Cyclohexylmethoxybenzyl-D-galactonoamidine (16y)**: Compound **28o** (0.0912 g, 0.1234 mmol); Pd/C (0.09 g) in 1 mL of trifluoroacetic acid and 5 mL ethanol; reaction time 72 h; ethanol amount for rinsing 2 mL each; compound **16y** (0.0738 g, 0.1950 mmol, 158%); yellowish foam. R_f = 0.27 (SiO_2, ethyl acetate/methanol = 5/1 v/v).

***N*-4-(2-Hydroxyethyl)benzyl-D-galactonoamidine (16z)**: Compound **28n** (0.0433 g, 0.0557 mmol); Pd/C (0.04 g) in 0.5 mL of trifluoroacetic acid and 5 mL ethanol; reaction time 25 h; ethanol amount for rinsing 2 mL each; compound **16z** (0.0385 g, 0.118 mmol, 211%); brown foam. R_f = 0.04 (SiO_2, ethyl acetate/methanol = 5/1 v/v)

5: NMR spectra of new compounds

^{1}H NMR (400.15 MHz, Acetone-d6)

Compound 29e

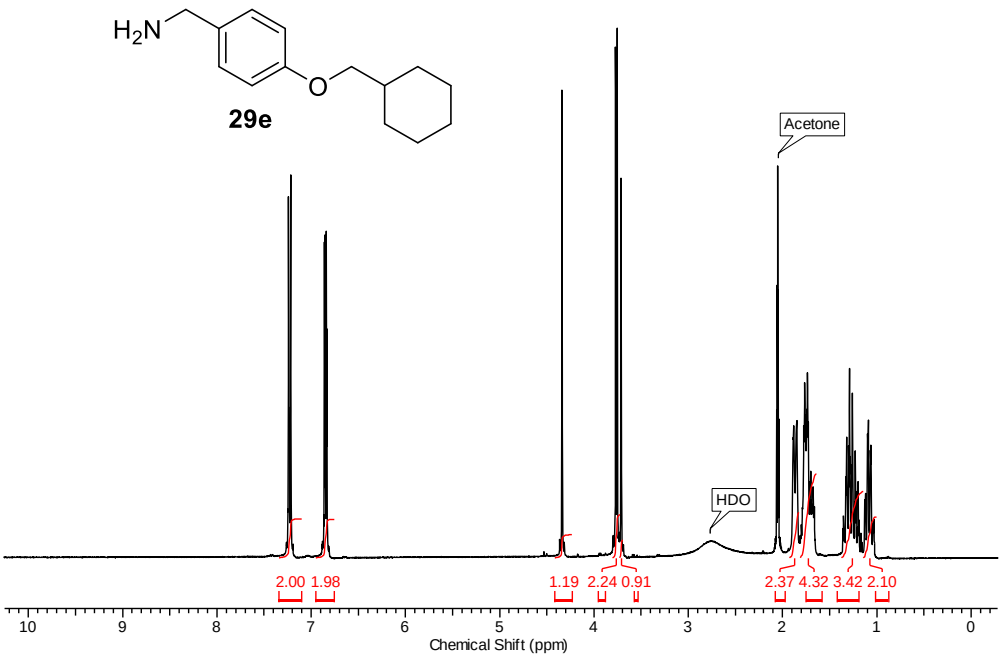

^{13}C NMR (100.6 MHz, Acetone)

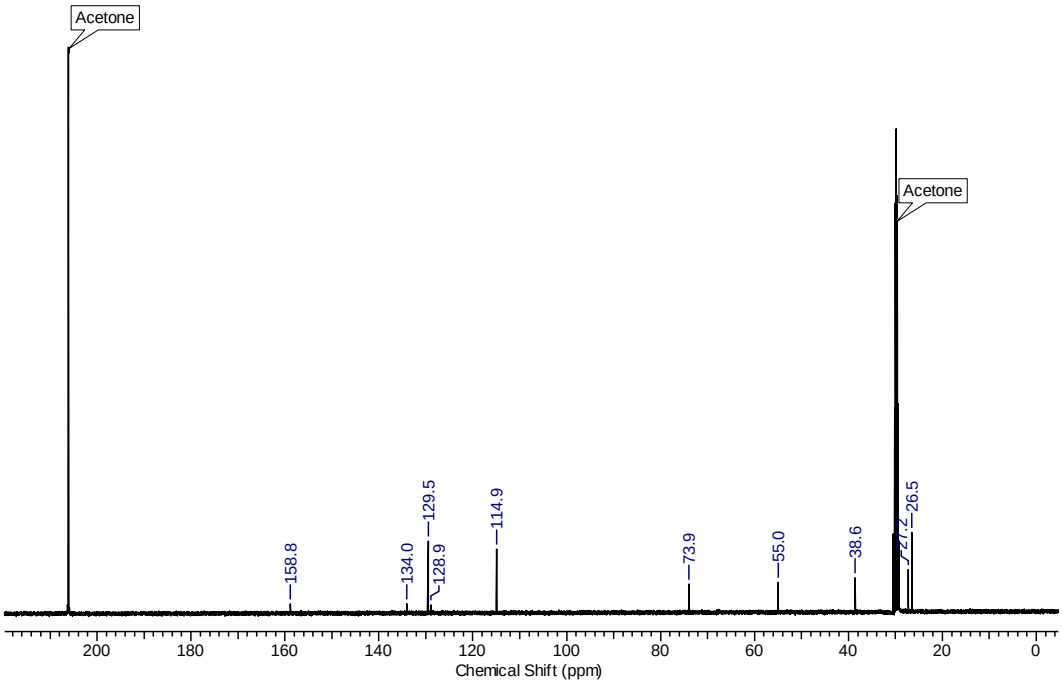

Compound 29l

^{1}H NMR (400.15 MHz, Methanol-d$_4$)

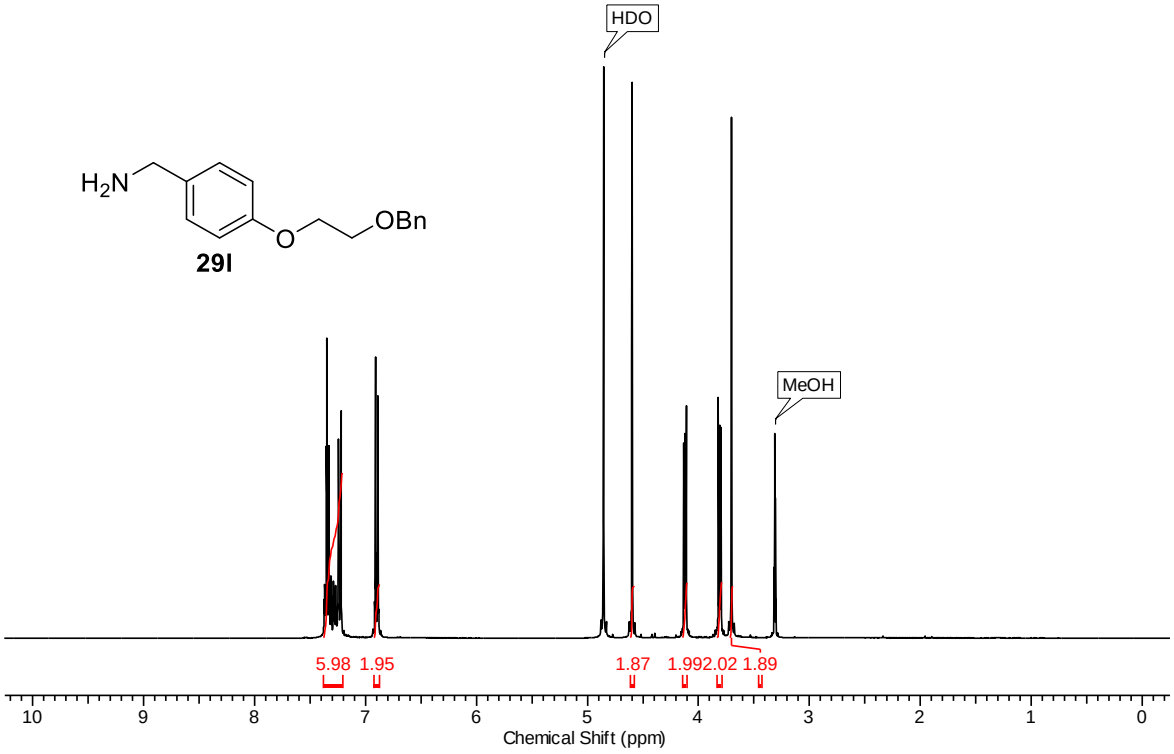

29l

^{13}C NMR (100.6 MHz, Methanol-d$_4$)

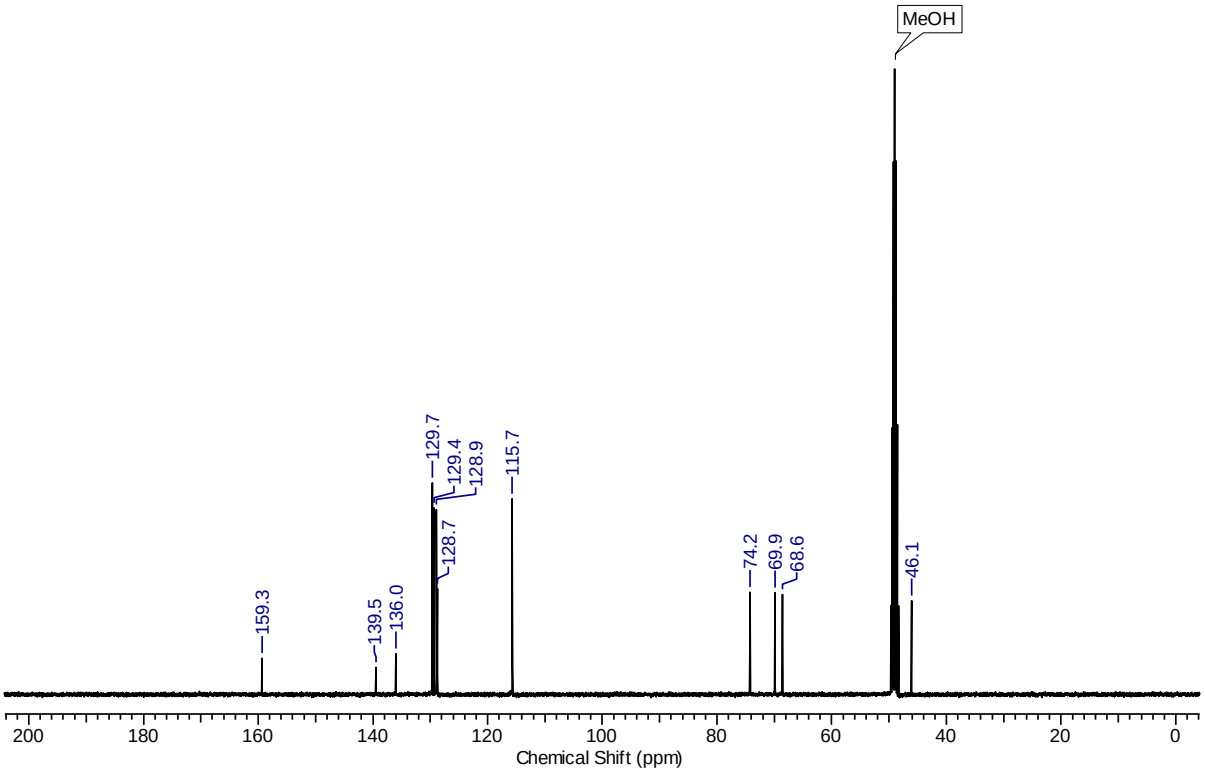

Compound 28a

^{1}H NMR (400.15 MHz, CD_2Cl_2)

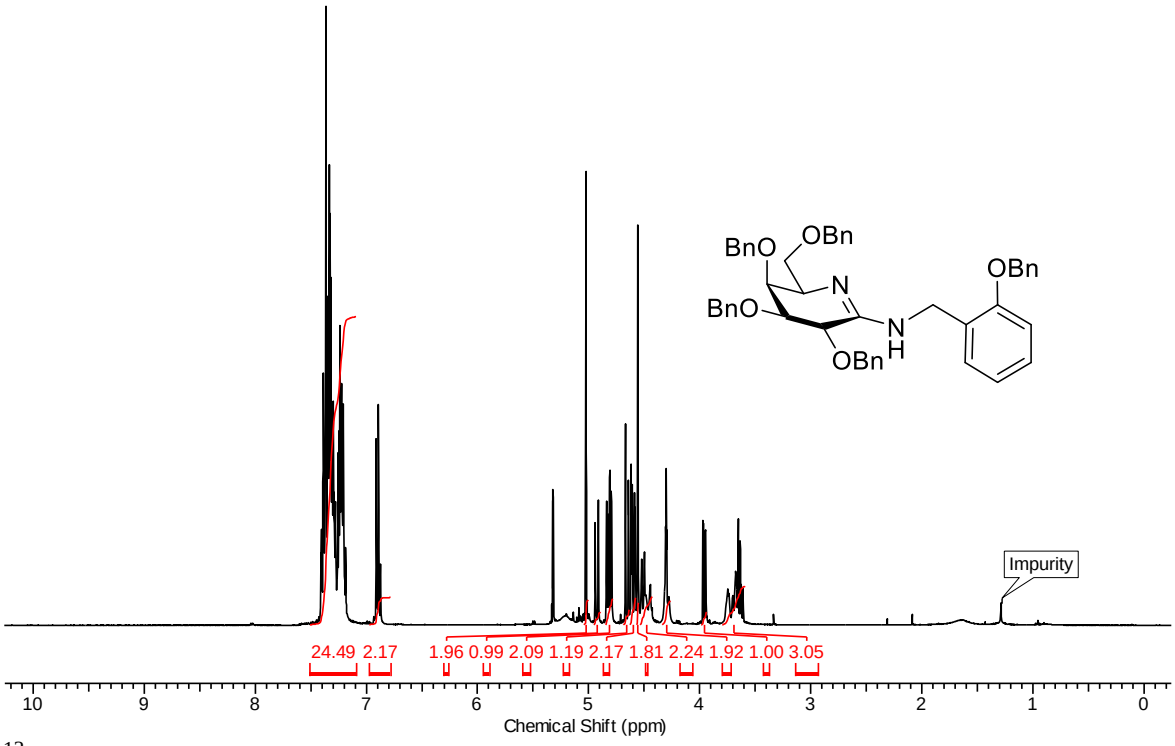

^{13}C NMR (100.6 MHz, CD_2Cl_2)

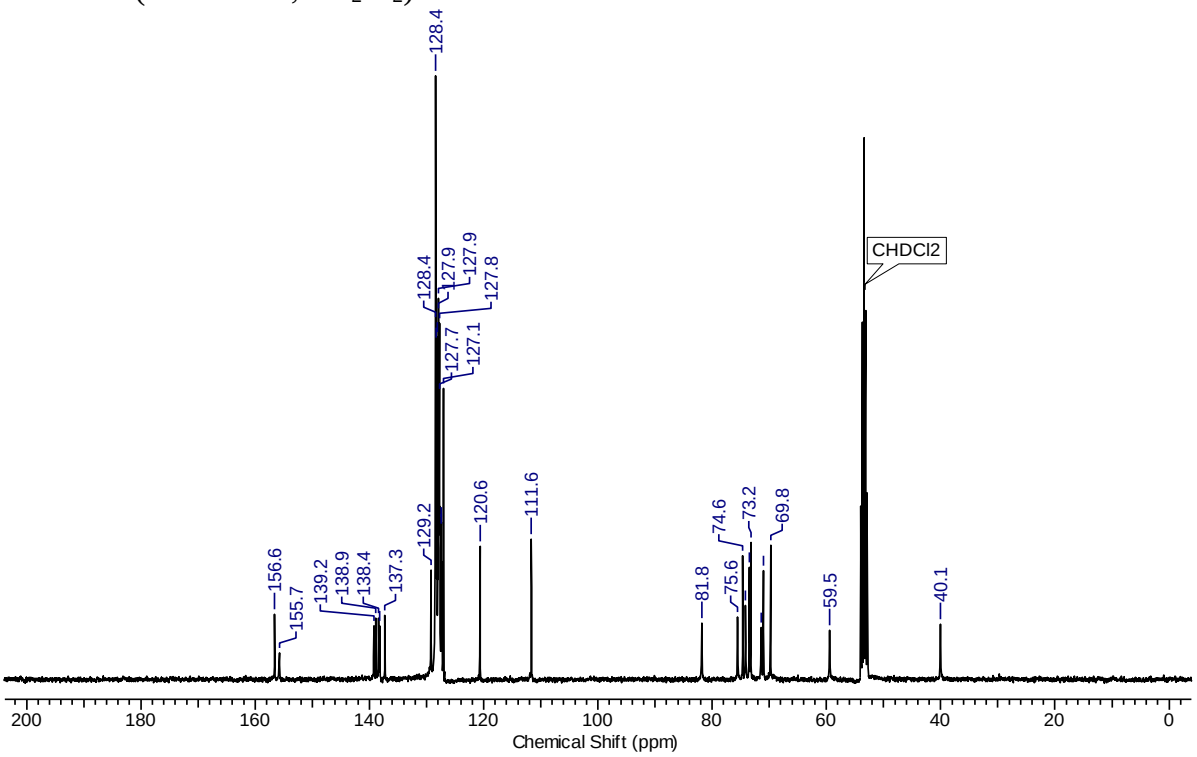

Compound 28b

^{1}H NMR (400.15 MHz, CD_2Cl_2)

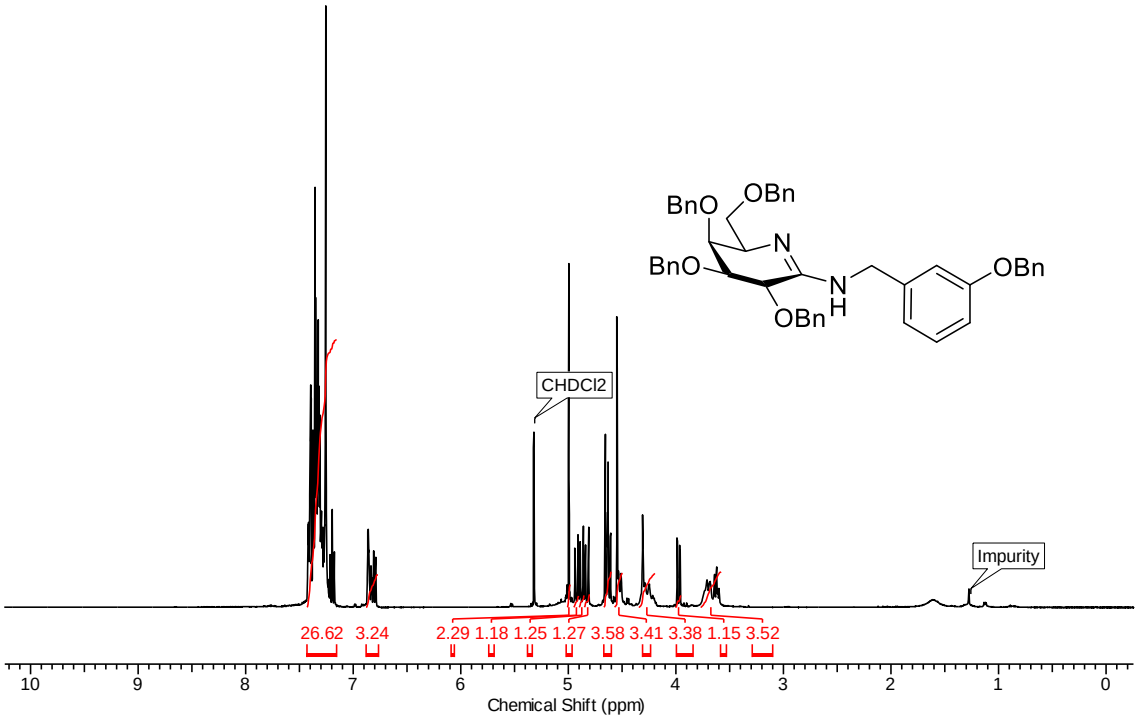

^{13}C NMR (100.6 MHz, CD_2Cl_2)

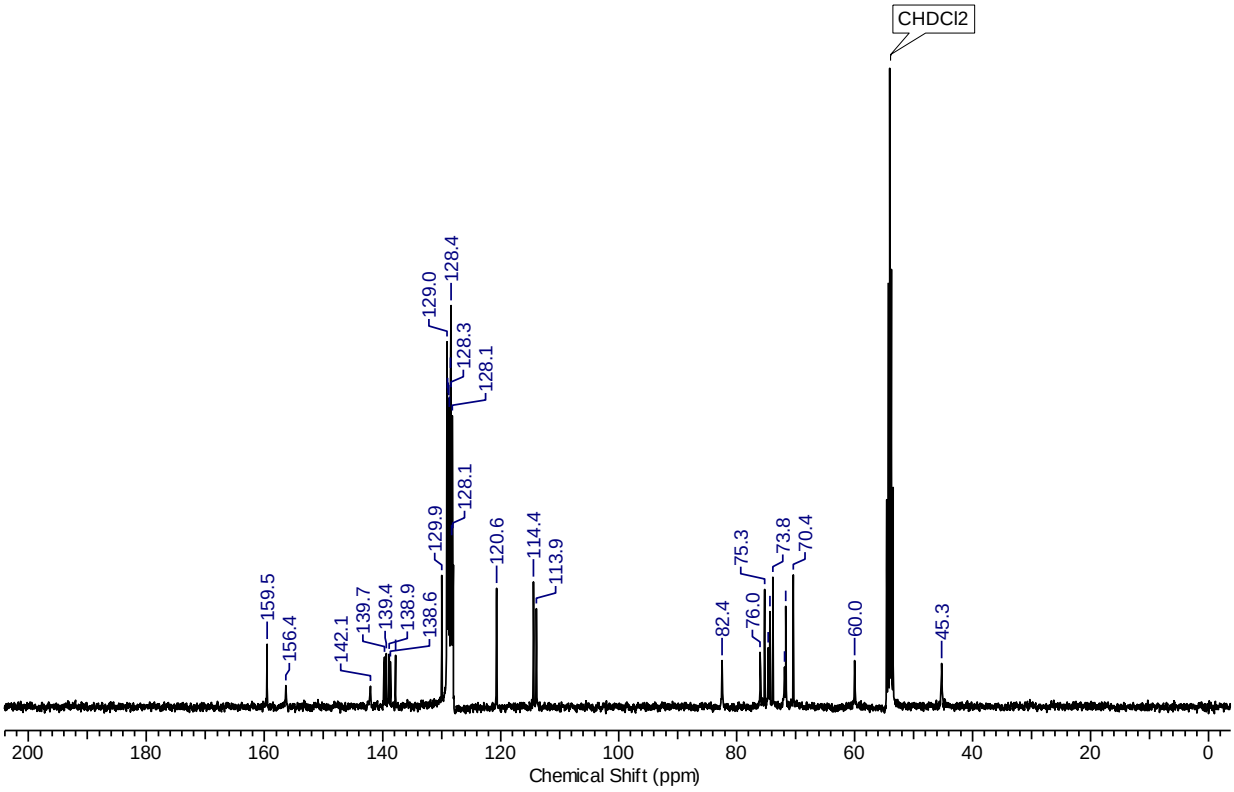

Compound 28c

^{1}H NMR (400.15 MHz, CD_2Cl_2)

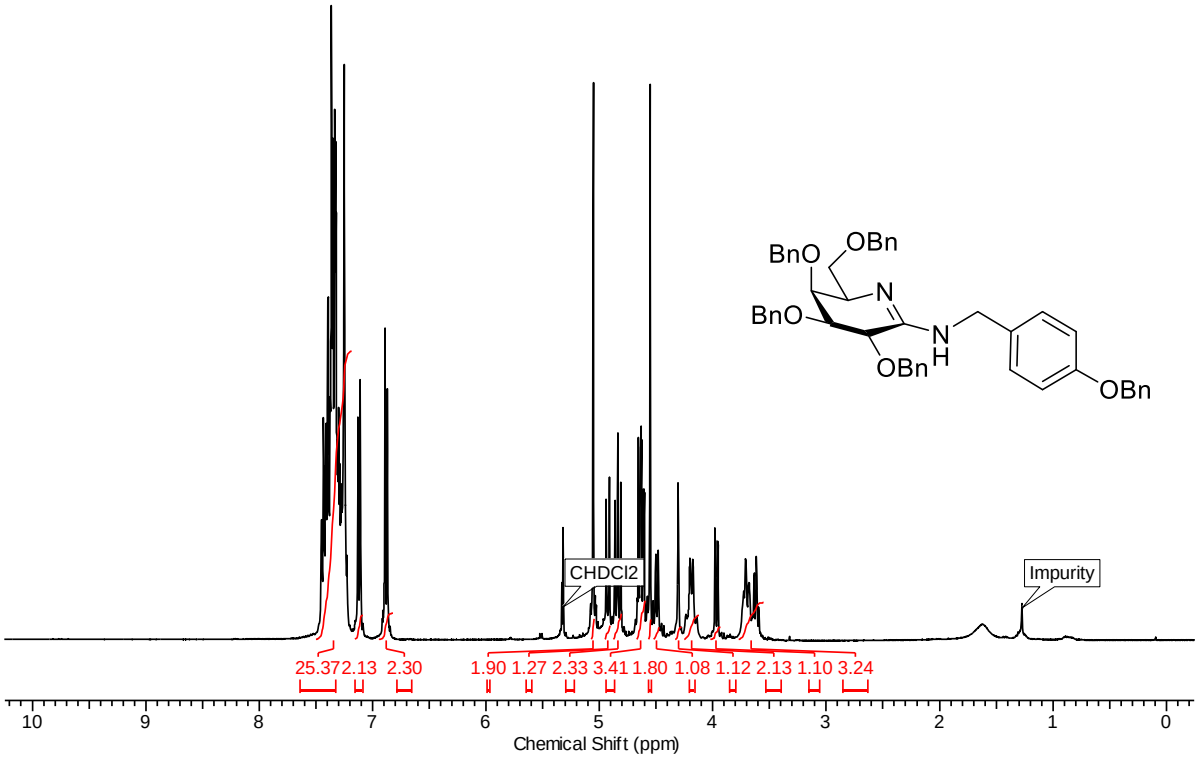

^{13}C NMR (100.6 MHz, CD_2Cl_2)

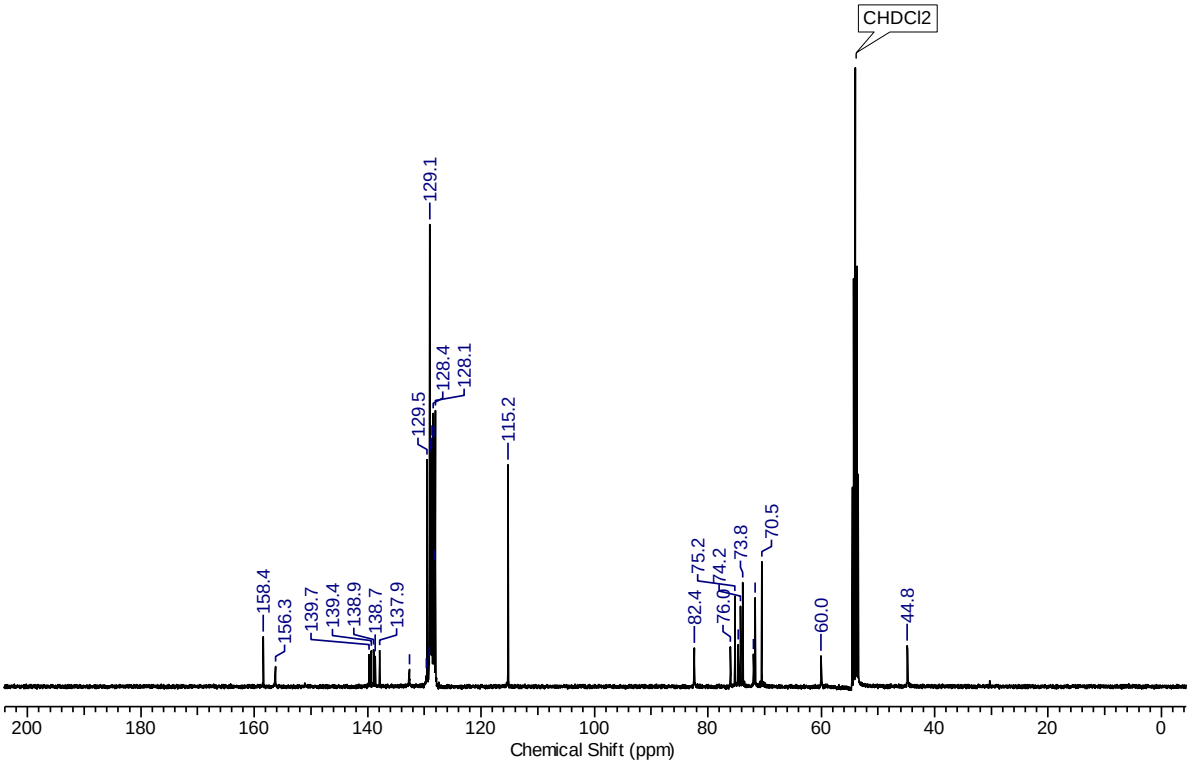

Compound 28d

^{1}H NMR (400.15 MHz, CD_2Cl_2)

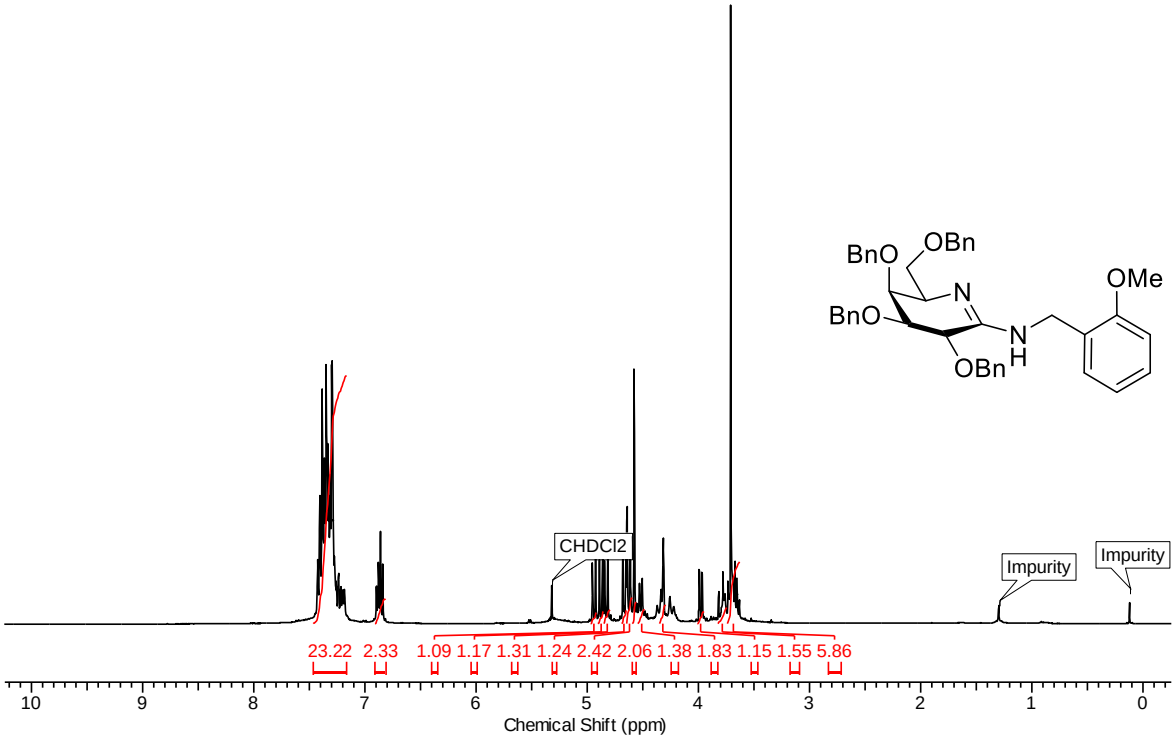

^{13}C NMR (100.6 MHz, CD_2Cl_2)

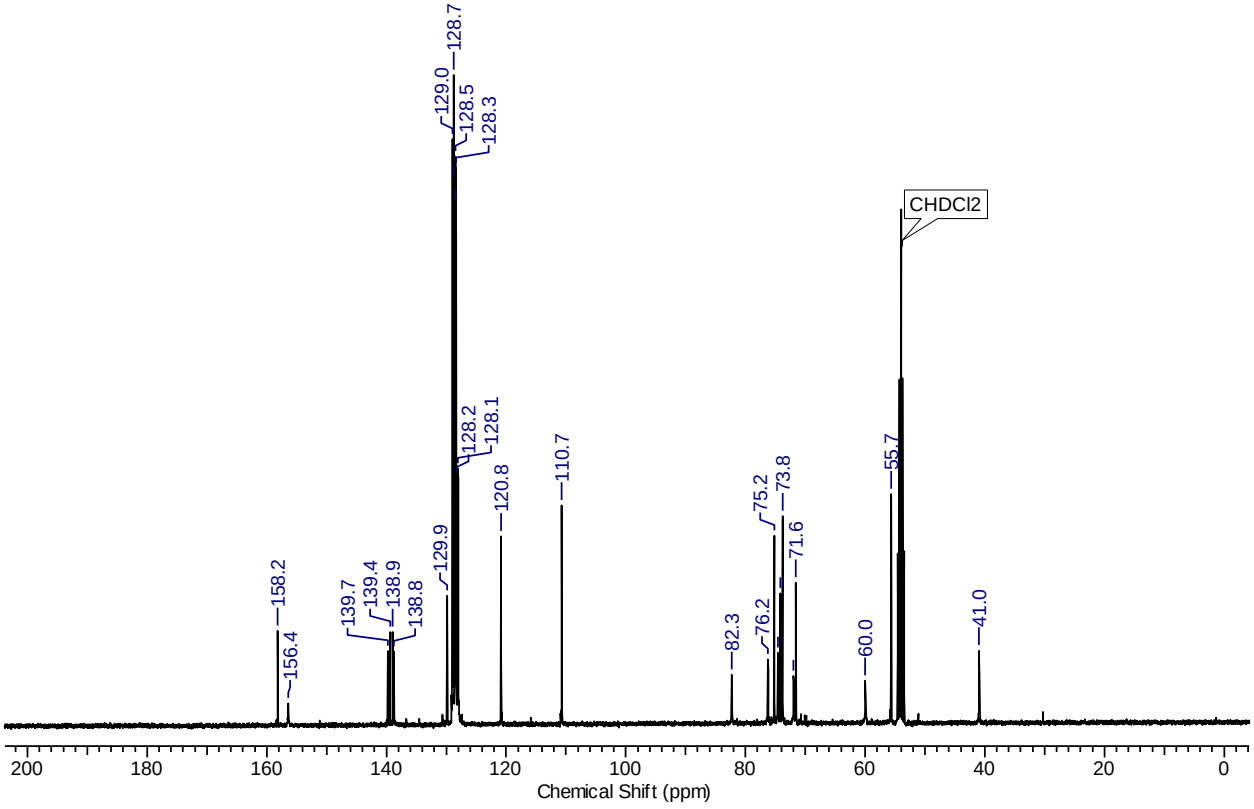

Compound 28e

^{1}H NMR (400.15 MHz, CD_2Cl_2)

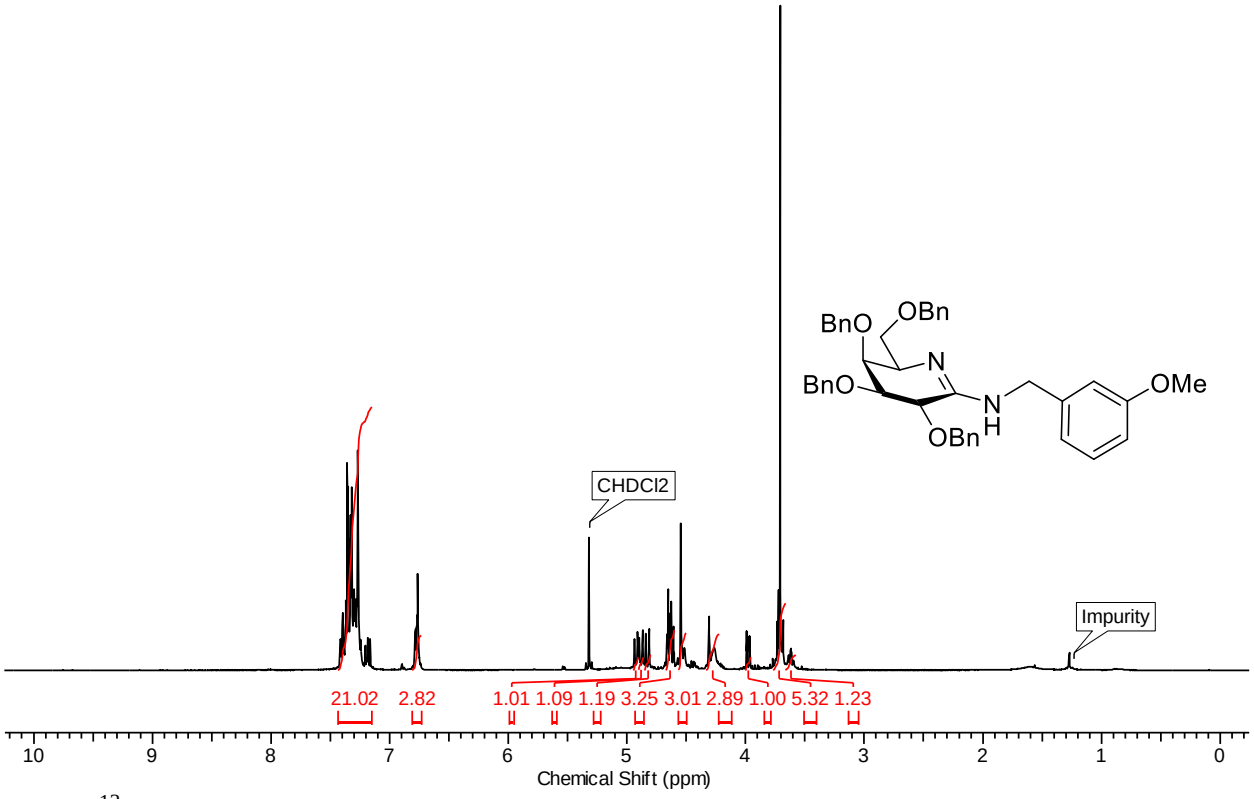

^{13}C NMR (100.6 MHz, CD_2Cl_2)

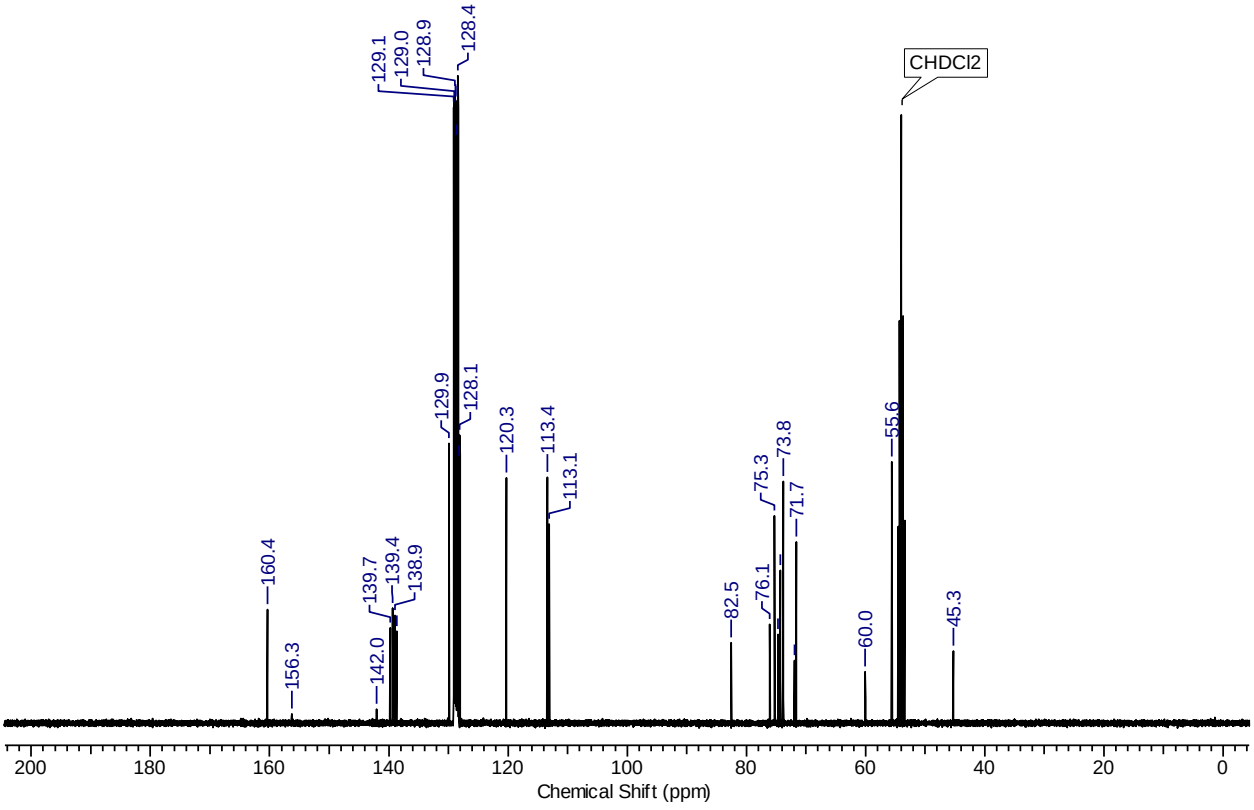

Compound 28f

^{1}H NMR (400.15 MHz, CD_2Cl_2)

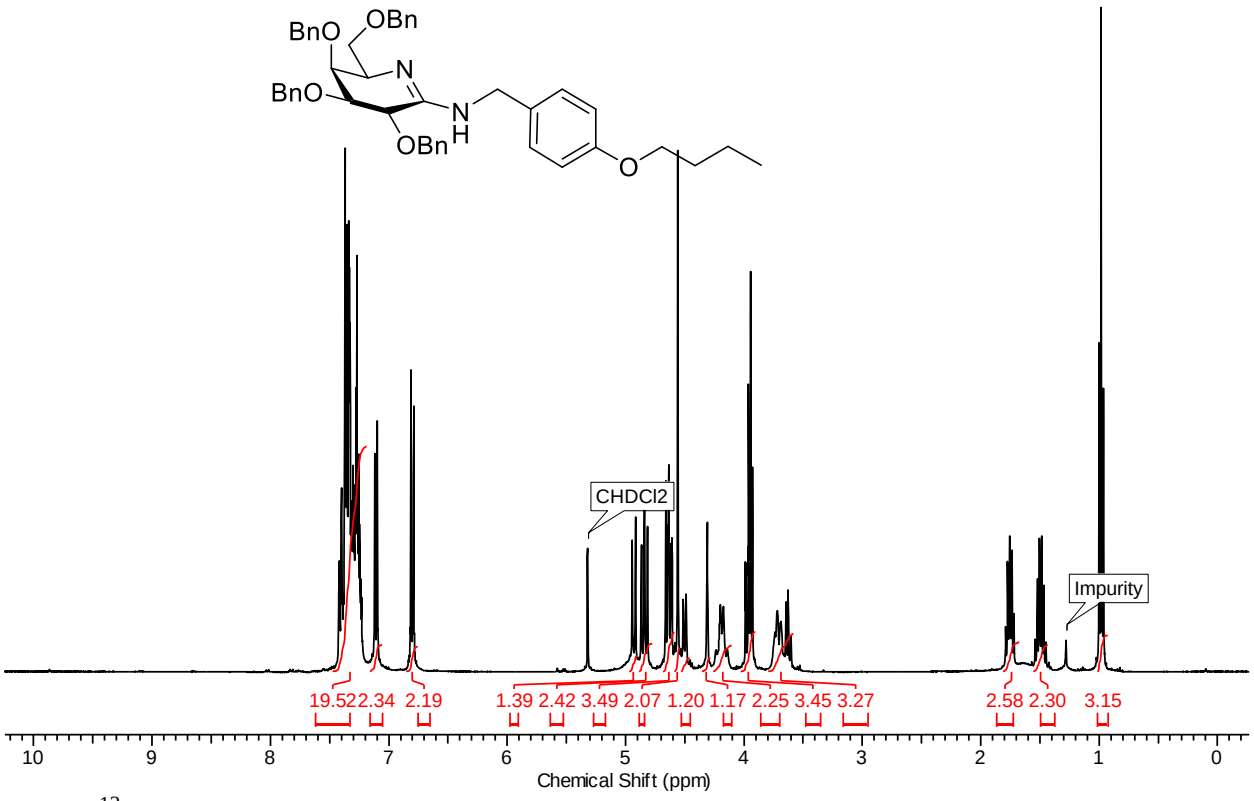

^{13}C NMR (100.6 MHz, CD_2Cl_2)

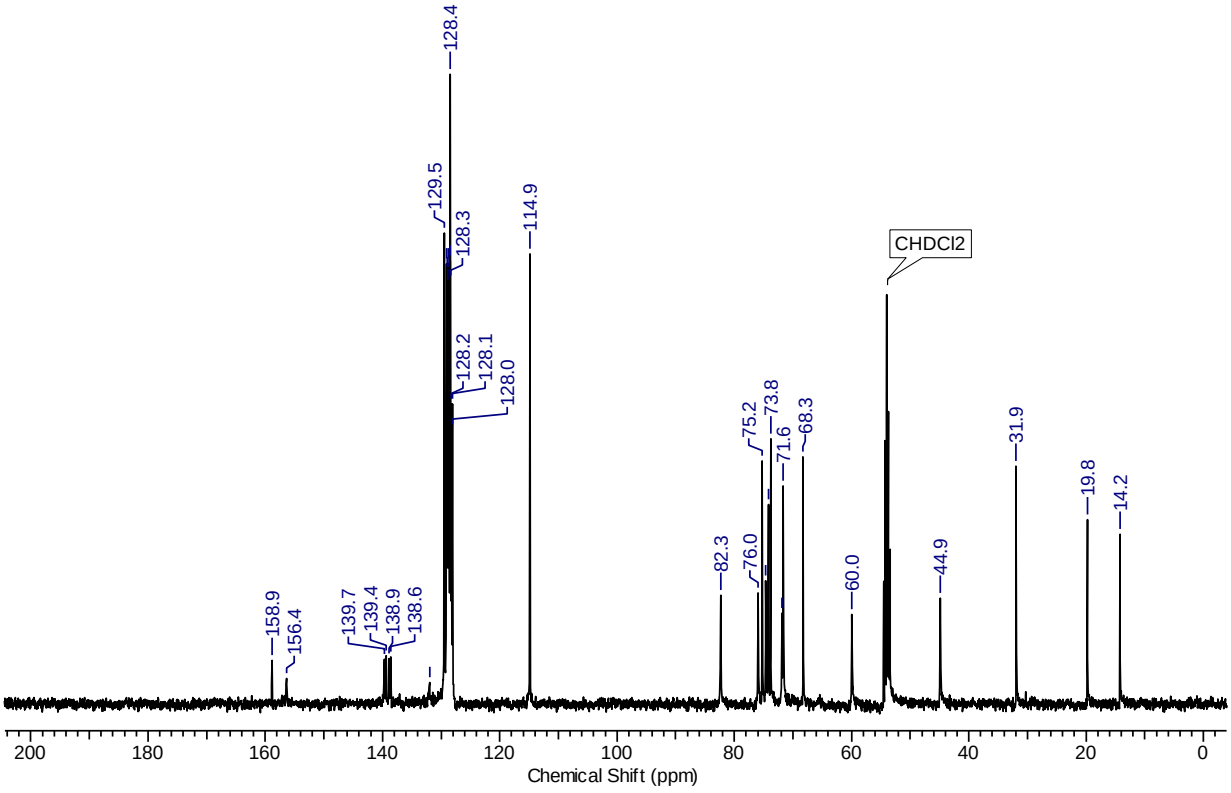

Compound 28h

^{1}H NMR (400.15 MHz, CD_2Cl_2)

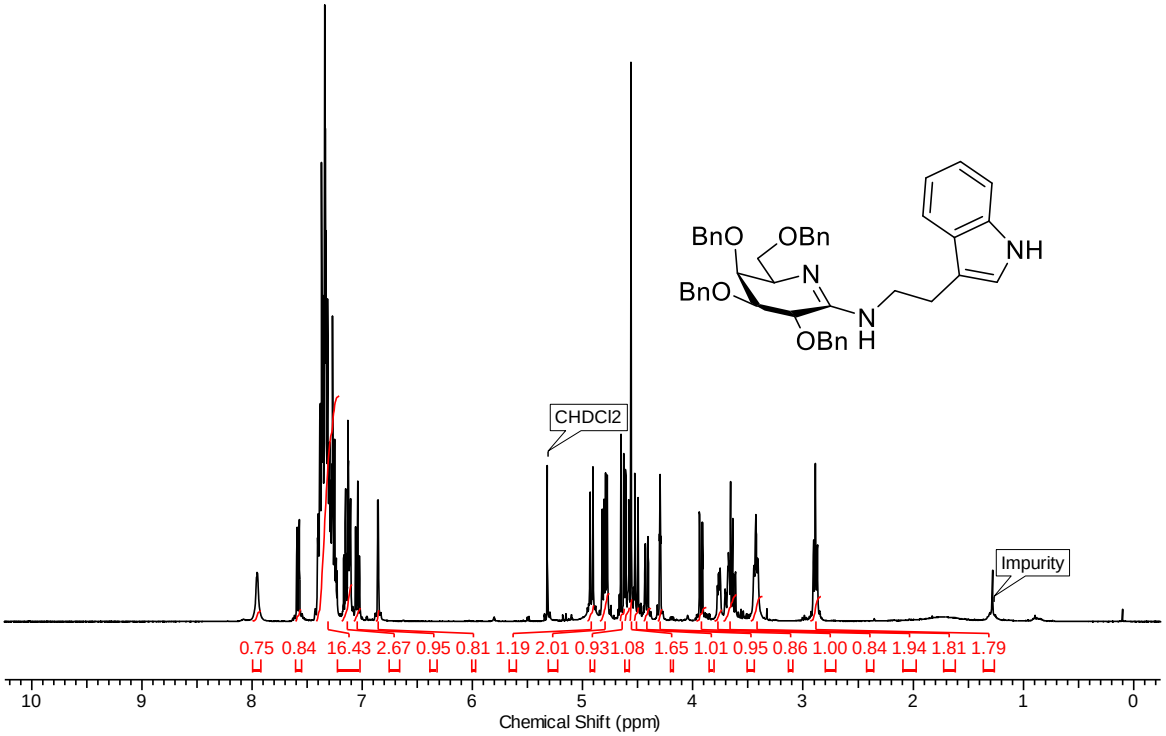

^{13}C NMR (100.6 MHz, CD_2Cl_2)

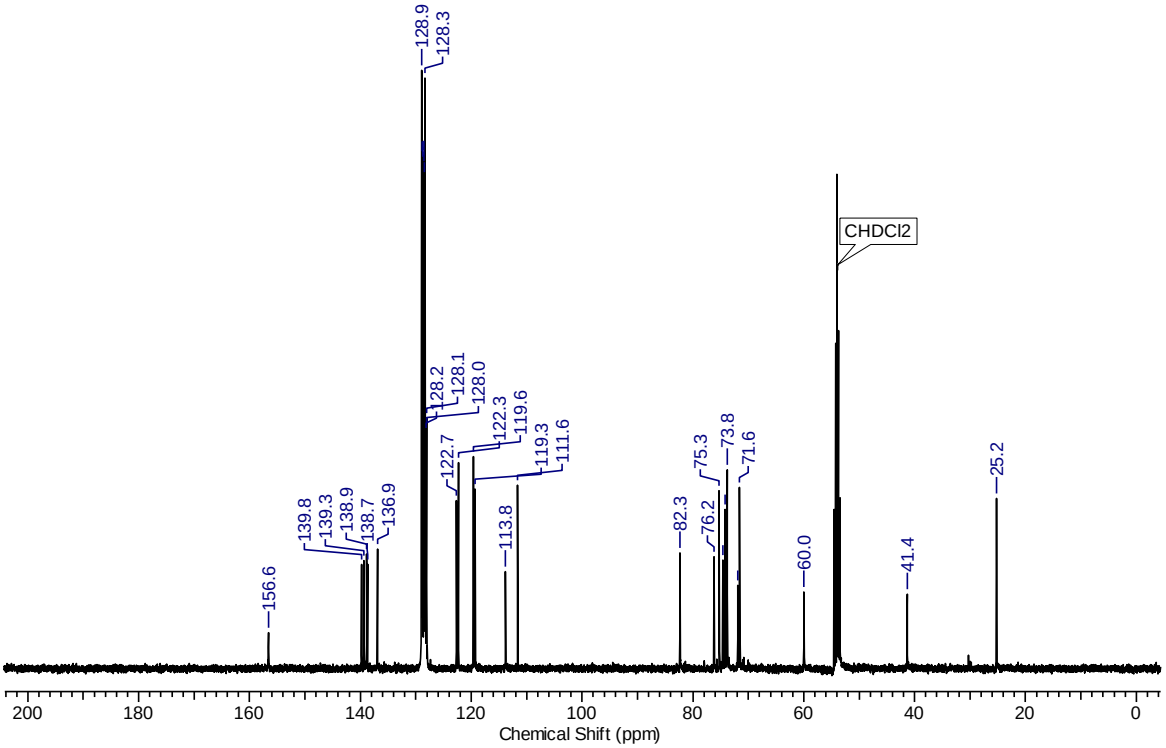

Compound 28i

^{1}H NMR (400.15 MHz, CD_2Cl_2)

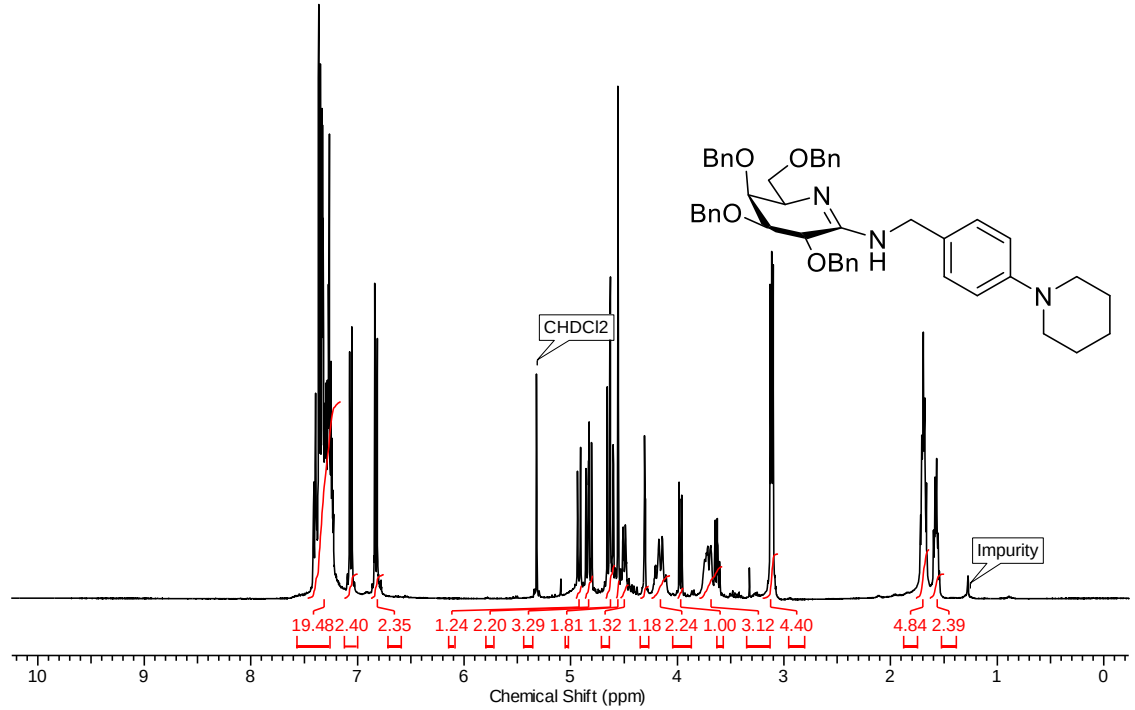

^{13}C NMR (100.6 MHz, CD_2Cl_2)

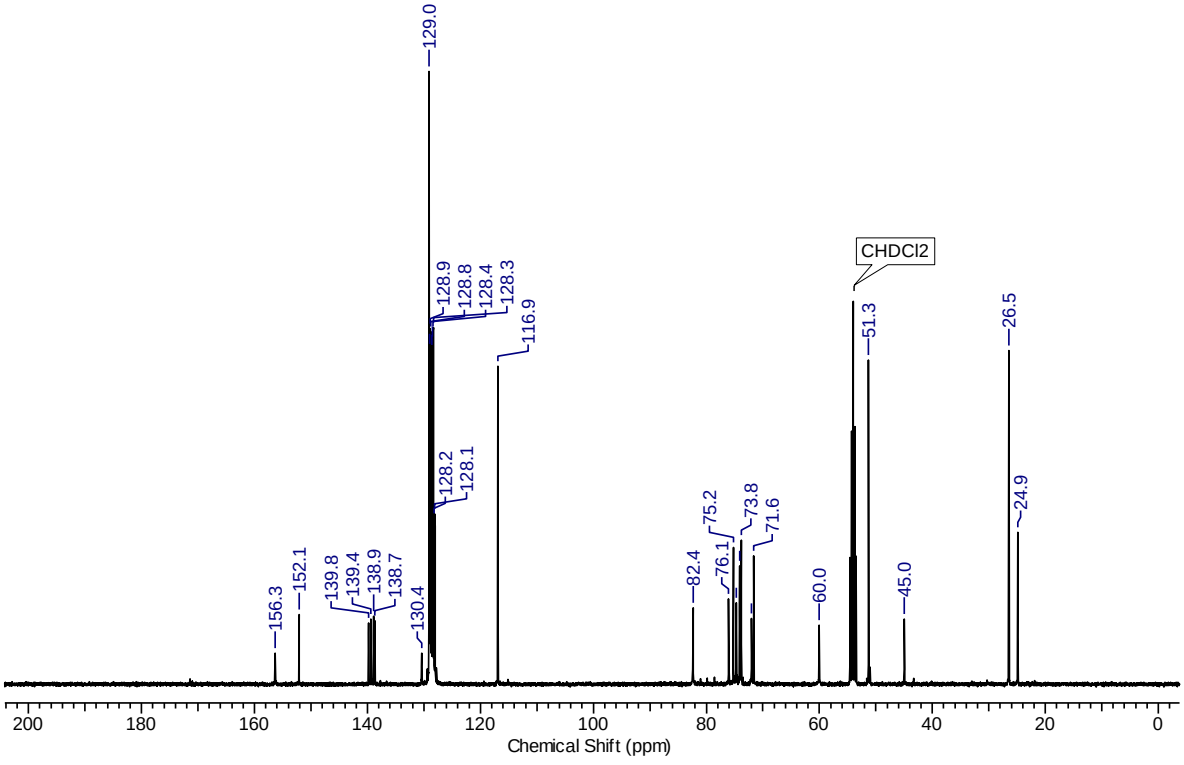

Compound 28i

^{1}H NMR (400.15 MHz, CD_2Cl_2)

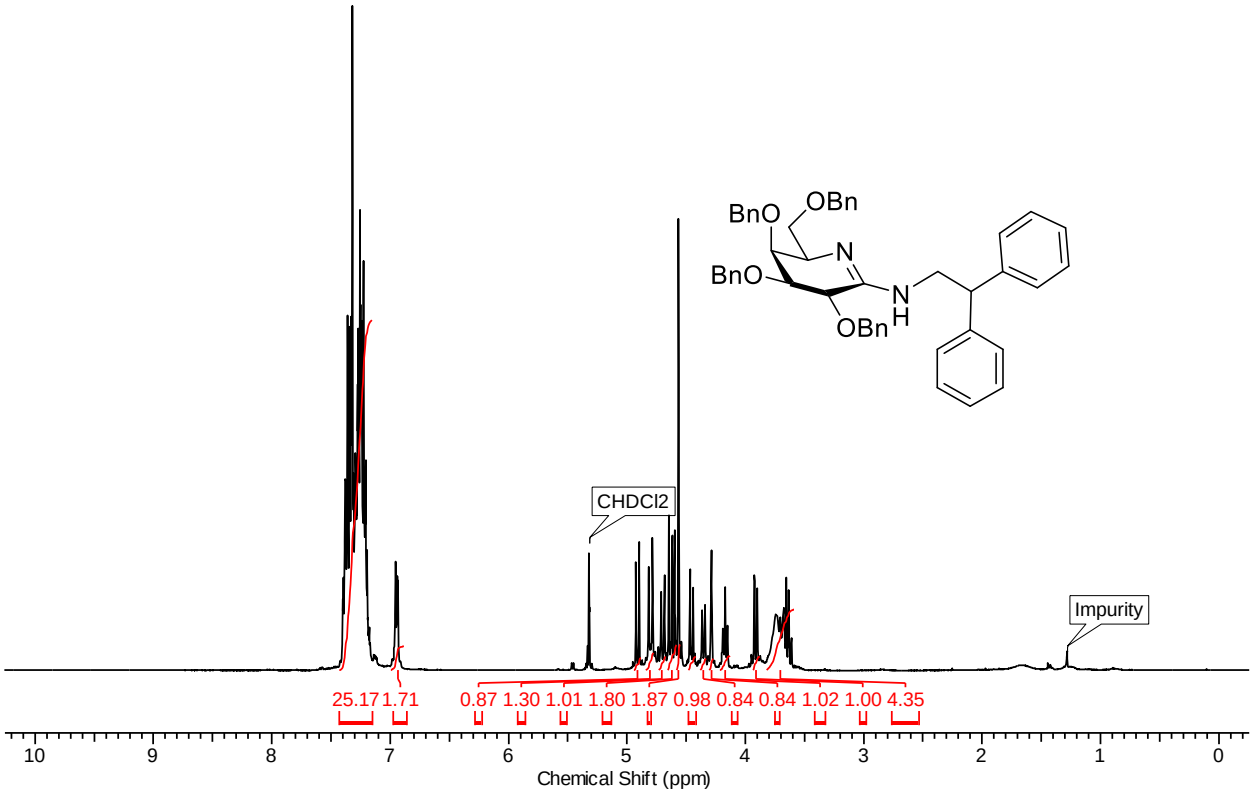

^{13}C NMR (100.6 MHz, CD_2Cl_2)

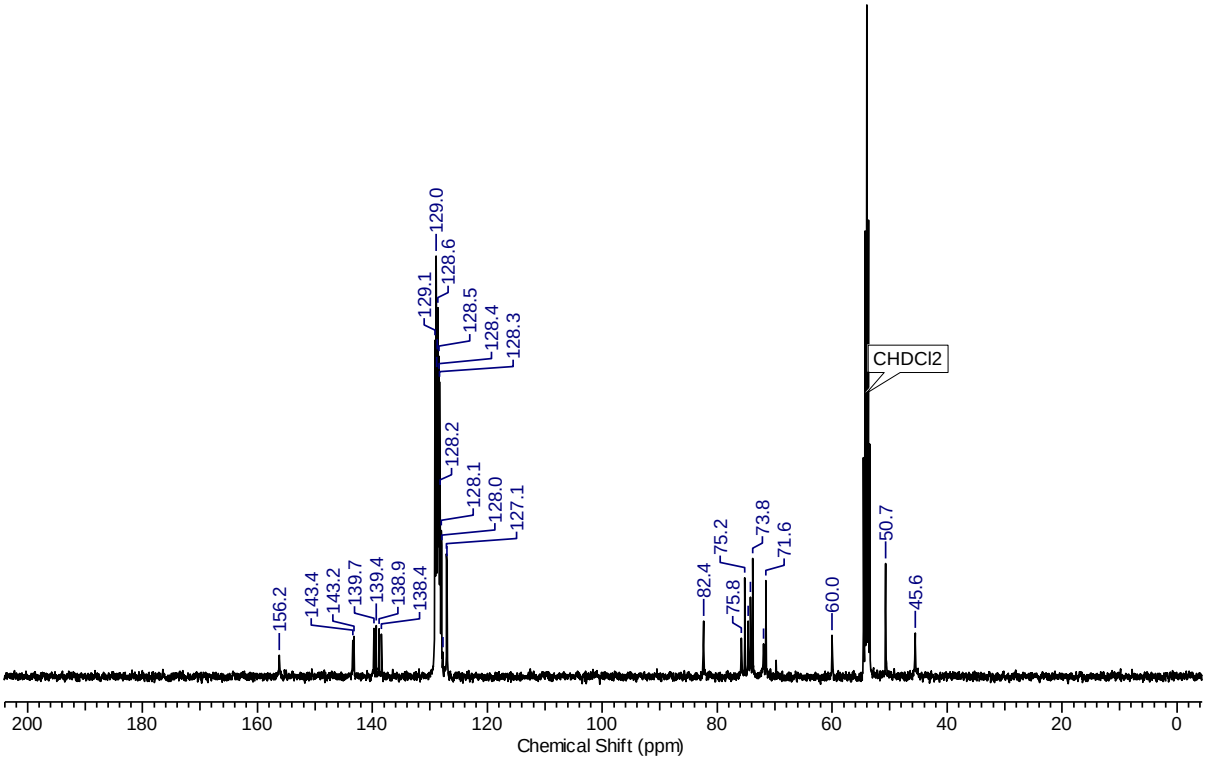

Compound 28j

^{1}H NMR (400.15 MHz, CD_2Cl_2)

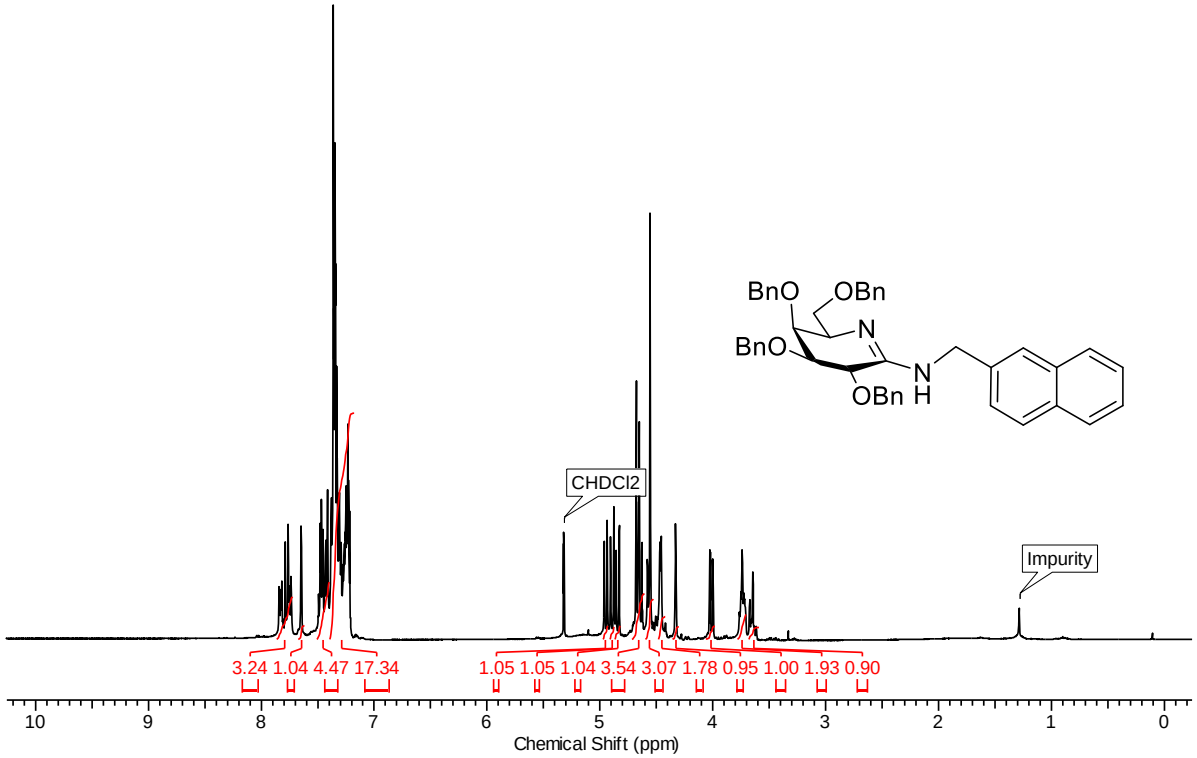

^{13}C NMR (100.6 MHz, CD_2Cl_2)

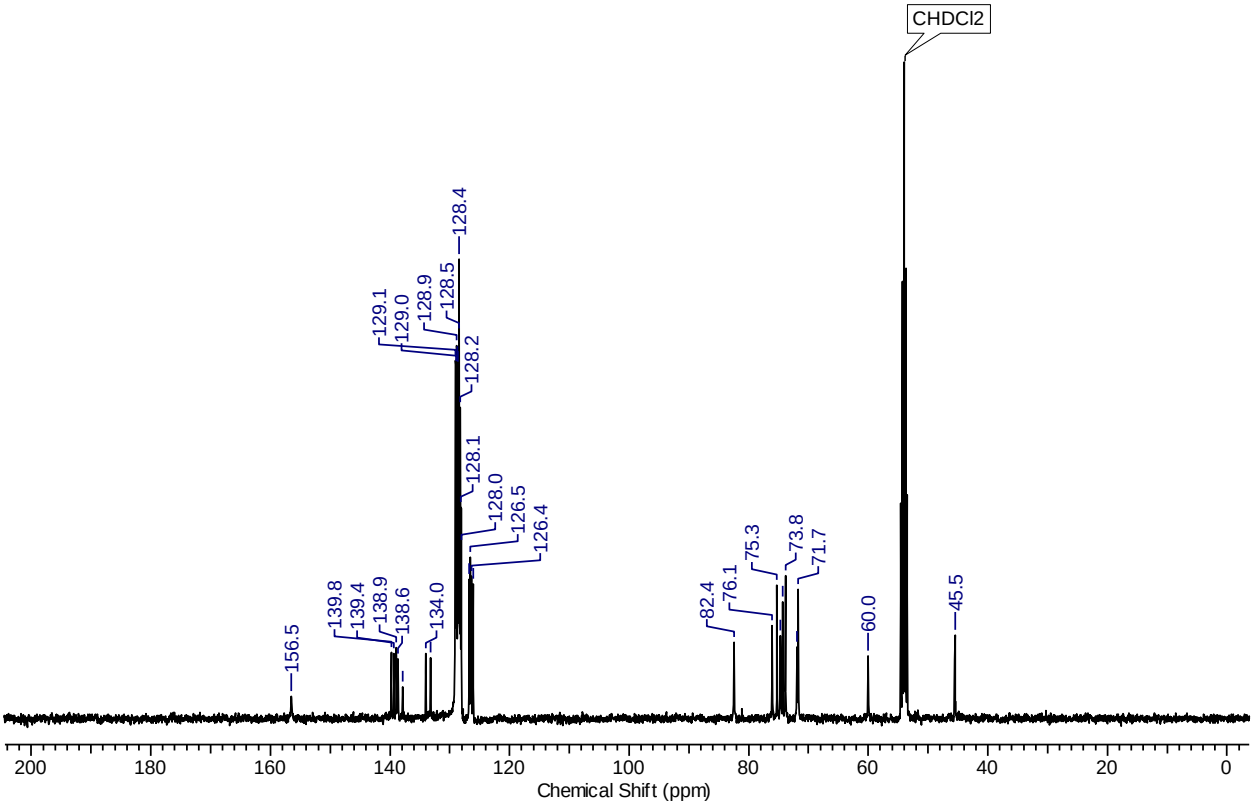

Compound 28k

^{1}H NMR (400.15 MHz, CD_2Cl_2)

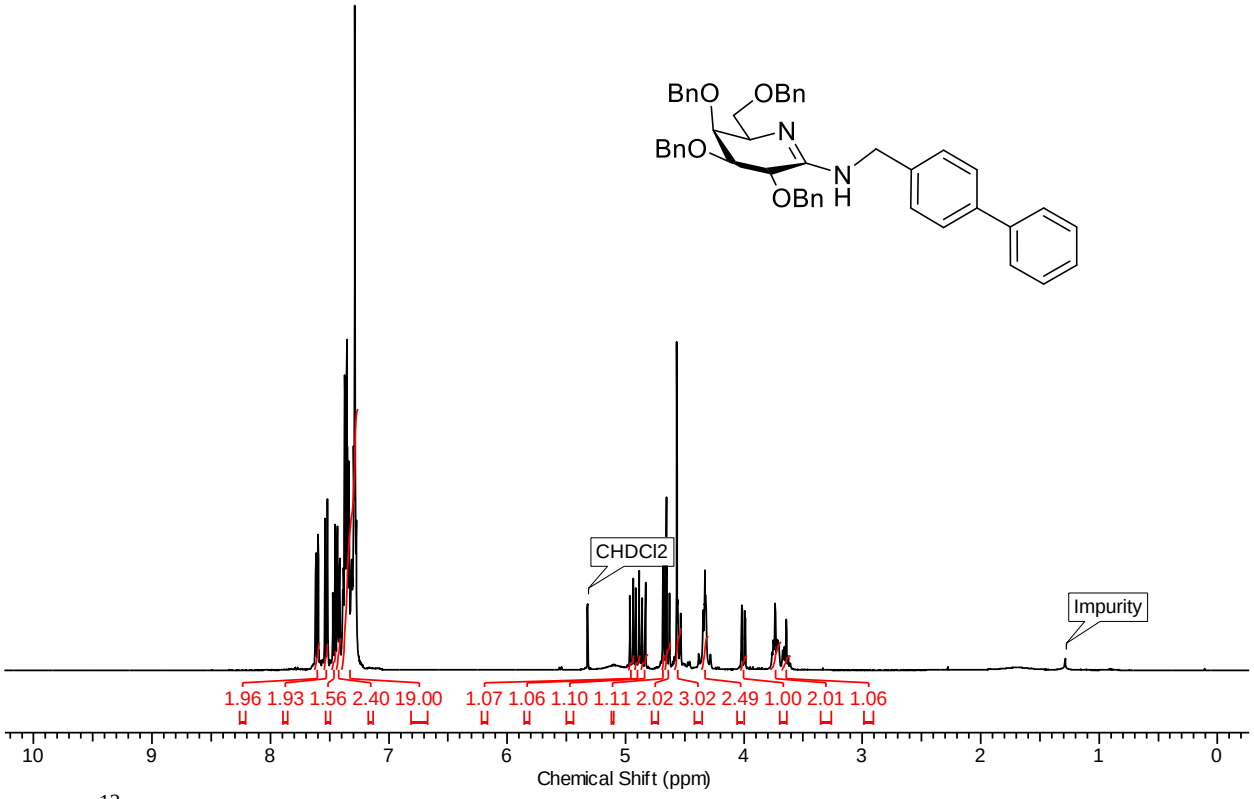

^{13}C NMR (100.6 MHz, CD_2Cl_2)

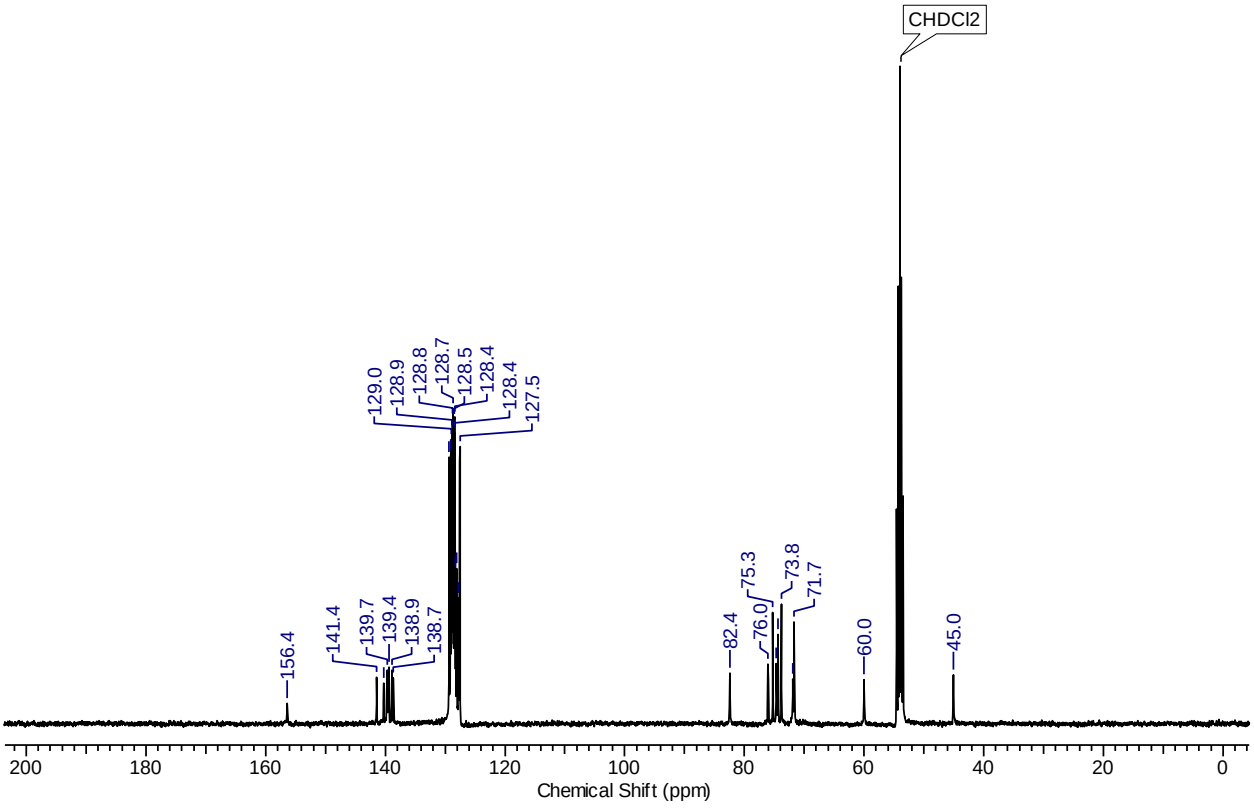

Compound 28l

^{1}H NMR (400.15 MHz, CD_2Cl_2)

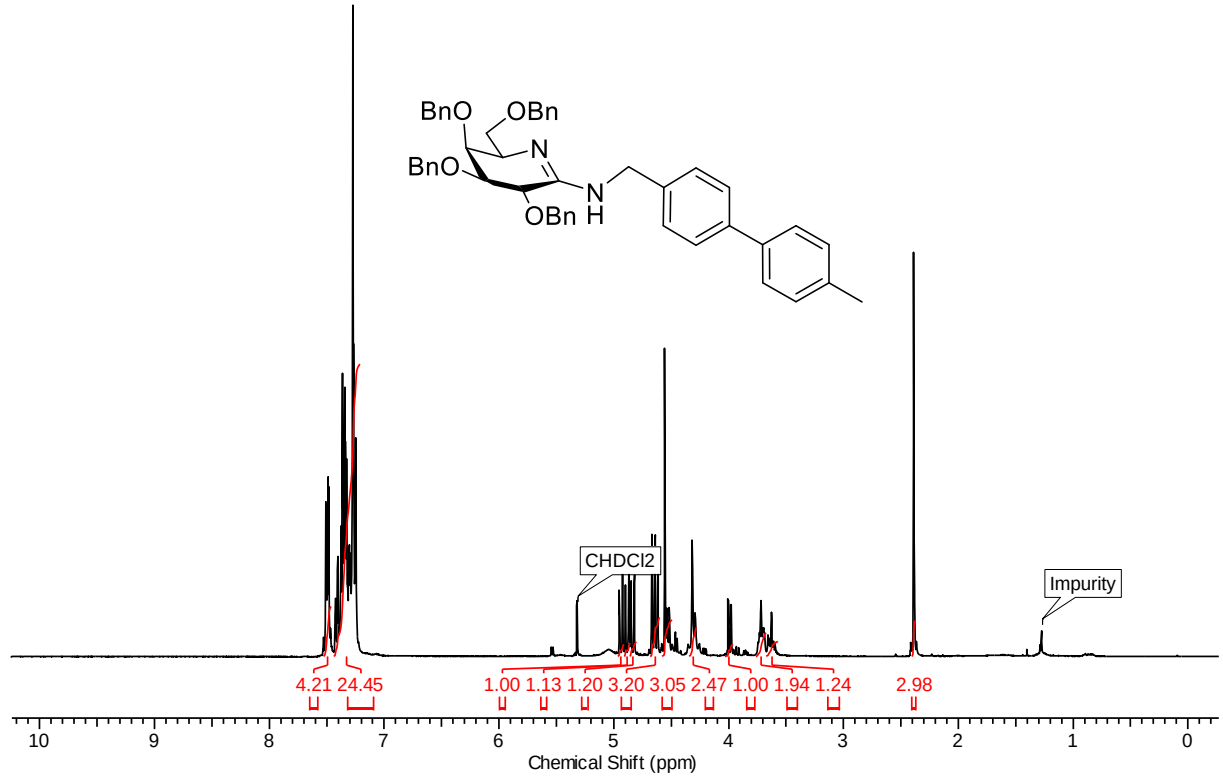

^{13}C NMR (100.6 MHz, CD_2Cl_2)

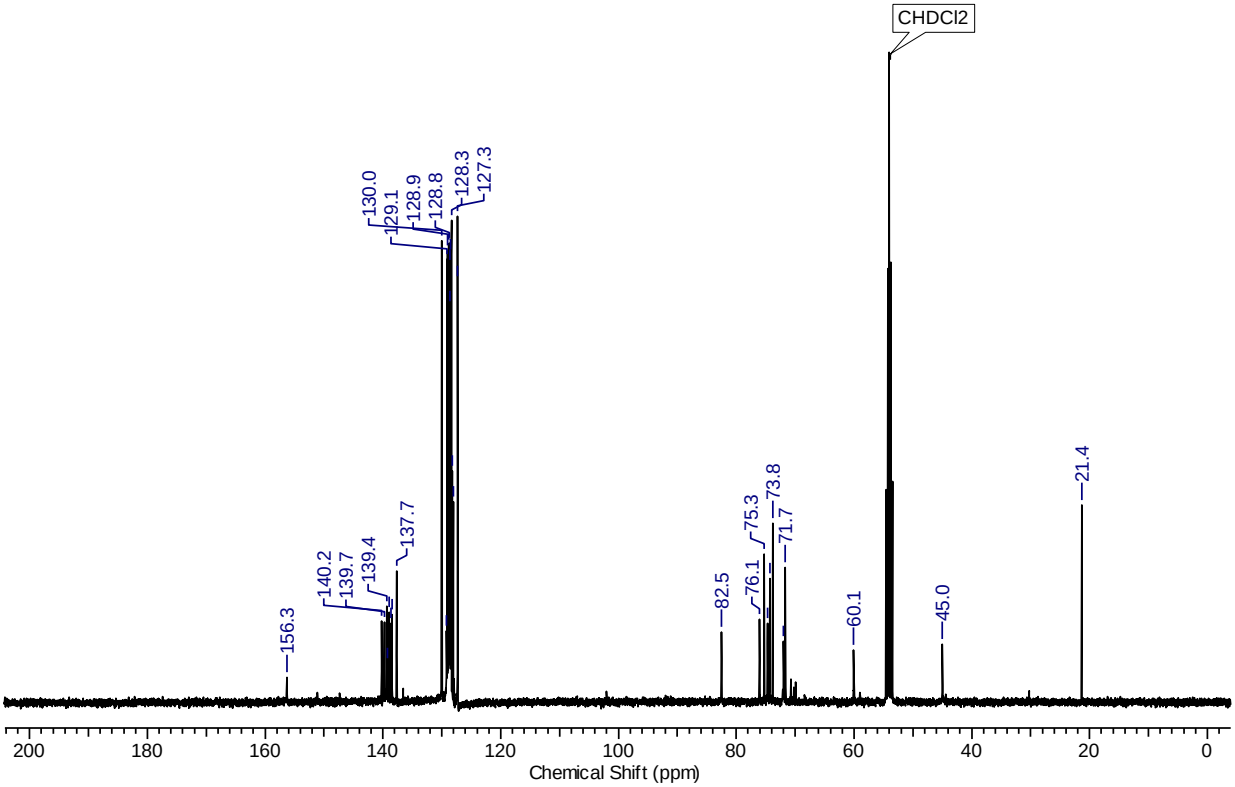

Compound 28m

^{1}H NMR (400.15 MHz, CD_2Cl_2)

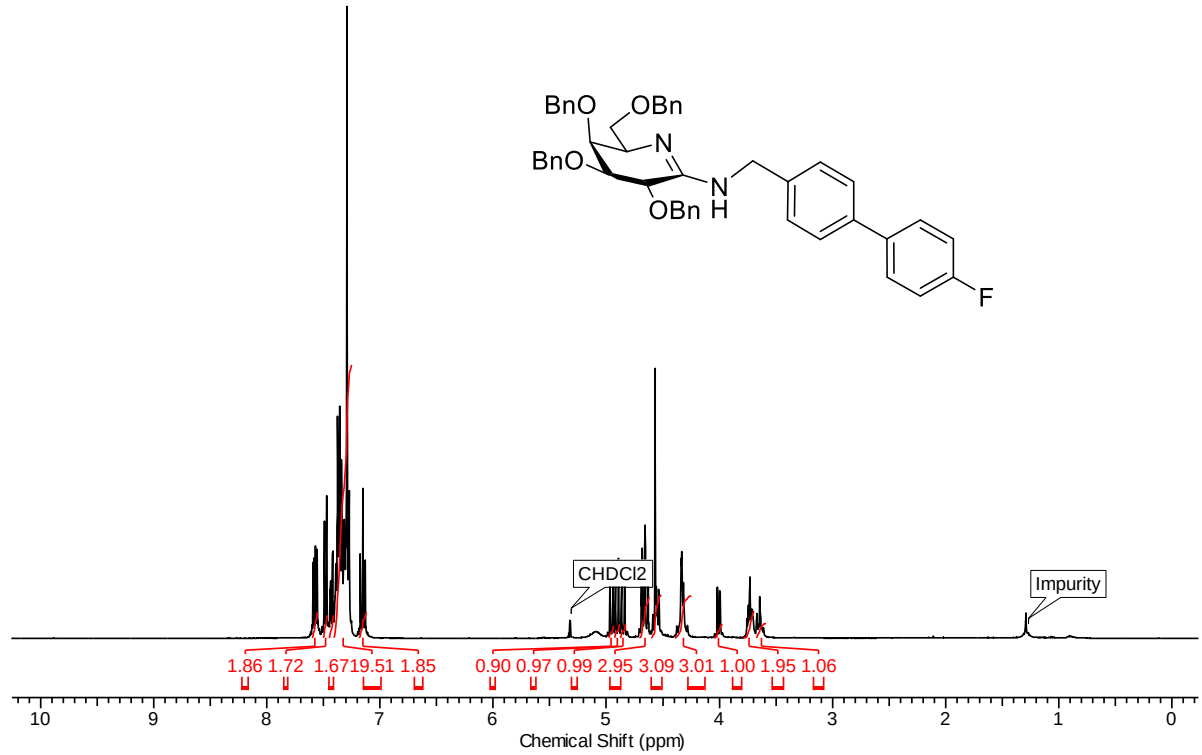

^{13}C NMR (100.6 MHz, CD_2Cl_2)

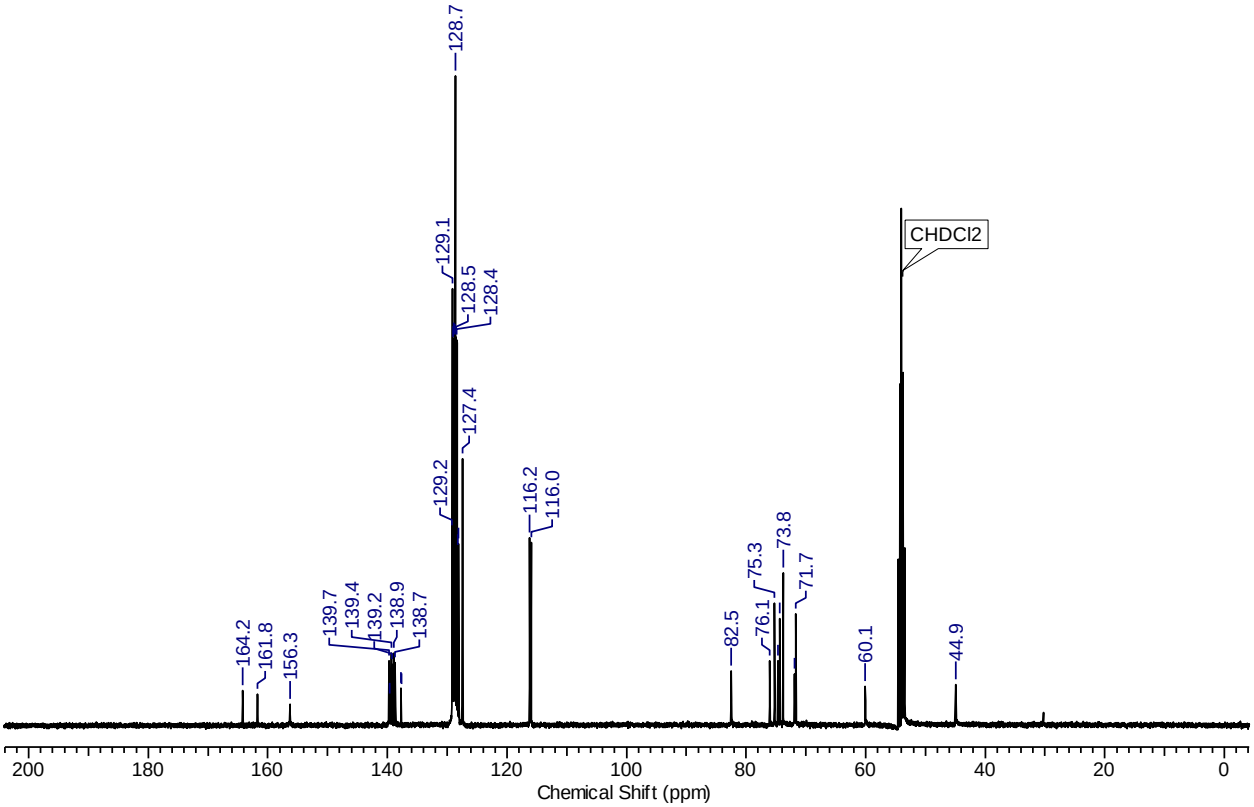

Compound 28n

^{1}H NMR (400.15 MHz, CD_2Cl_2)

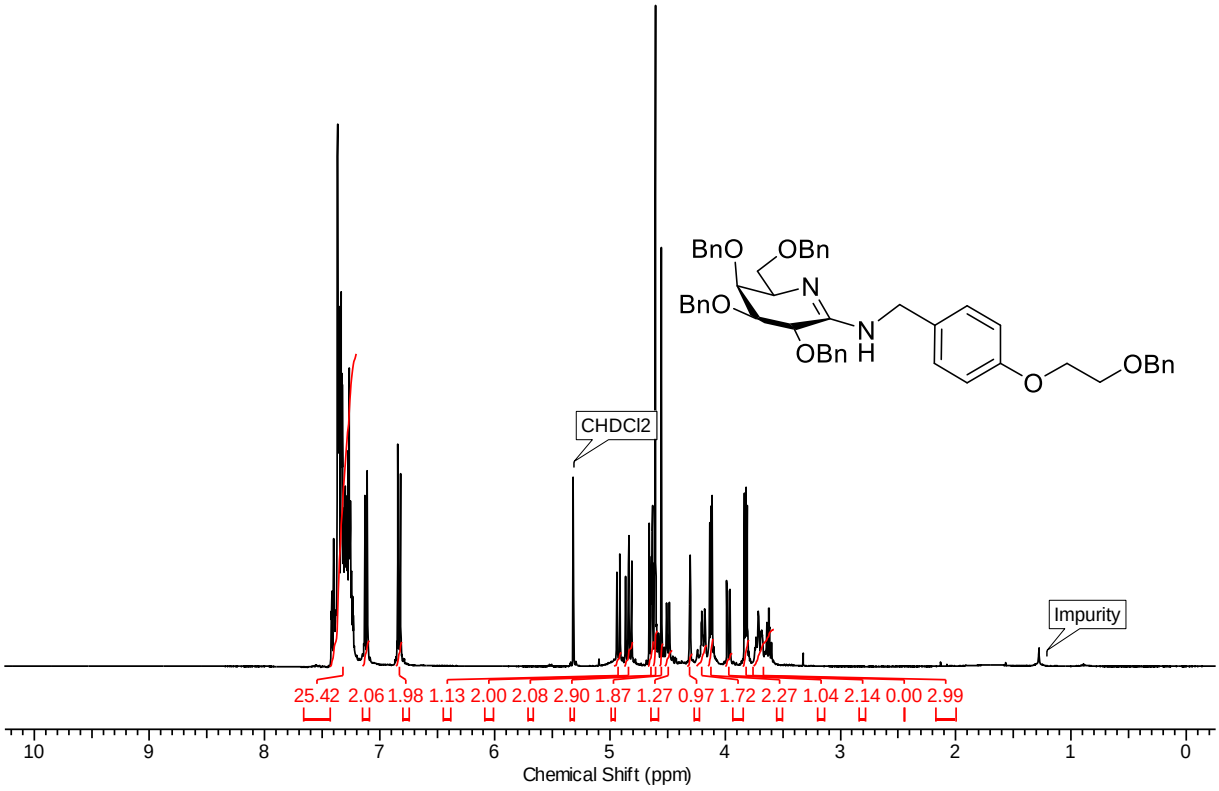

^{13}C NMR (100.6 MHz, CD_2Cl_2)

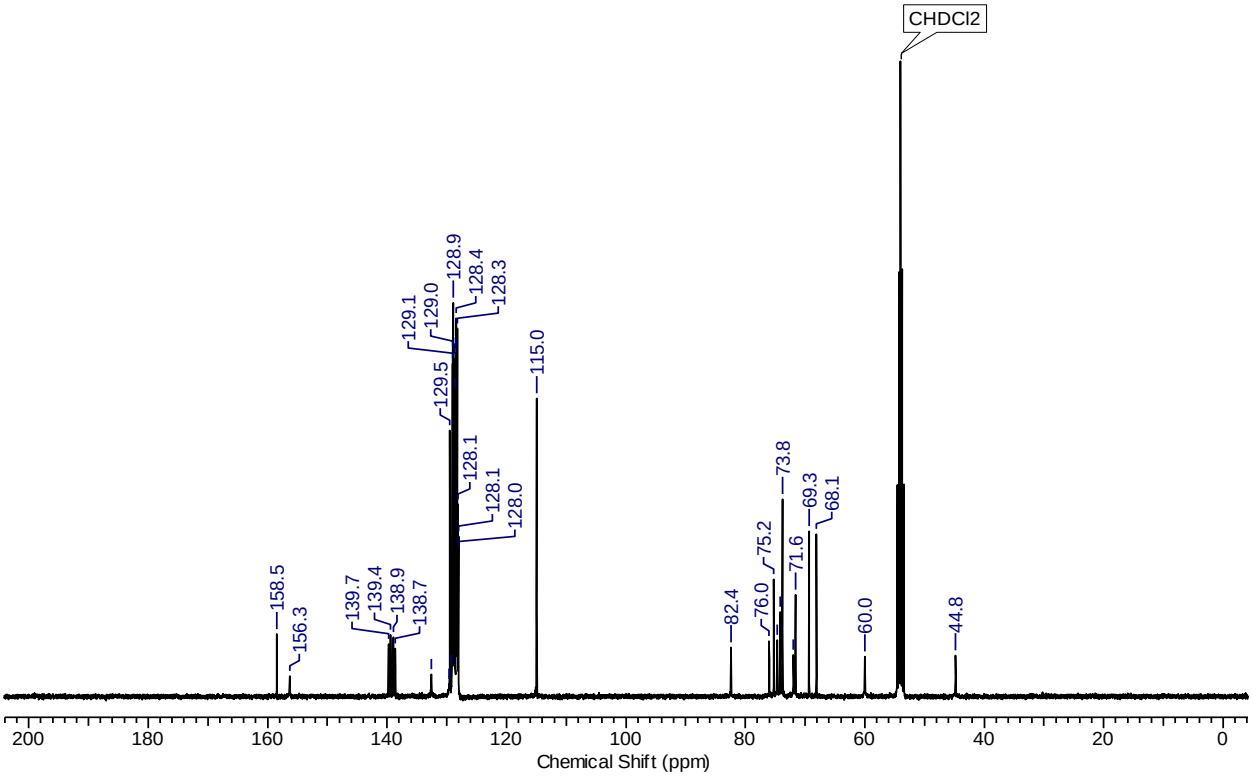

Compound 28o

^{1}H NMR (400.15 MHz, CD_2Cl_2)

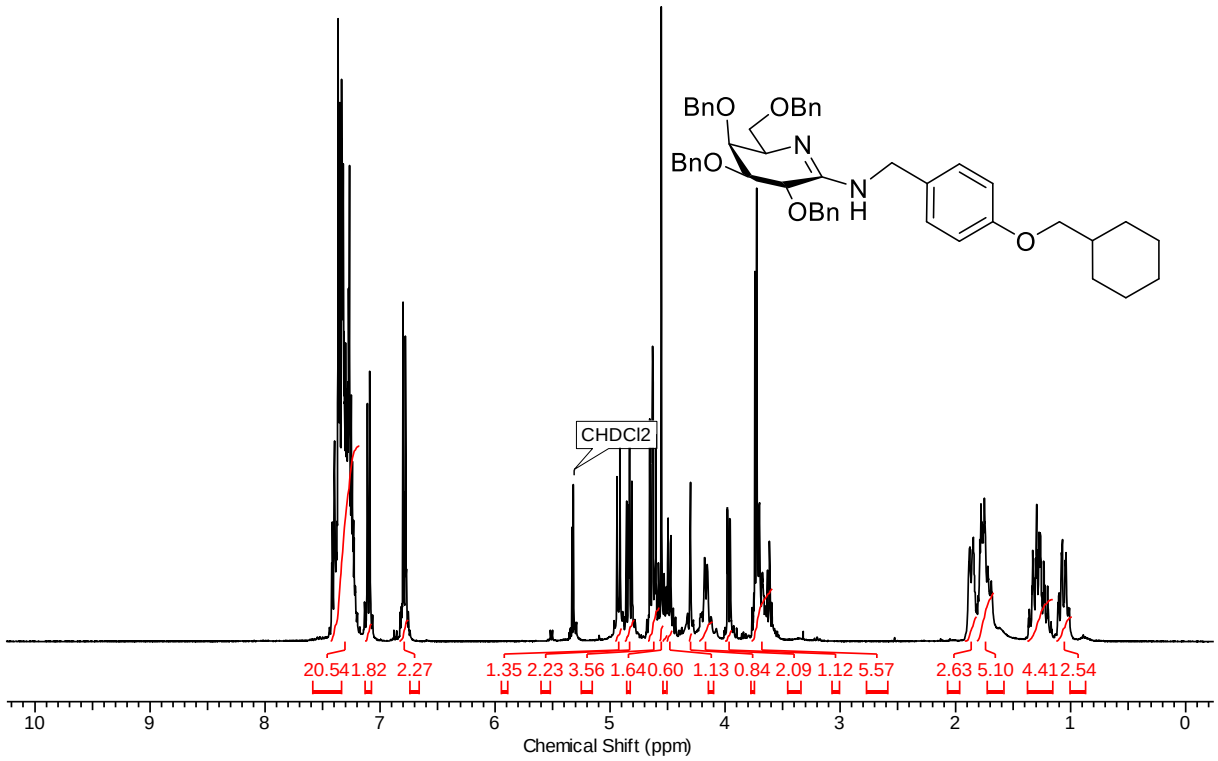

^{13}C NMR (100.6 MHz, CD_2Cl_2)

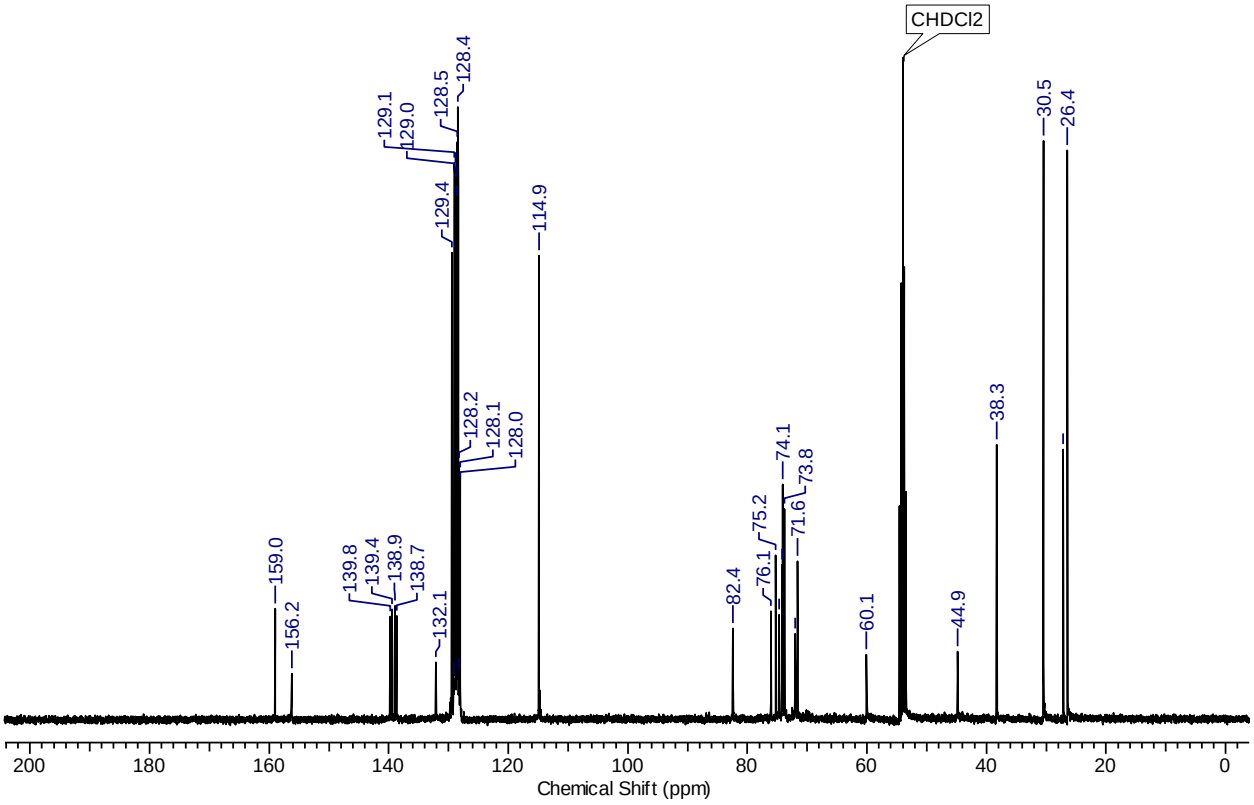

Compound 28p

^{1}H NMR (400.15 MHz, CD_2Cl_2)

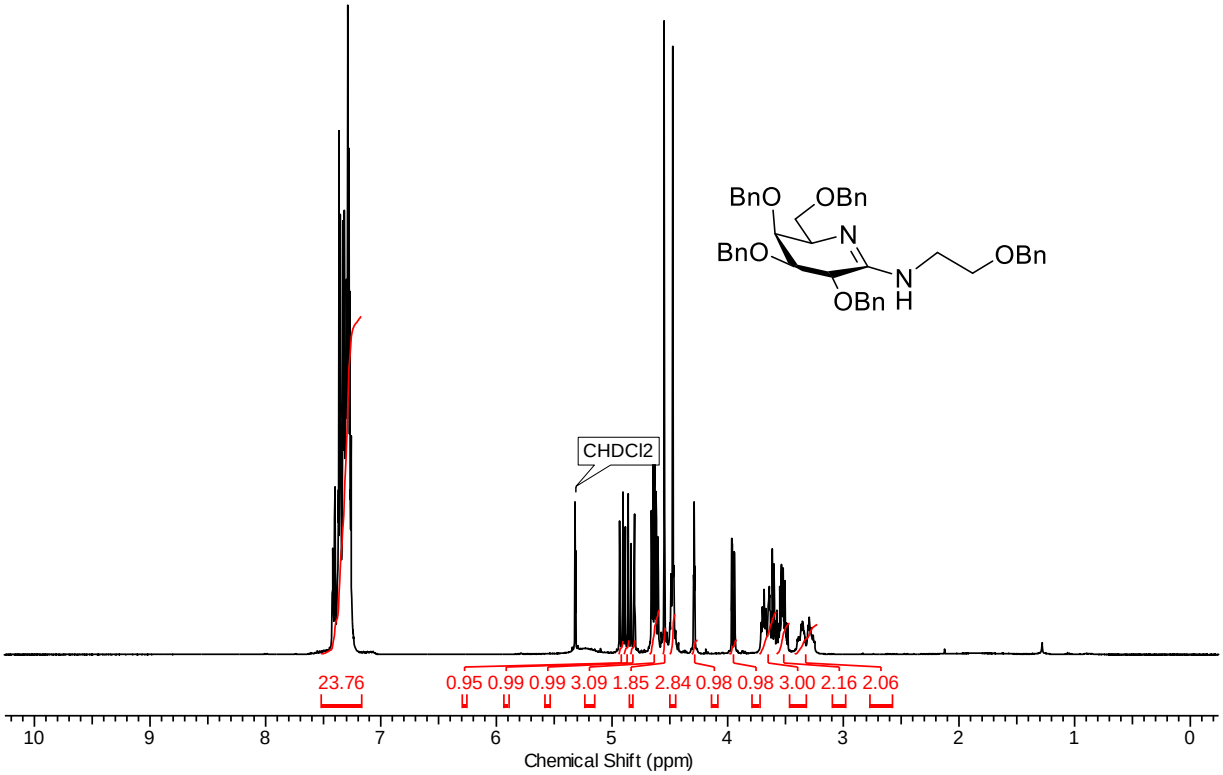

^{13}C NMR (100.6 MHz, CD_2Cl_2)

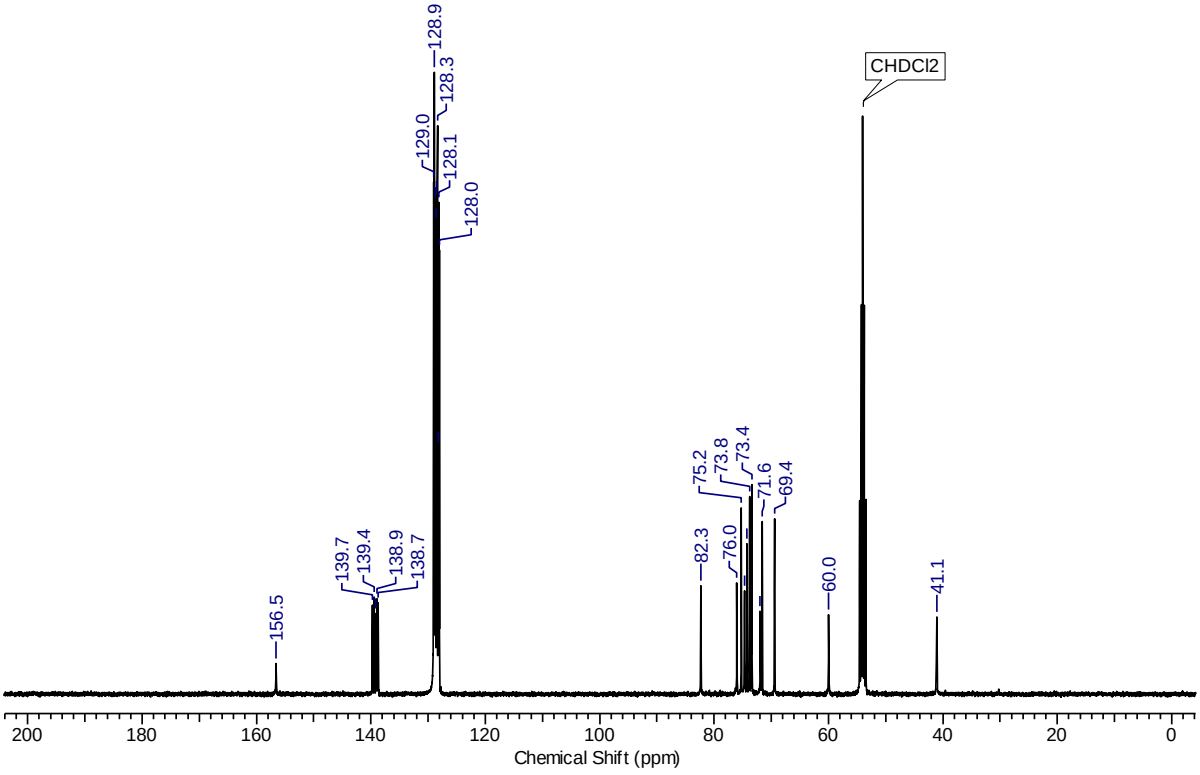

Compound 28p'

^{1}H NMR (400.15 MHz, $CDCl_3$)

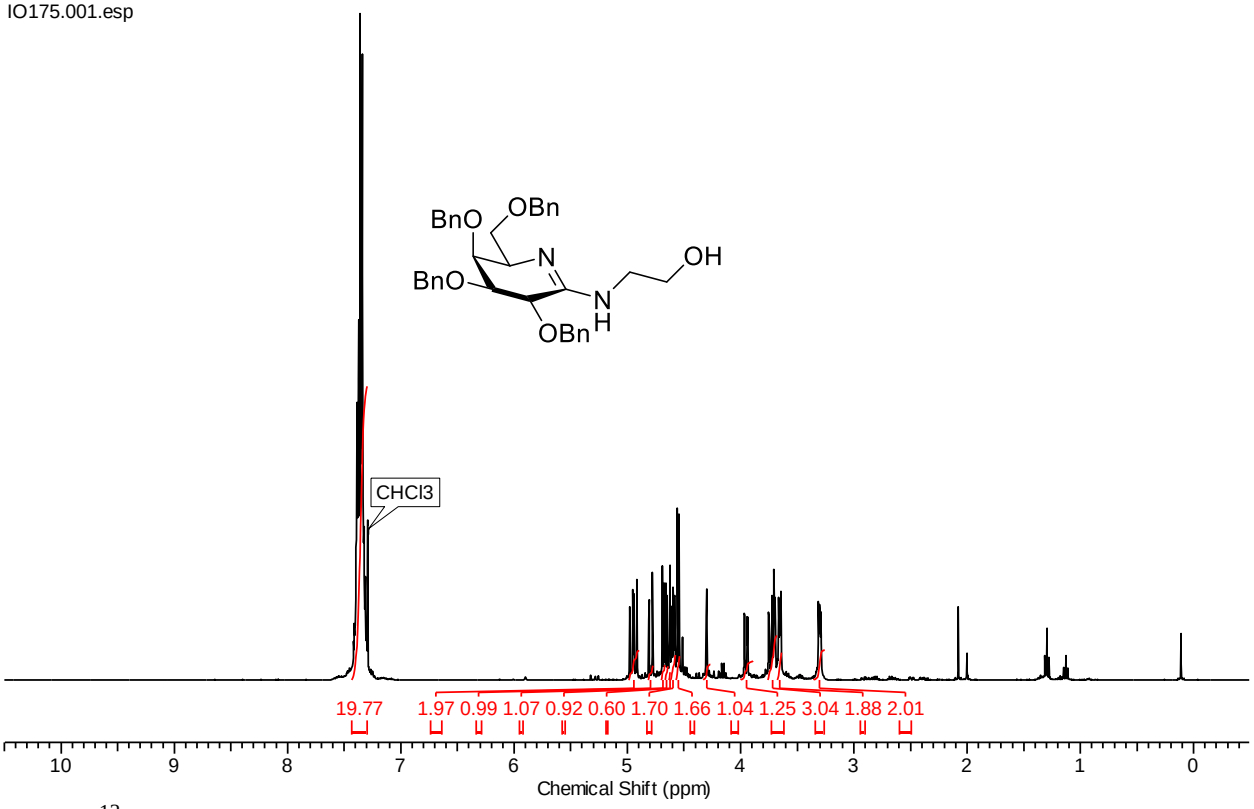

^{13}C NMR (100.6 MHz, $CDCl_3$)

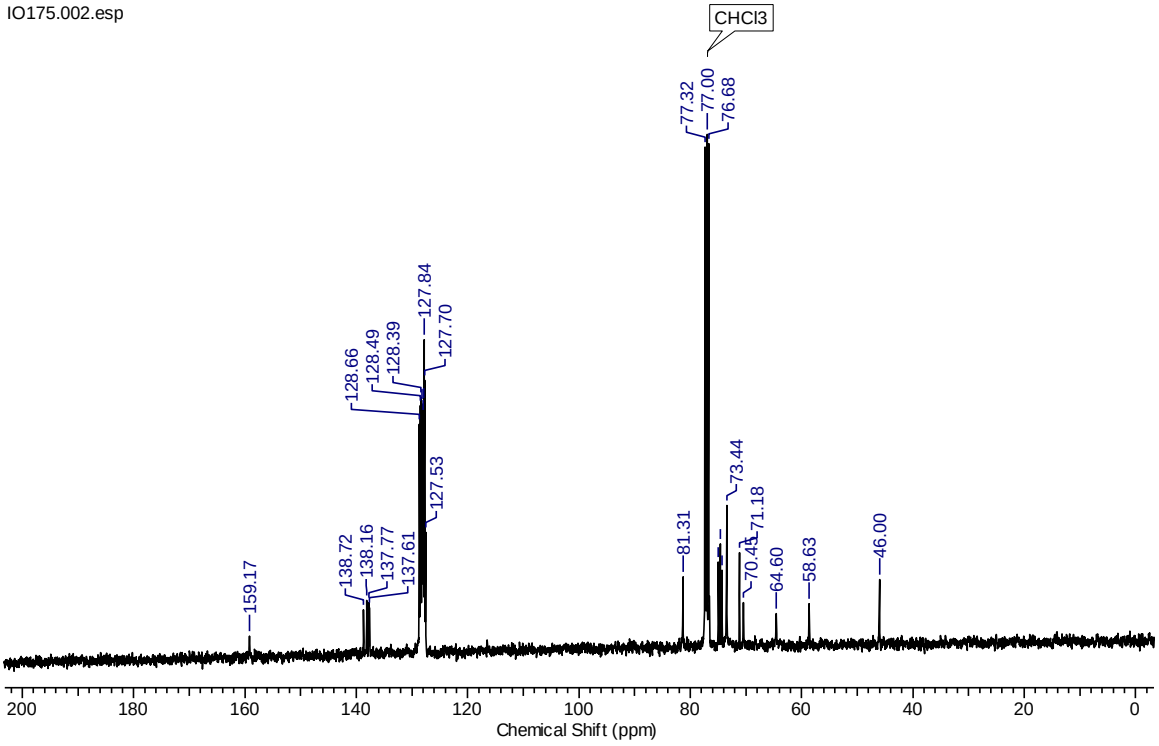

Compound 16k

^{1}H NMR (400 MHz, D_2O)

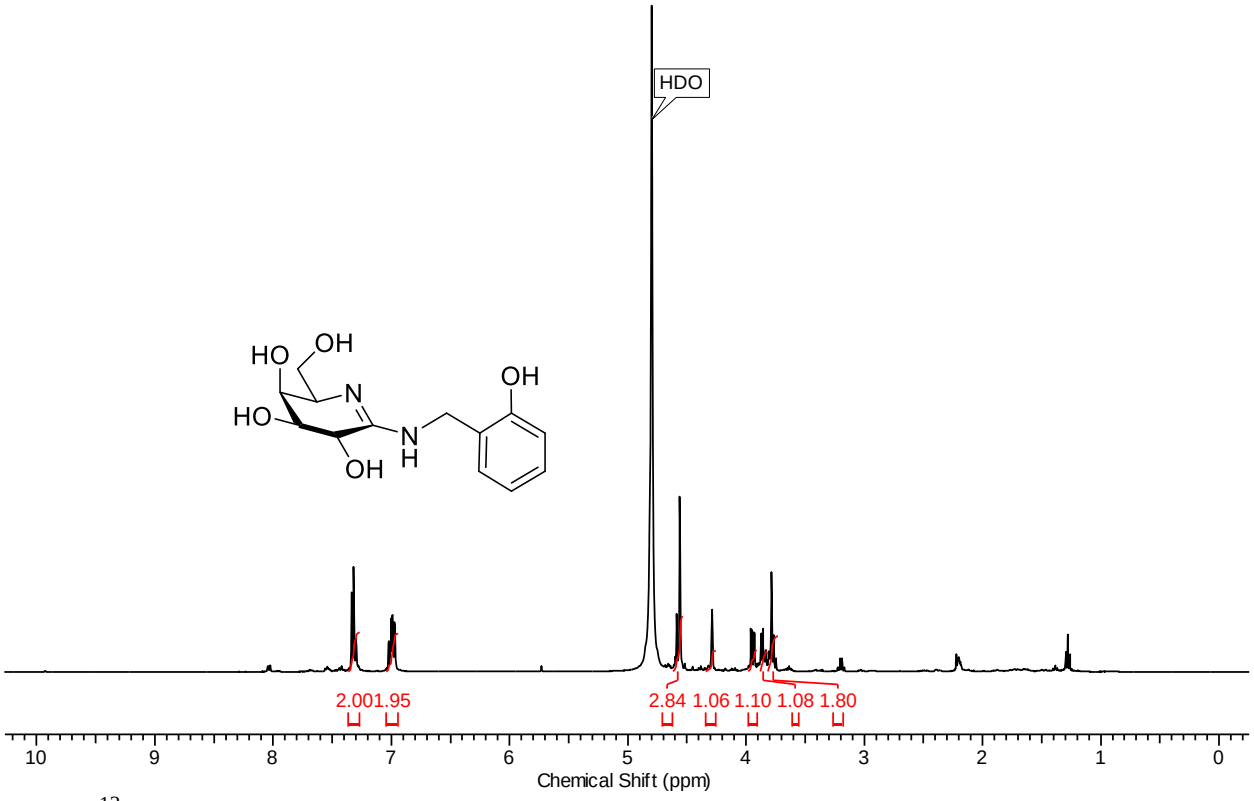

^{13}C NMR (101 MHz, D_2O + MeOD-d_4)

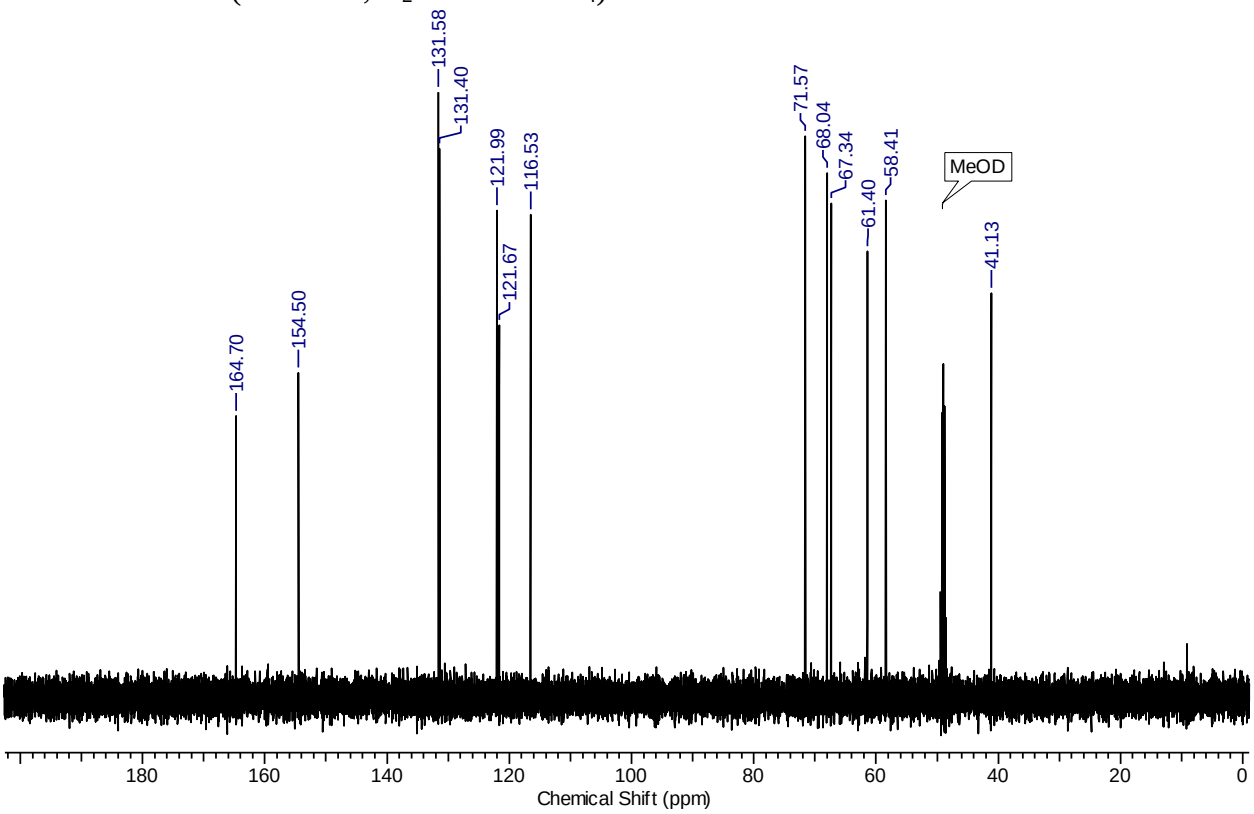

IO268

^{1}H NMR (400 MHz, D_2O)

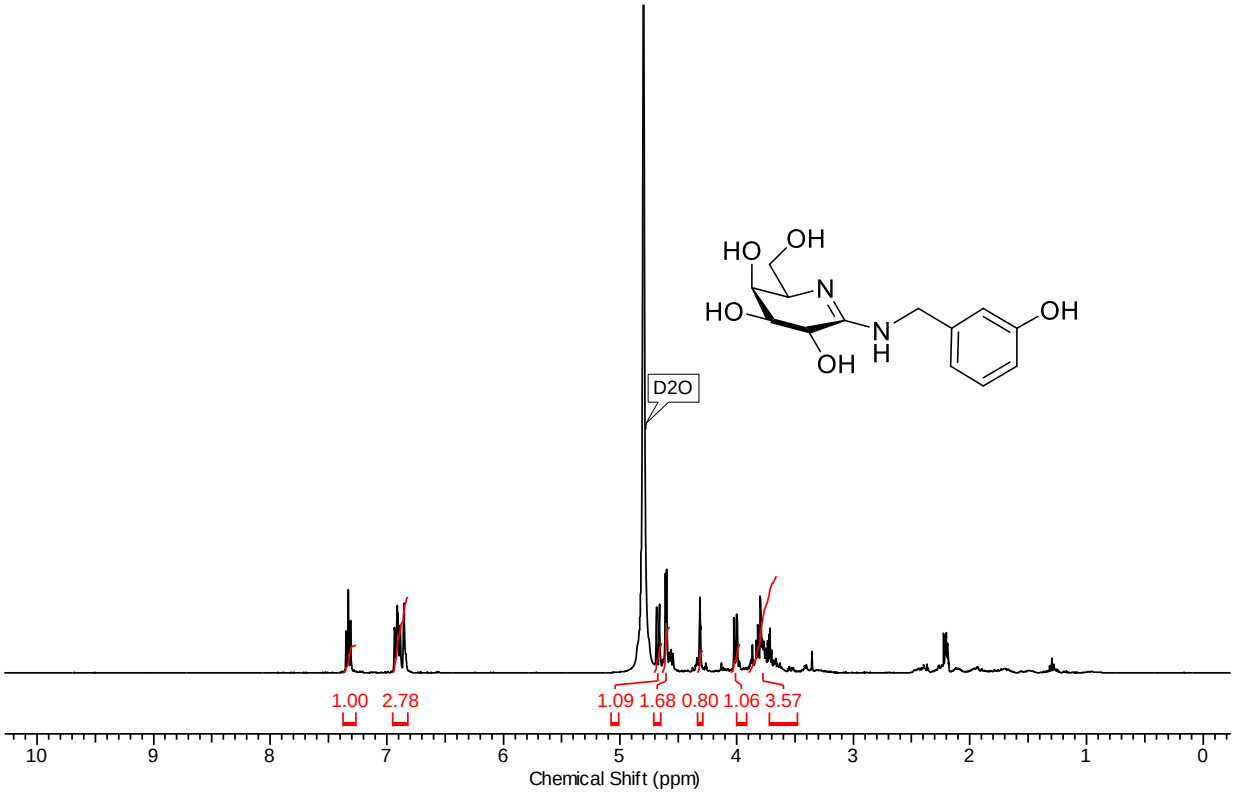

^{13}C NMR (101 MHz, D_2O + MeOD-d_4)

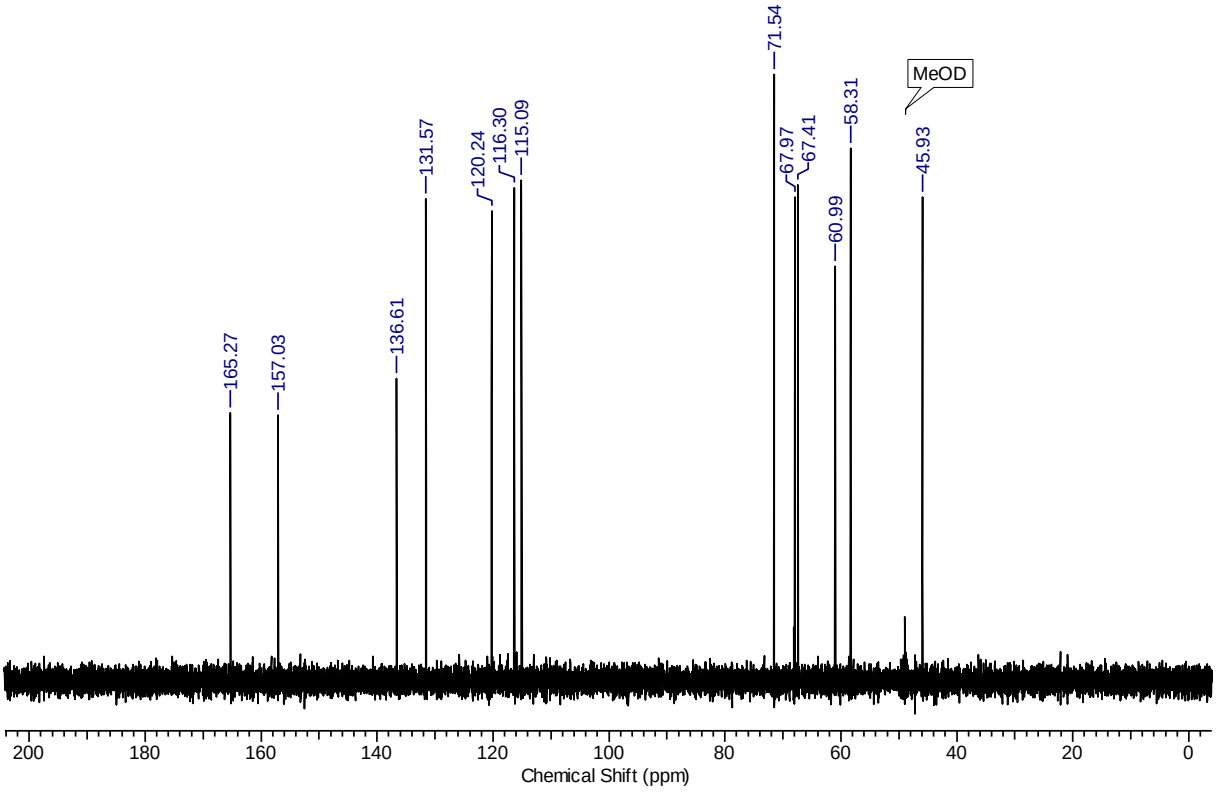

Compound 16m

^{1}H NMR (400.15 MHz, D_2O)

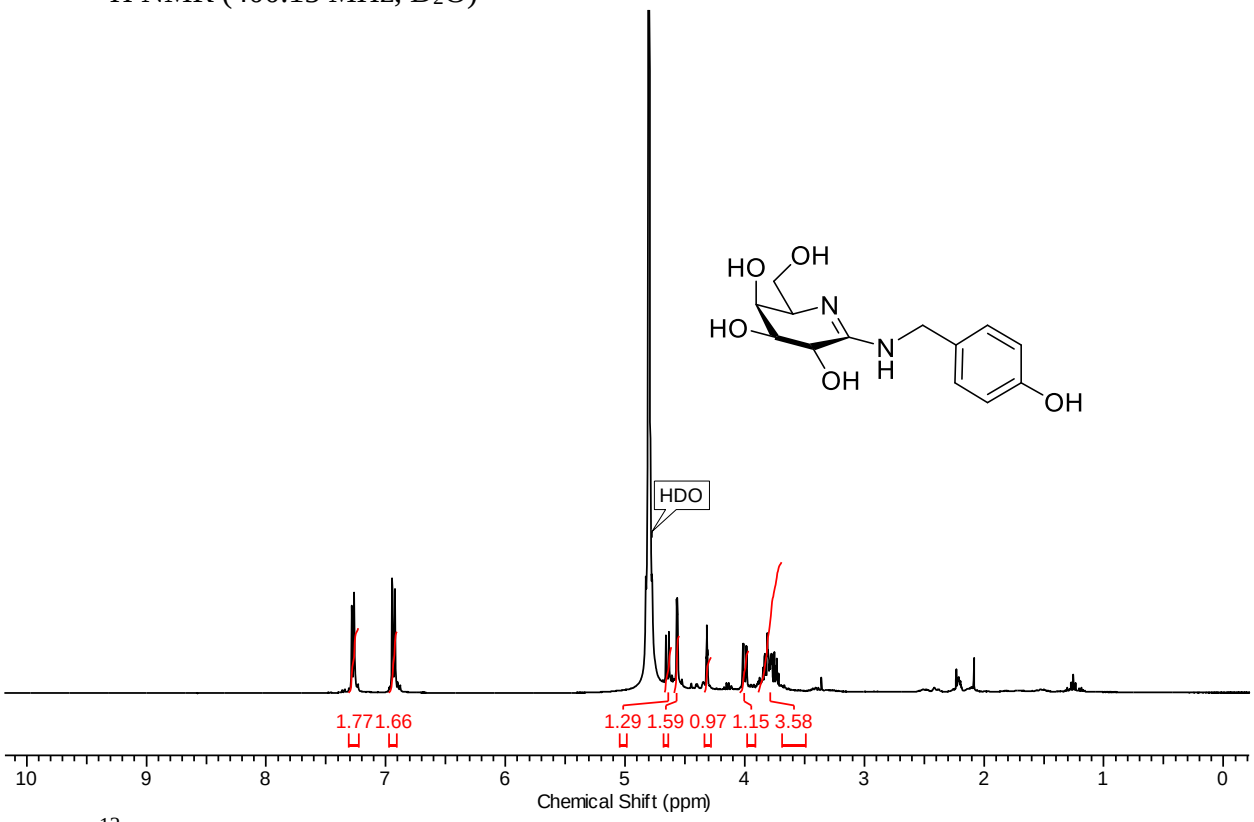

^{13}C NMR (100.6 MHz, D_2O + DMSO-d_6)

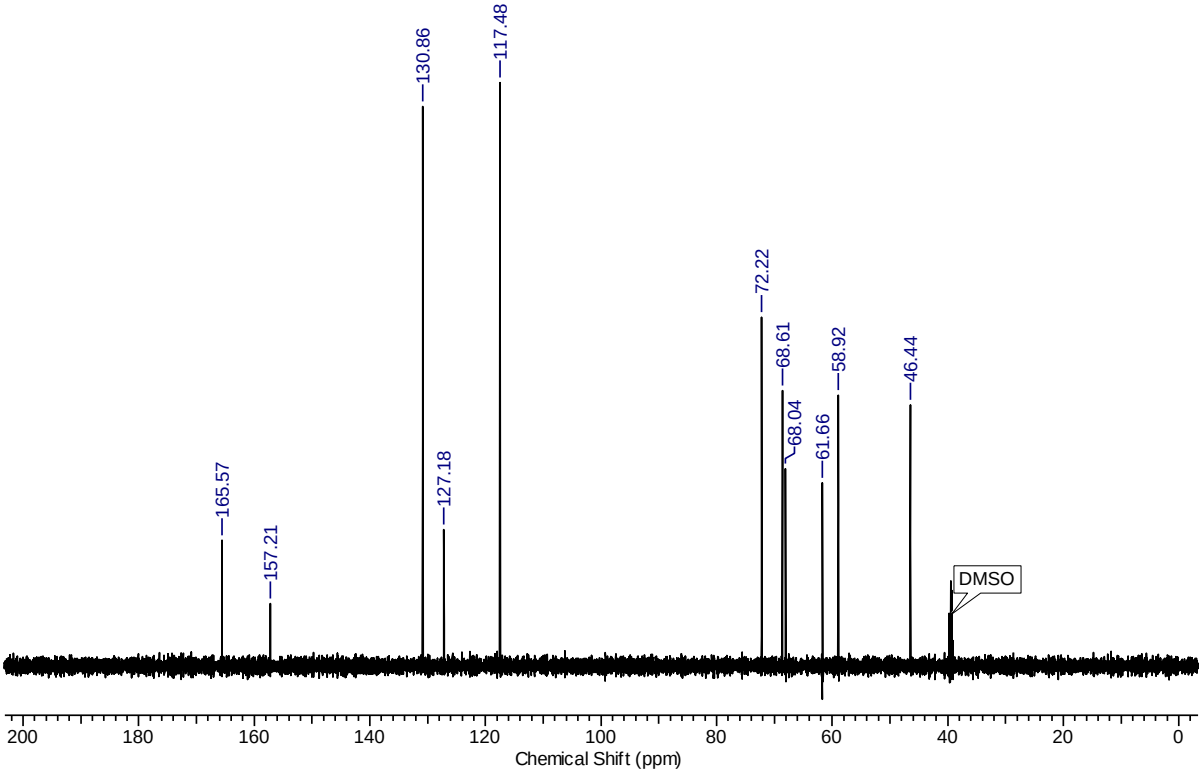

Compound 16n

^{1}H NMR (400.15 MHz, D_2O)

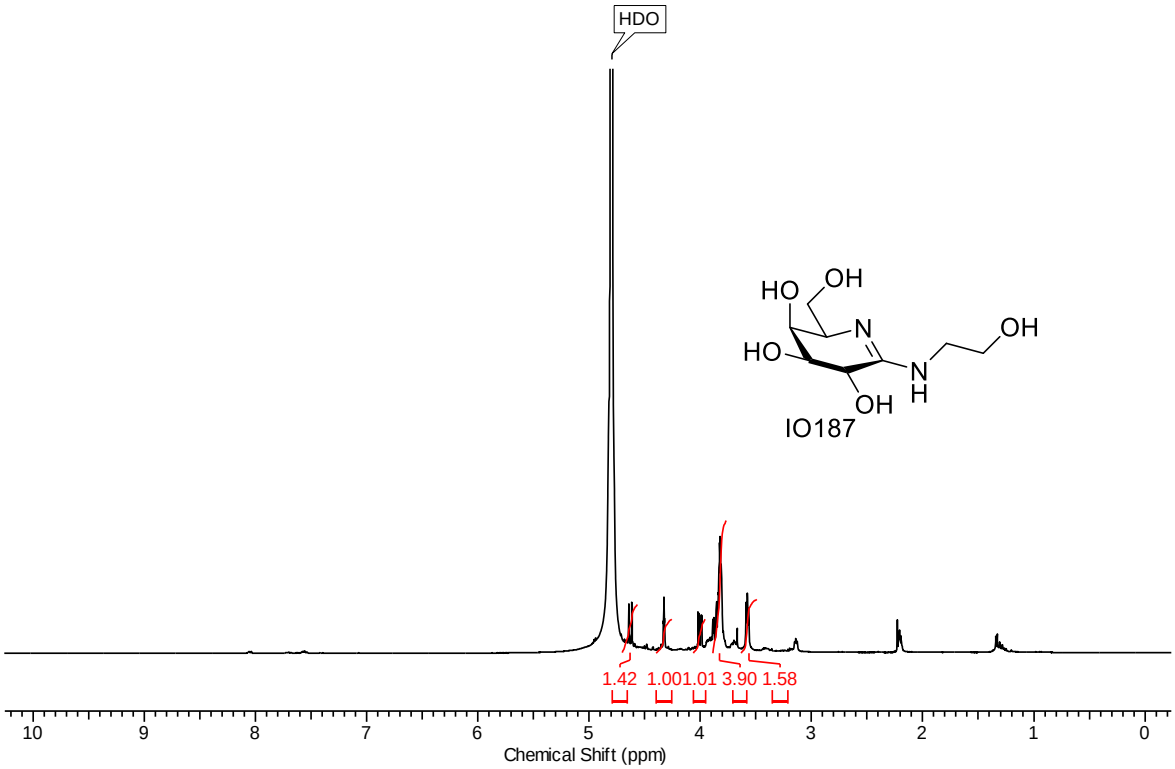

^{13}C NMR (100.6 MHz, D_2O + DMSO-d_6)

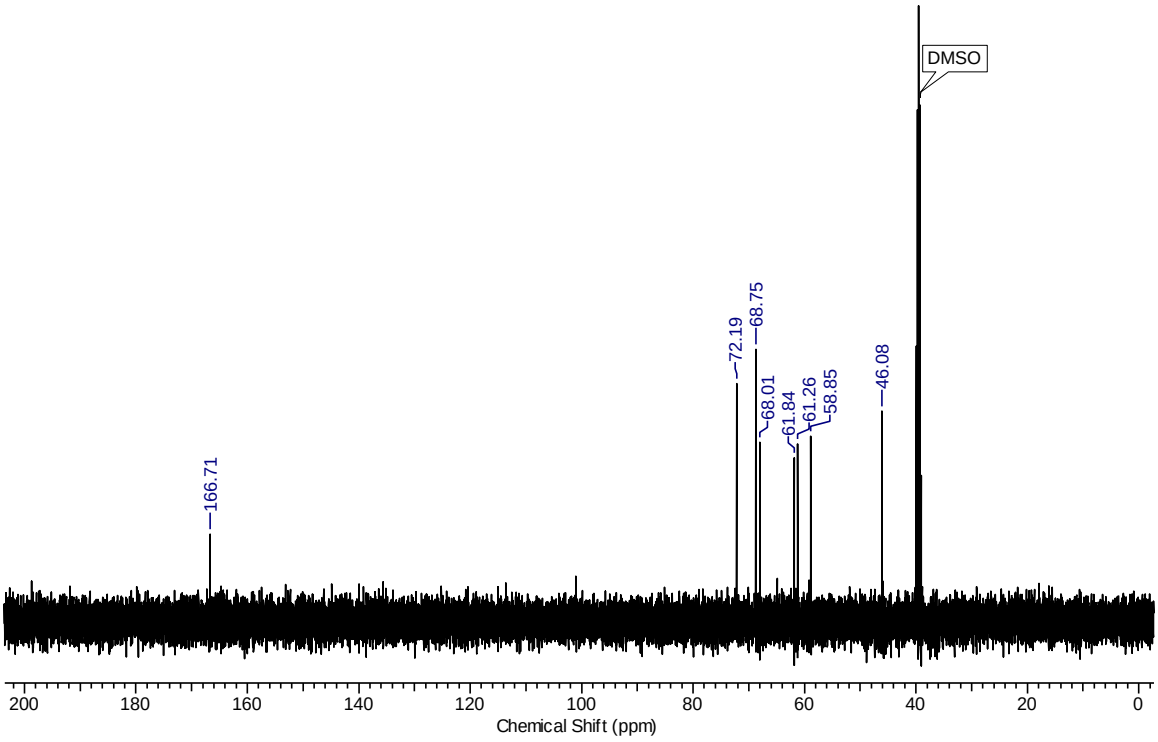

Compound 16o

^{1}H NMR (400 MHz, D_2O)

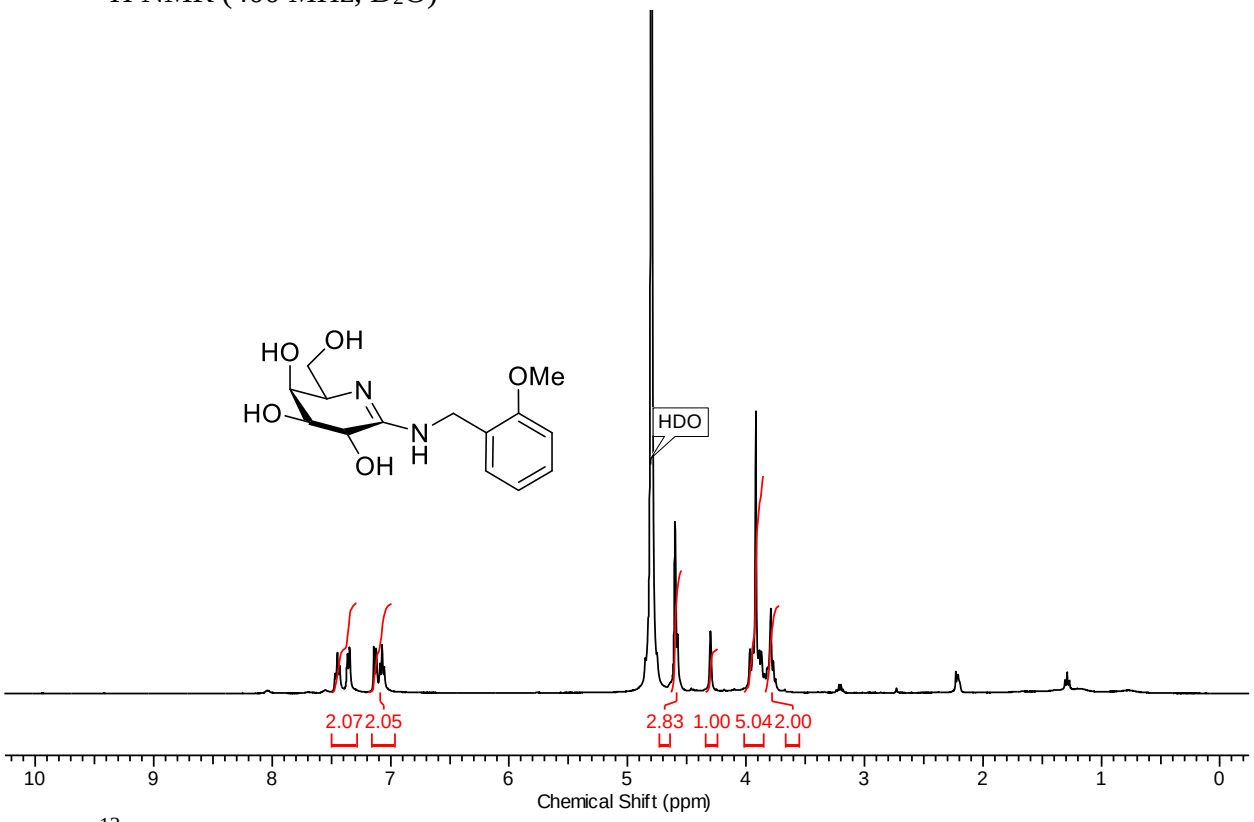

^{13}C NMR (101 MHz, D_2O + MeOD-d_4)

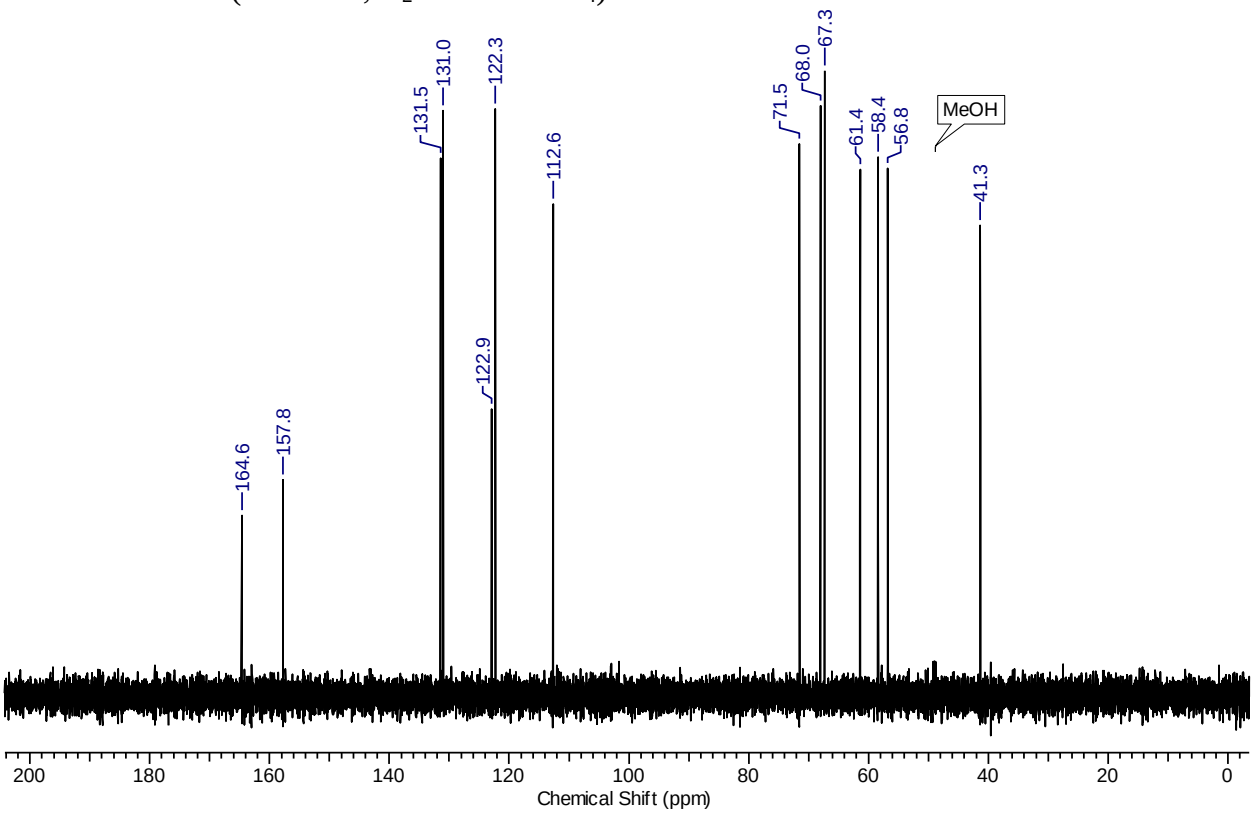

Compound 16p

^{1}H NMR (400.15 MHz, D_2O)

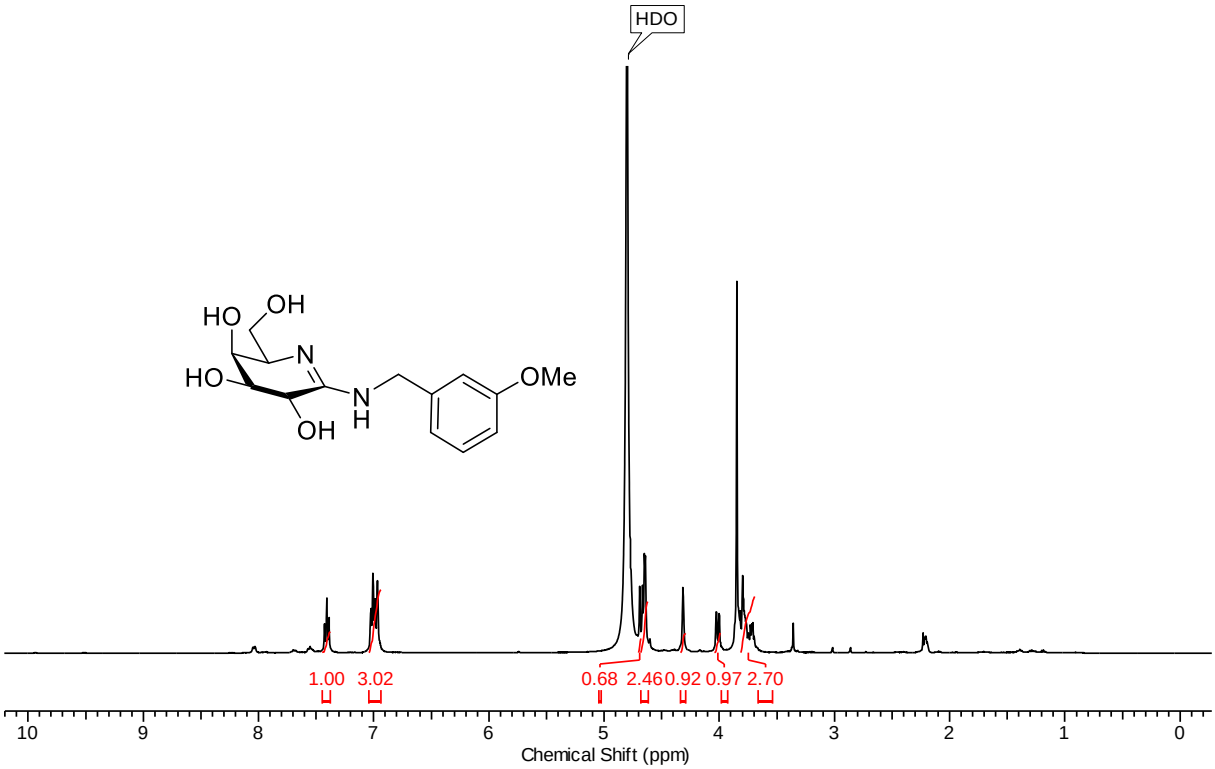

^{13}C NMR (100.6 MHz, D_2O + DMSO-d_6)

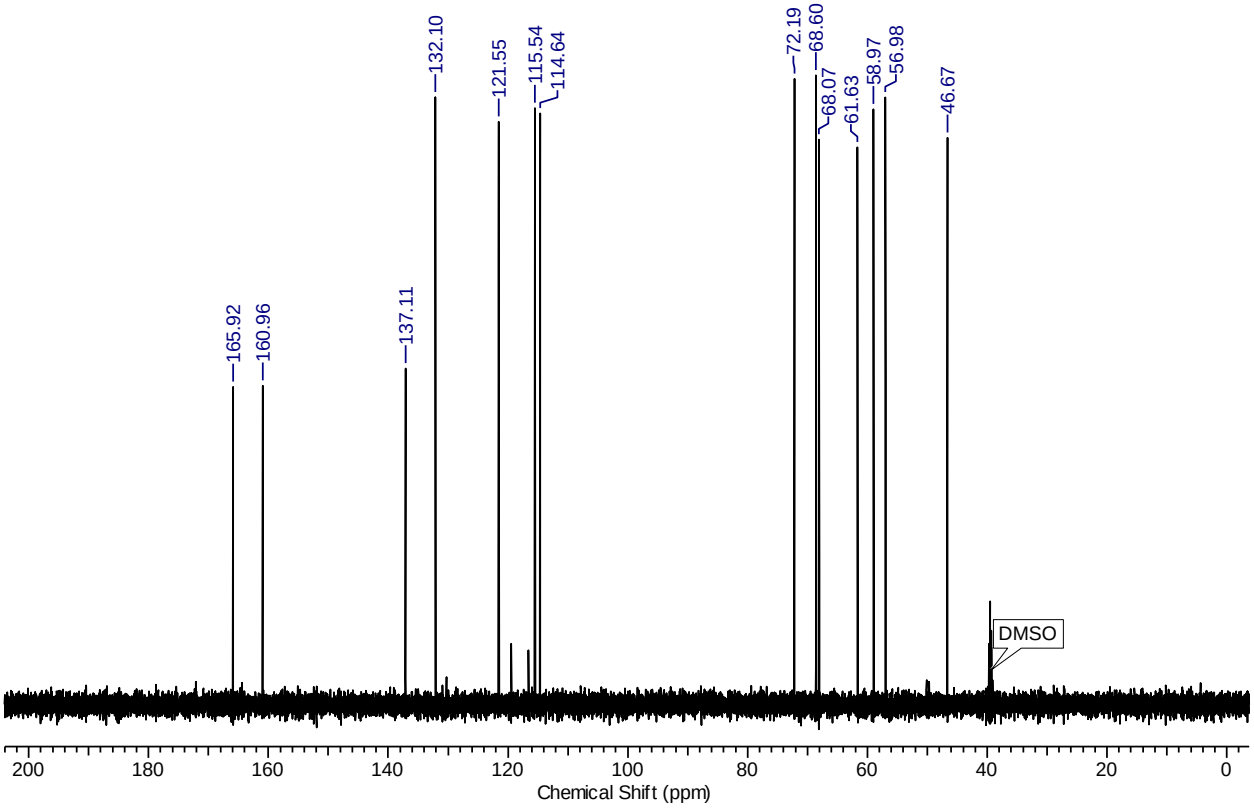

Compound 16q

^{1}H NMR (400.15 MHz, D_2O)

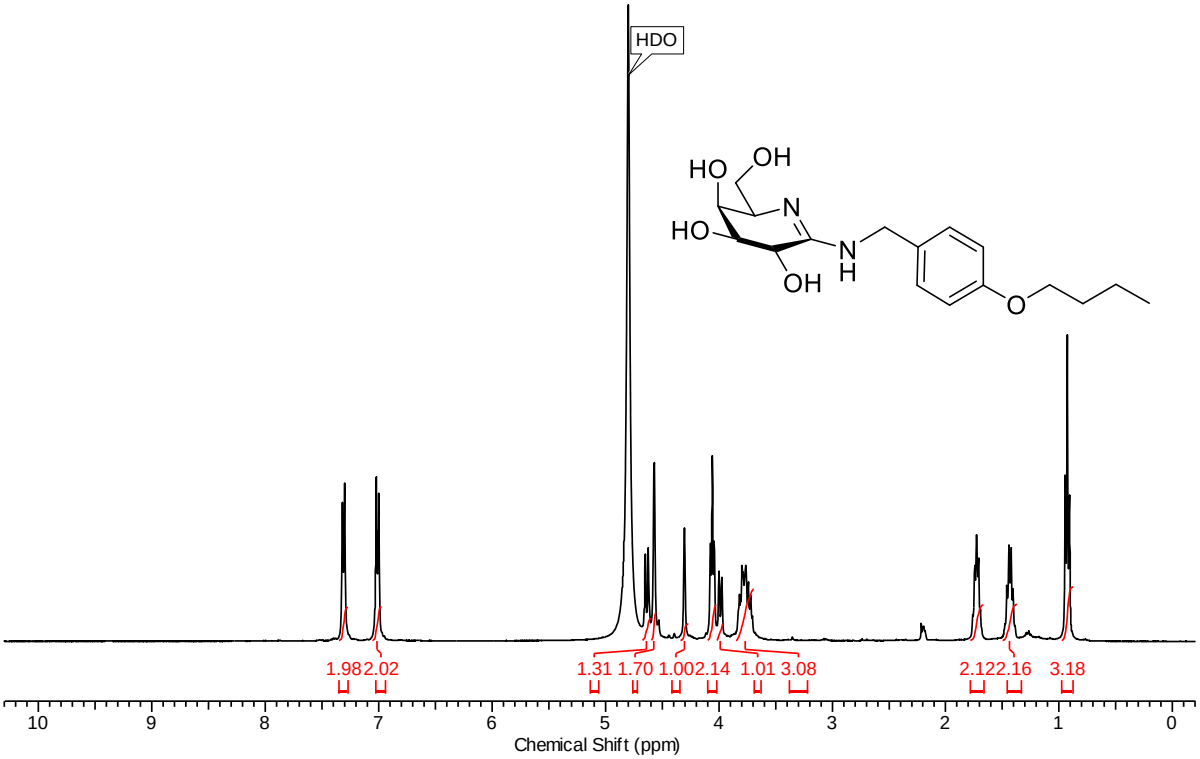

^{13}C NMR (100.6 MHz, D_2O + DMSO-d_6)

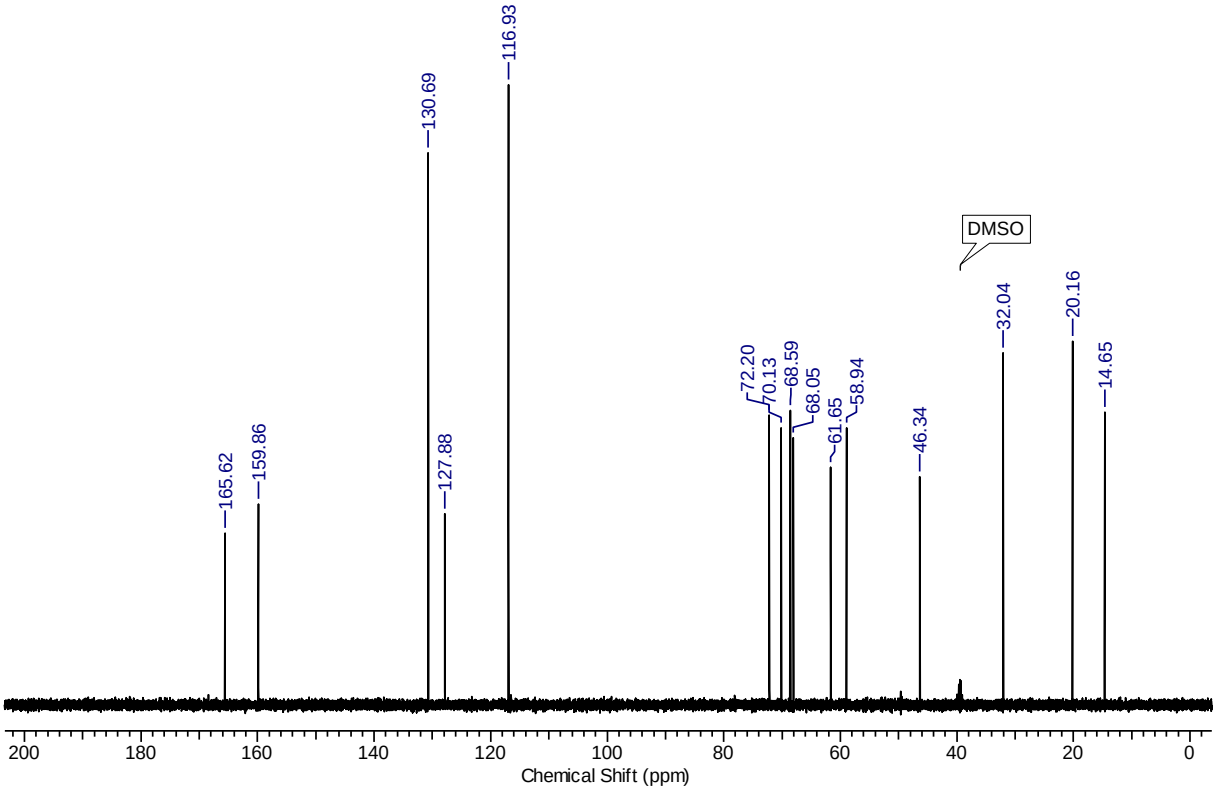

Compound 16r

^{1}H NMR (400.15 MHz, MeOD)

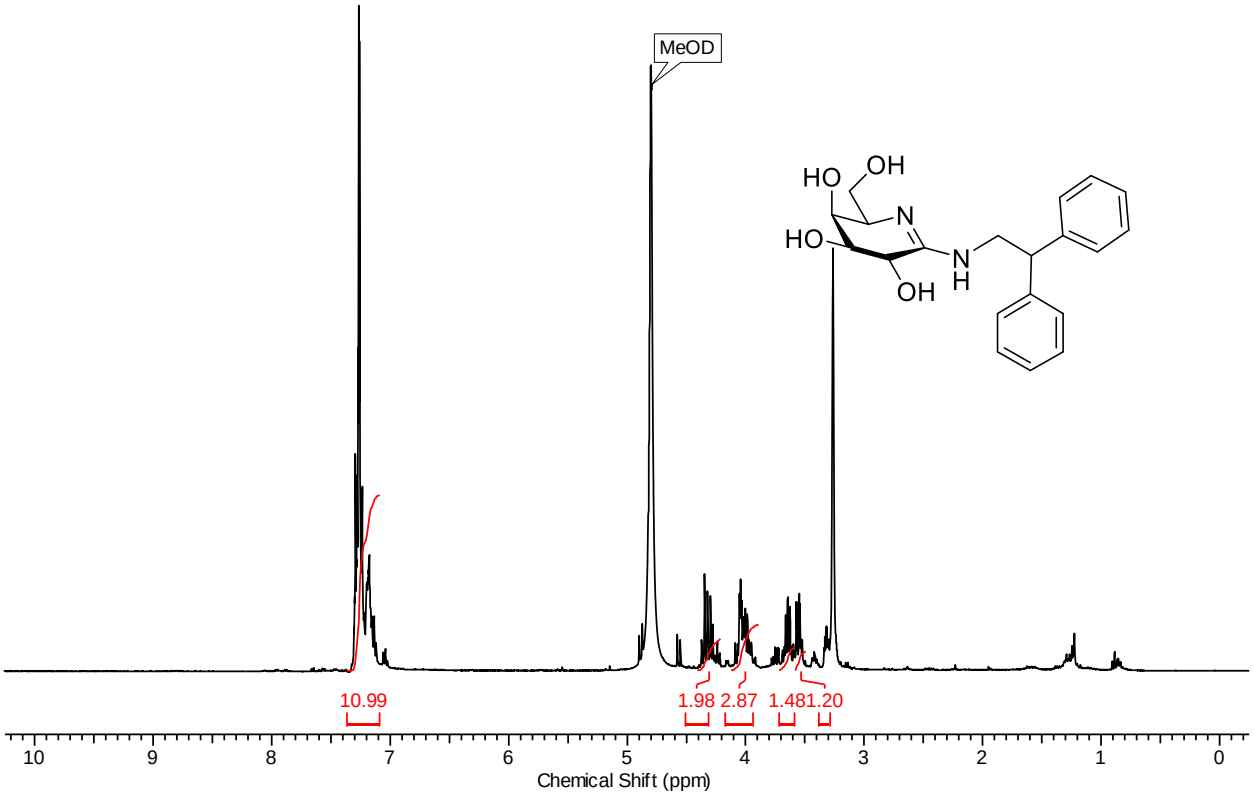

^{13}C NMR (100.6 MHz, MeOD)

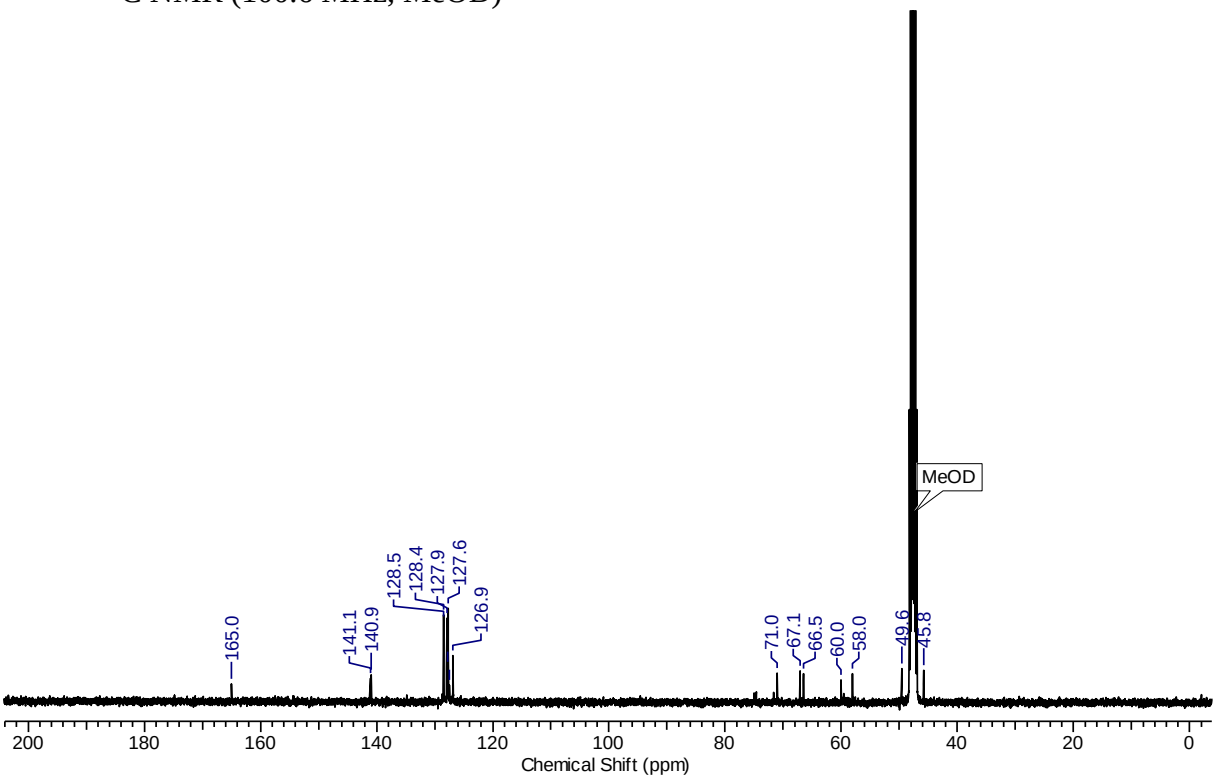

Compound 16s

^{1}H NMR (400 MHz, MeOD-d_4)

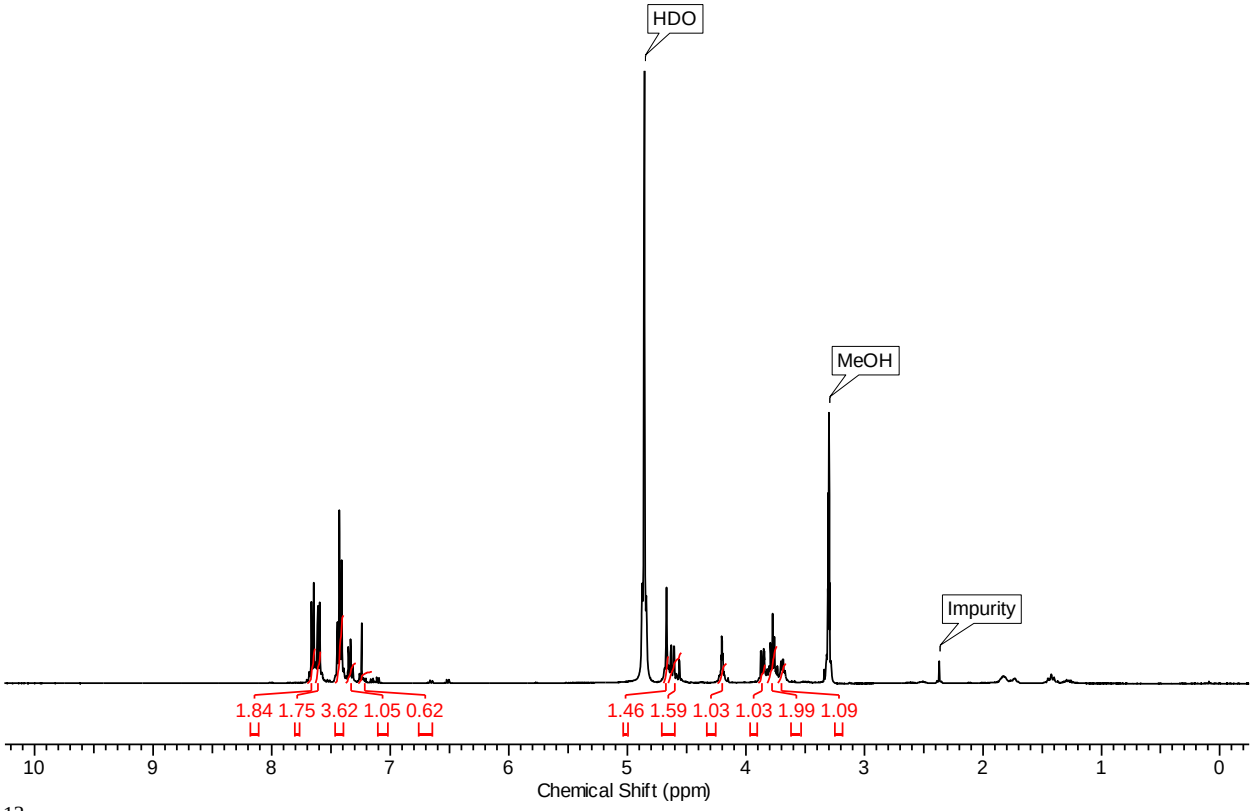

^{13}C NMR (100.6 MHz, D_2O + MeOD-d_4)

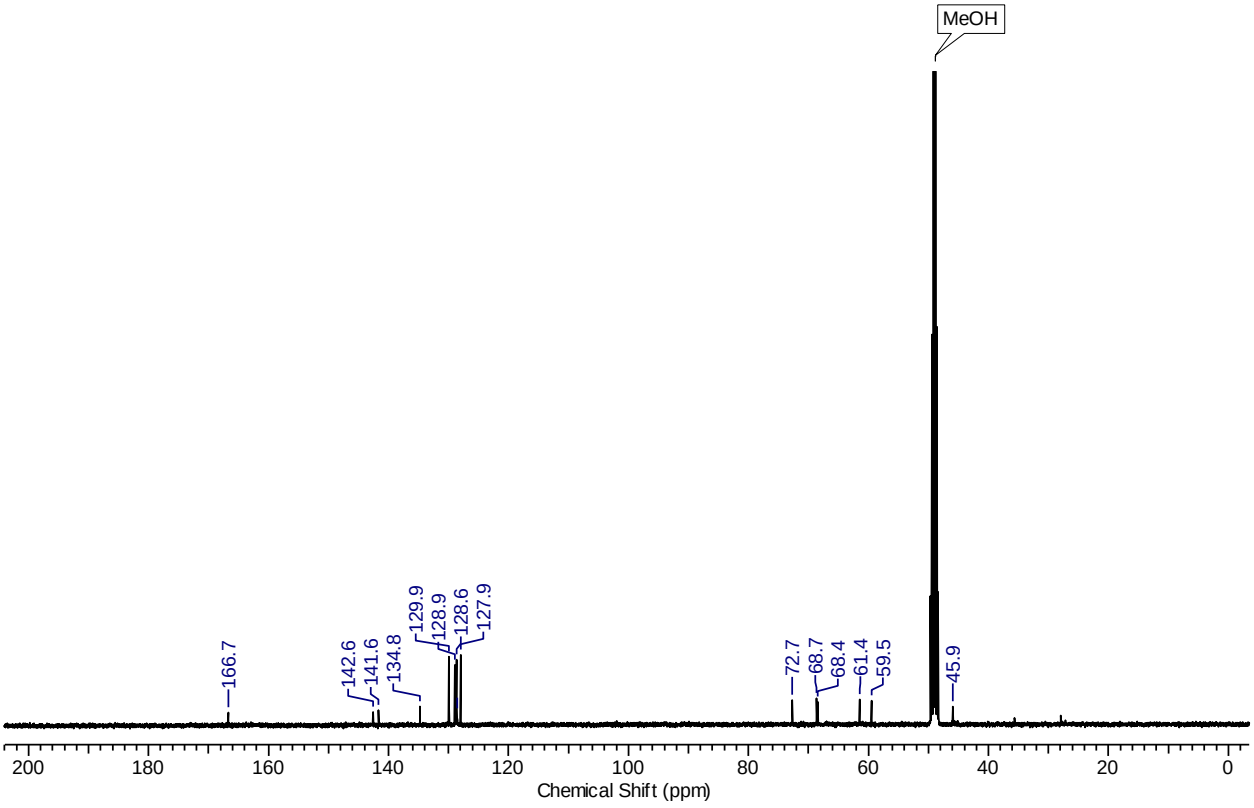

Compound 16t

^{1}H NMR (400 MHz, D_2O)

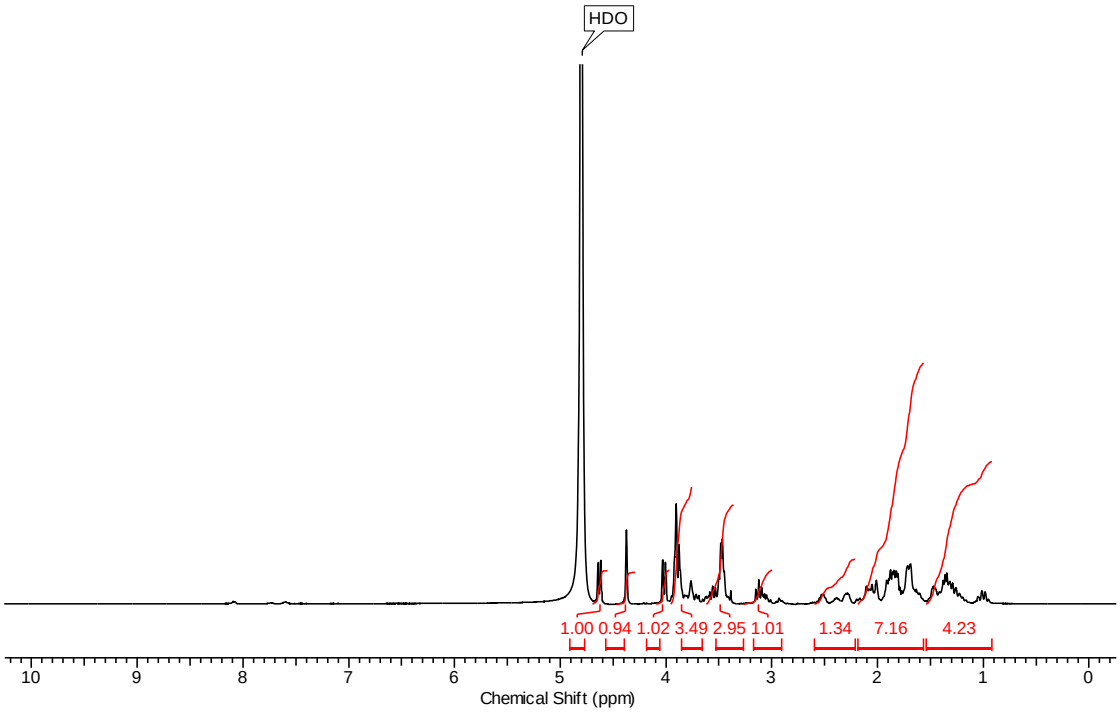

^{13}C NMR (100.6 MHz, D_2O + MeOD-d_4)

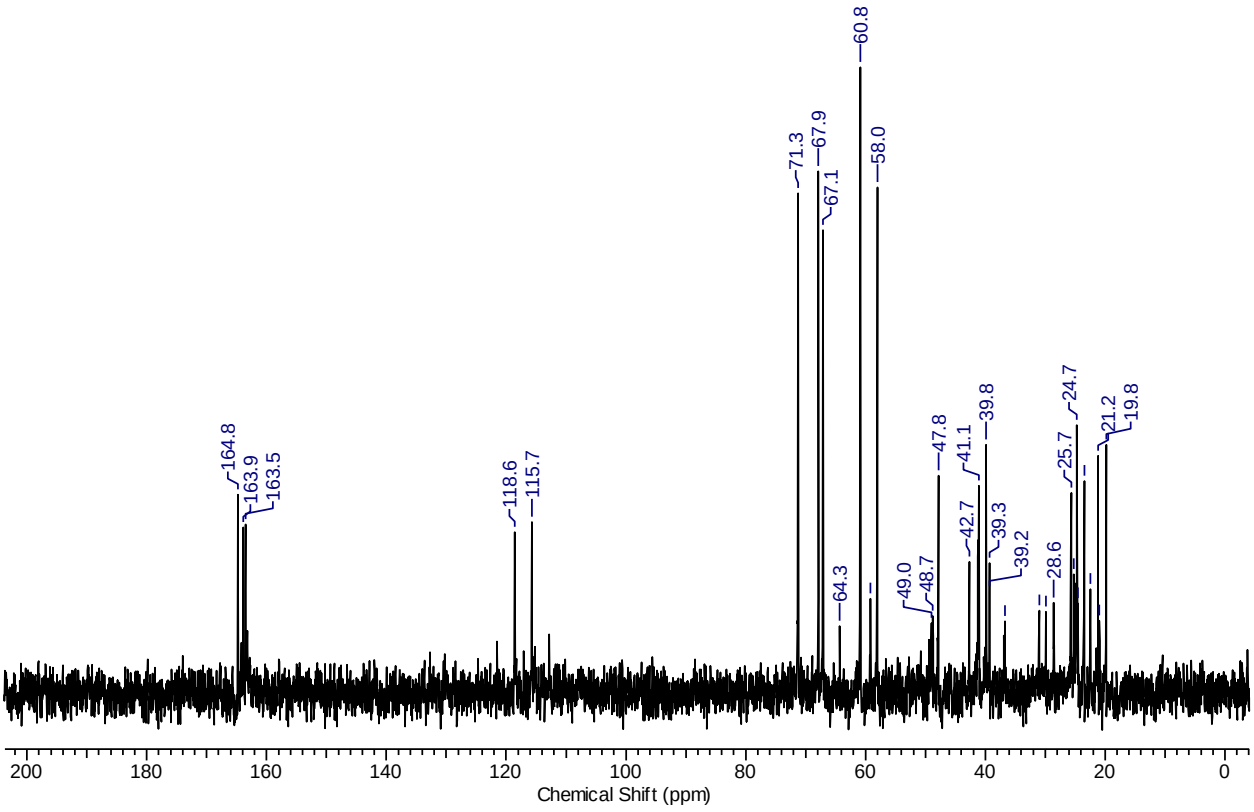

6: References

1. Gloster, T. M.; Vocadlo, D. J., Developing inhibitors of glycan processing enzymes as tools for enabling glycobiology. *Nature Chemical Biology* **2012,** *8*, 683-694.

2. Alonso, M. D.; Lomako, J.; Lomako, W. M.; Whelan, W. J., Catalytic activities of glycogenin additional to autocatalytic self-glucosylation. *Journal of Biological Chemistry* **1995,** *270*, 15315-15319.

3. Bigg, H. F.; Wait, R.; Rowan, A. D.; Cawston, T. E., The mammalian chitinase-like lectin, YKL-40, binds specifically to type I collagen and modulates the rate of type I collagen fibril formation. *Journal of Biological Chemistry* **2006,** *281*, 21082-21095.

4. Vasudevan, D.; Takeuchi, H.; Johar, S. S.; Majerus, E.; Haltiwanger, R. S., Peters plus syndrome mutations disrupt a noncanonical er quality-control mechanism. *Current Biology* **2015,** *25*, 286-295.

5. Williams, C.; Pazos, R.; Royo, F.; Gonzalez, E.; Roura-Ferrer, M.; Martinez, A.; Gamiz, J.; Reichardt, N. C.; Falcon-Perez, J. M., Assessing the role of surface glycans of extracellular vesicles on cellular uptake. *Scientific Reports* **2019,** *9*.

6. Asano, N., Sugar-mimicking glycosidase inhibitors: bioactivity and application. *Cellular and Molecular Life Sciences* **2009,** *66*, 1479-1492.

7. Dou, H. Q.; Sun, G. R.; Zhang, L. J., CA242 as a biomarker for pancreatic cancer and other diseases. *Glycans and Glycosaminoglycans as Clinical Biomarkers and Therapeutics, Pt A* **2019,** *162*, 229-239.

8. Haglund, C.; Lindgren, J.; Roberts, P. J.; Kuusela, P.; Nordling, S., Tissue expression of the tumor associated antigen-ca242 in benign and malignant pancreatic lesions - a comparison with CA-50 and CA-19-9. *British Journal of Cancer* **1989,** *60*, 845-851.

9. Kajimoto, T.; Node, M., Inhibitors against glycosidases as medicines. *Current Topics in Medicinal Chemistry* **2009,** *9*, 13-33.

10. Henrissat, B.; Bairoch, A., Updating the sequence-based classification of glycosyl hydrolases. *Biochemical Journal* **1996,** *316*, 695-696.

11. Henrissat, B.; Davies, G., Structural and sequence-based classification of glycoside hydrolases. *Current Opinion in Structural Biology* **1997,** *7*, 637-644.

12. Henrissat, B.; Callebaut, I.; Fabrega, S.; Lehn, P.; Mornon, J. P.; Davies, G., Conserved catalytic machinery and the prediction of a common fold for several families of glycosyl hydrolases. *Proceedings of the National Academy of Sciences of the United States of America* **1995,** *92*, 7090-7094.

13. Koshland, D. E., Stereochemistry and the mechanism of enzymatic reactions. *Biological Reviews of the Cambridge Philosophical Society* **1953,** *28*, 416-436.

14. Sinnott, M. L., Catalytic mechanisms of enzymatic glycosyl transfer. *Chemical Reviews* **1990,** *90*, 1171-1202.

15. Martin, A.; Arda, A.; Desire, J.; Martin-Mingot, A.; Probst, N.; Sinay, P.; Jimenez-Barbero, J.; Thibaudeau, S.; Bleriot, Y., Catching elusive glycosyl cations in a condensed phase with HF/SbF5 superacid. *Nature Chemistry* **2016,** *8*, 186-191.

16. Frihed, T. G.; Bols, M.; Pedersen, C. M., Mechanisms of Glycosylation reactions studied by low-temperature nuclear magnetic resonance. *Chemical Reviews* **2015,** *115*, 4963-5013.

17. Denekamp, C.; Sandlers, Y., Anomeric distinction and oxonium ion formation in acetylated glycosides. *Journal of Mass Spectrometry* **2005,** *40*, 765-771.

18. Denekamp, C.; Sandlers, Y., Formation and stability of oxocarbenium ions from glycosides. *Journal of Mass Spectrometry* **2005,** *40*, 1055-1063.

19. Crich, D.; Chandrasekera, N. S., Mechanism of 4,6-0-benzylidene-directed beta-mannosylation as determined by alpha-deuterium kinetic isotope effects. *Angewandte Chemie-International Edition* **2004,** *43*, 5386-5389.

20. Elferink, H.; Severijnen, M. E.; Martens, J.; Mensink, R. A.; Berden, G.; Oomens, J.; Rutjes, F.; Rijs, A. M.; Boltje, T. J., Direct experimental characterization of glycosyl cations by infrared ion spectroscopy. *Journal of the American Chemical Society* **2018,** *140*, 6034-6038.

21. Mucha, E.; Marianski, M.; Xu, F. F.; Thomas, D. A.; Meijer, G.; von Helden, G.; Seeberger, P. H.; Pagel, K., Unravelling the structure of glycosyl cations via cold-ion infrared spectroscopy. *Nature Communications* **2018,** *9*, 5.

22. Davies, G. J.; Planas, A.; Rovira, C., Conformational analyses of the reaction coordinate of glycosidases. *Accounts of Chemical Research* **2012,** *45*, 308-316.

23. Vasella, A.; Davies, G. J.; Bohm, M., Glycosidase mechanisms. *Current Opinion in Chemical Biology* **2002,** *6*, 619-629.

24. Davies, G.; Henrissat, B., Structures and mechanisms of glycosyl hydrolases. *Structure* **1995,** *3*, 853-859.

25. Knapp, S.; Vocadlo, D.; Gao, Z. N.; Kirk, B.; Lou, J. P.; Withers, S. G., NAG-thiazoline, an N-acetyl-beta-hexosaminidase inhibitor that implicates acetamido participation. *Journal of the American Chemical Society* **1996,** *118*, 6804-6805.

26. Coines, J.; Raich, L.; Rovira, C., Modeling catalytic reaction mechanisms in glycoside hydrolases. *Current Opinion in Chemical Biology* **2019,** *53*, 183-191.

27. Newstead, S. L.; Potter, J. A.; Wilson, J. C.; Xu, G. G.; Chien, C. H.; Watts, A. G.; Withers, S. G.; Taylor, G. L., The structure of Clostridium perfringens NanI sialidase and its catalytic intermediates. *Journal of Biological Chemistry* **2008,** *283*, 9080-9088.

28. Rogers, I. L.; Naidoo, K. J., Profiling transition-state configurations on the trypanosoma cruzi trans-sialidase free-energy reaction surfaces. *Journal of Physical Chemistry B* **2015,** *119*, 1192-1201.

29. Sobala, L. F.; Speciale, G.; Zhu, S.; Raich, L.; Sannikova, N.; Thompson, A. J.; Hakki, Z.; Lu, D.; Abadi, S. S. K.; Lewis, A. R.; Rojas-Cervellera, V.; Bernardo-Seisdedos, G.; Zhang, Y. M.; Millet, O.; Jimenez-Barbero, J.; Bennet, A. J.; Sollogoub, M.; Rovira, C.; Davies, G. J.; Williams, S. J., An epoxide intermediate in glycosidase catalysis. *Acs Central Science* **2020,** *6*, 760-770.

30. Petricevic, M.; Sobala, L. F.; Fernandes, P. Z.; Raich, L.; Thompson, A. J.; Bernardo-Seisdedos, G.; Millet, O.; Zhu, S.; Sollogoub, M.; Jimenez-Barbero, J.; Rovira, C.; Davies, G. J.; Williams, S. J., Contribution of shape and charge to the inhibition of a family GH99 endo-alpha-1,2-Mannanase. *Journal of the American Chemical Society* **2017,** *139*, 1089-1097.

31. Adero, P. O.; Amarasekara, H.; Wen, P.; Bohe, L.; Crich, D., The experimental evidence in support of glycosylation mechanisms at the S(N)1-S(N)2 interface. *Chemical Reviews* **2018,** *118*, 8242-8284.

32. Vocadlo, D. J.; Davies, G. J., Mechanistic insights into glycosidase chemistry. *Current Opinion in Chemical Biology* **2008,** *12*, 539-555.

33. Gloster, T. M.; Roberts, S.; Perugino, G.; Rossi, M.; Moracci, M.; Panday, N.; Terinek, M.; Vasella, A.; Davies, G. J., Structural, kinetic, and thermodynamic analysis of glucoimidazole-derived glycosidase inhibitors. *Biochemistry* **2006,** *45*, 11879-11884.

34. Hovel, K.; Shallom, D.; Niefind, K.; Belakhov, V.; Shoham, G.; Baasov, T.; Shoham, Y.; Schomburg, D., Crystal structure and snapshots along the reaction pathway of a family 51 alpha-L-arabinofuranosidase. *Embo Journal* **2003,** *22*, 4922-4932.

35. Artola, M.; Hedberg, C.; Rowland, R. J.; Raich, L.; Kytidou, K.; Wu, L.; Schaaf, A.; Ferraz, M. J.; van der Marel, G. A.; Codee, J. D. C.; Rovira, C.; Aerts, J.; Davies, G. J.; Overkleeft, H. S., alpha-d-Gal-cyclophellitol cyclosulfamidate is a Michaelis complex analog that stabilizes therapeutic lysosomal alpha-galactosidase A in Fabry disease. *Chemical Science* **2019,** *10*, 9233-9243.

36. McGregor, N. G. S.; Artola, M.; Nin-Hill, A.; Linzel, D.; Haon, M.; Reijngoud, J.; Ram, A.; Rosso, M. N.; van der Marel, G. A.; Codee, J. D. C.; van Wezel, G. P.; Berrin, J. G.; Rovira, C.; Overkleeft, H. S.; Davies, G. J., Rational design of mechanism-based inhibitors and activity-based probes for the identification of retaining alpha-L-arabinofuranosidases. *Journal of the American Chemical Society* **2020,** *142*, 4648-4662.

37. Cremer, D.; Pople, J. A., General definition of ring puckering coordinates. *Journal of the American Chemical Society* **1975,** *97*, 1354-1358.

38. Kallemeijn, W. W.; Witte, M. D.; Wennekes, T.; Aerts, J., Mechanism-based inhibitors of glycosidases: design and applications. *Advances in Carbohydrate Chemistry and Biochemistry, Vol 71* **2014,** *71*, 297-338.

39. Pauling, L., Nature of forces between large molecules of biological interest. *Nature* **1948,** *161*, 707-709.

40. Wolfenden, R.; Lu, X. D.; Young, G., Spontaneous hydrolysis of glycosides. *Journal of the American Chemical Society* **1998,** *120*, 6814-6815.

41. Gloster, T. M.; Meloncelli, P.; Stick, R. V.; Zechel, D.; Vasella, A.; Davies, G. J., Glycosidase inhibition: An assessment of the binding of 18 putative transition-state mimics. *Journal of the American Chemical Society* **2007,** *129*, 2345-2354.

42. Tailford, L. E.; Offen, W. A.; Smith, N. L.; Dumon, C.; Morland, C.; Gratien, J.; Heck, M. P.; Stick, R. V.; Bleriot, Y.; Vasella, A.; Gilbert, H. J.; Davies, G. J., Structural and biochemical evidence for a boat-like transition state in beta-mannosidases. *Nature Chemical Biology* **2008,** *4*, 306-312.

43. Gloster, T. M.; Davies, G. J., Glycosidase inhibition: assessing mimicry of the transition state. *Organic & Biomolecular Chemistry* **2010,** *8*, 305-320.

44. Heightman, T. D.; Vasella, A. T., Recent insights into inhibition, structure, and mechanism of configuration-retaining glycosidases. *Angewandte Chemie-International Edition* **1999,** *38*, 750-770.

45. Ganem, B., Inhibitors of carbohydrate-processing enzymes: Design and synthesis of sugar-shaped heterocycles. *Accounts of Chemical Research* **1996,** *29*, 340-347.

46. Terinek, M.; Vasella, A., Synthesis of C(2)-substituted manno-configured tetrahydroimidazopyridines and their evaluation as inhibitors of snail beta-mannosidase. *Helvetica Chimica Acta* **2003,** *86*, 3482-3509.

47. Terinek, M.; Vasella, A., Synthesis of tetrahydropyridoimidazole-2-acetates: Effect of carboxy and methoxycarbonyl groups at C(2) on the inhibition of some beta- and alpha-glycosidases. *Helvetica Chimica Acta* **2004,** *87*, 3035-3049.

48. Tong, M. K.; Papandreou, G.; Ganem, B., Potent, broad-spectrum inhibition of glycosidases by an amidine derivative of d-glucose. *Journal of the American Chemical Society* **1990,** *112*, 6137-6139.

49. Ganem, B.; Papandreou, G., Mimicking the glucosidase transition-state - shape charge considerations. *Journal of the American Chemical Society* **1991,** *113*, 8984-8985.

50. Papandreou, G.; Tong, M. K.; Ganem, B., Amidine, amidrazone, and amidoxime derivatives of monosaccharide aldonolactams - synthesis and evaluation as glycosidase inhibitors. *Journal of the American Chemical Society* **1993,** *115*, 11682-11690.

51. Bleriot, Y.; Genregrandpierre, A.; Tellier, C., Synthesis of a benzylamidine derived from d-mannose - a potent mannosidase inhibitor. *Tetrahedron Letters* **1994,** *35*, 1867-1870.

52. Bleriot, Y.; Dintinger, T.; Genregrandpierre, A.; Padrines, M.; Tellier, C., Inhibition of glycosidases by substituted amidines. *Bioorganic & Medicinal Chemistry Letters* **1995,** *5*, 2655-2660.

53. Heck, M. P.; Vincent, S. P.; Murray, B. W.; Bellamy, F.; Wong, C. H.; Mioskowski, C., Cyclic amidine sugars as transition-state analogue inhibitors of glycosidases: Potent competitive inhibitors of mannosidases. *Journal of the American Chemical Society* **2004,** *126*, 1971-1979.

54. Striegler, S.; Dittel, M., A sugar's choice: Coordination to a mononuclear or a dinuclear copper(II) complex? *Inorganic Chemistry* **2005,** *44*, 2728-2733.

55. Striegler, S., Binuclear metal complexes in molecular recognition and catalysis. *Current Organic Chemistry* **2007,** *11*, 1543-1565.

56. Striegler, S.; Gichinga, M. G., Disaccharide recognition by binuclear copper(II) complexes. *Chemical Communications* **2008**, 5930-5932.

57. Striegler, S.; Dunaway, N. A.; Gichinga, M. G.; Milton, L. K., Binuclear complexes for aerobic oxidation of primary alcohols and carbohydrates. *Tetrahedron* **2010,** *66*, 7927-7932.

58. Fan, Q. H.; Striegler, S.; Langston, R. G.; Barnett, J. D., Evaluating N-benzylgalactonoamidines as putative transition state analogs for beta-galactoside hydrolysis. *Organic & Biomolecular Chemistry* **2014,** *12*, 2792-2800.

59. Gichinga, M. G.; Striegler, S.; Dunaway, N. A.; Barnett, J. D., Miniemulsion polymers as solid support for transition metal catalysts. *Polymer* **2010,** *51*, 606-615.

60. Striegler, S.; Barnett, J. D.; Dunaway, N. A., Glycoside hydrolysis with sugar-templated microgel catalysts. *Acs Catalysis* **2012,** *2*, 50-55.

61. Matsuda, J.; Suzuki, O.; Oshima, A.; Yamamoto, Y.; Noguchi, A.; Takimoto, K.; Itoh, M.; Matsuzaki, Y.; Yasuda, Y.; Ogawa, S.; Sakata, Y.; Nanba, E.; Higaki, K.; Ogawa, Y.; Tominaga, L.; Ohno, K.; Iwasaki, H.; Watanabe, H.; Brady, R. O.; Suzuki, Y., Chemical chaperone therapy for brain pathology in G(M1)-gangliosidosis. *Proceedings of the National Academy of Sciences of the United States of America* **2003,** *100*, 15912-15917.

62. Kanso, R.; Striegler, S., Multi gram-scale synthesis of galactothionolactam and its transformation into a galactonoamidine. *Carbohydrate Research* **2011,** *346*, 897-904.

63. Kanso, R.; Yancey, E. A.; Striegler, S., N-Benzylgalactonoamidines as potent beta-galactosidase inhibitors. *Tetrahedron* **2012,** *68*, 47-52.

64. Ermert, P.; Vasella, A.; Weber, M.; Rupitz, K.; Withers, S. G., Configurationally selective transition-state analog inhibitors of glycosidases - a study with nojiritetrazoles, a new class of glycosidase inhibitors. *Carbohydrate Research* **1993,** *250*, 113-128.

65. Davies, G. J.; Ducros, V. M. A.; Varrot, A.; Zechel, D. L., Mapping the conformational itinerary of beta-glycosidases by X-ray crystallography. *Biochemical Society Transactions* **2003,** *31*, 523-527.

66. Sabini, E.; Wilson, K. S.; Danielsen, S.; Schulein, M.; Davies, G. J., Oligosaccharide binding to family 11 xylanases: both covalent intermediate and mutant product complexes display B-2,B-5 conformations at the active centre. *Acta Crystallographica Section D-Structural Biology* **2001,** *57*, 1344-1347.

67. Bartlett, P. A.; Marlowe, C. K., Phosphonamidates as transition-state analog inhibitors of thermolysin. *Biochemistry* **1983,** *22*, 4618-4624.

68. Mader, M. M.; Bartlett, P. A., Binding energy and catalysis: The implications for transition-state analogs and catalytic antibodies. *Chemical Reviews* **1997,** *97*, 1281-1301.

69. Fan, Q. H.; Claunch, K. A.; Striegler, S., Structure-activity relationship of highly potent galactonoamidine inhibitors toward beta-galactosidase (*Aspergillus oryzae*). *Journal of Medicinal Chemistry* **2014,** *57*, 8999-9009.

70. Pickens; Jessica; B. Probing of carbohydrate-protein interactions using galactonoamidine inhibitors. University of Arkansas, Arkansas, 2019.

71. Fan, Q. H.; Pickens, J. B.; Striegler, S.; Gervaise, C. D., Illuminating the binding interactions of galactonoamidines during the inhibition of beta-galactosidase (E-coli). *Bioorganic & Medicinal Chemistry* **2016,** *24*, 661-671.

72. Varrot, A.; Tarling, C. A.; Macdonald, J. M.; Stick, R. V.; Zechel, D. L.; Withers, S. G.; Davies, G. J., Direct observation of the protonation state of an imino sugar glycosidase inhibitor upon binding. *Journal of the American Chemical Society* **2003,** *125*, 7496-7497.

73. Zechel, D. L.; Withers, S. G., Glycosidase mechanisms: Anatomy of a finely tuned catalyst. *Accounts of Chemical Research* **2000,** *33*, 11-18.

74. Williams, S. J.; Notenboom, V.; Wicki, J.; Rose, D. R.; Withers, S. G., A new, simple, high-affinity glycosidase inhibitor: Analysis of binding through X-ray crystallography, mutagenesis, and kinetic analysis. *Journal of the American Chemical Society* **2000,** *122*, 4229-4230.

75. Pickens, J. B.; Wang, F.; Striegler, S., Picomolar inhibition of beta-galactosidase (bovine liver) attributed to loop closure. *Bioorganic & Medicinal Chemistry* **2017,** *25*, 5194-5202.

76. Garman, S. C.; Garboczi, D. N., The molecular defect leading to Fabry disease: Structure of human alpha-galactosidase. *Journal of Molecular Biology* **2004,** *337*, 319-335.

77. Guce, A. I.; Clark, N. E.; Salgado, E. N.; Ivanen, D. R.; Kulminskaya, A. A.; Brumer, H.; Garman, S. C., Catalytic mechanism of human alpha-galactosidase. *Journal of Biological Chemistry* **2010,** *285*, 3625-3632.

78. Lemansky, P.; Bishop, D. F.; Desnick, R. J.; Hasilik, A.; Vonfigura, K., Synthesis and processing of alpha-galactosidase-a in human-fibroblasts - evidence for different mutations in fabry disease. *Journal of Biological Chemistry* **1987,** *262*, 2062-2065.

79. Aerts, J. M.; Groener, J. E.; Kuiper, S.; Donker-Koopman, W. E.; Strijland, A.; Ottenhoff, R.; van Roomen, C.; Mirzaian, M.; Wijburg, F. A.; Linthorst, G. E.; Vedder, A. C.; Rombach, S. M.; Cox-Brinkman, J.; Somerharju, P.; Boot, R. G.; Hollak, C. E.; Brady, R. O.; Poorthuis, B. J., Elevated globotriaosylsphingosine is a hallmark of Fabry disease. *Proceedings of the National Academy of Sciences of the United States of America* **2008,** *105*, 2812-2817.

80. Gold, H.; Mirzaian, M.; Dekker, N.; Ferraz, M. J.; Lugtenburg, J.; Codee, J. D. C.; van der Marel, G. A.; Overkleeft, H. S.; Linthorst, G. E.; Groener, J. E. M.; Aerts, J. M.; Poorthuis, B., Quantification of globotriaosylsphingosine in plasma and urine of fabry patients by stable isotope ultraperformance liquid chromatography-tandem mass spectrometry. *Clinical Chemistry* **2013,** *59*, 547-556.

81. Eng, C. M.; Guffon, N.; Wilcox, W. R.; Germain, D. P.; Lee, P.; Waldek, S.; Caplan, L.; Linthorst, G. E.; Desnick, R. J.; Int Collaborative Fabry Dis, S., Safety and efficacy of recombinant human alpha-galactosidase a replacement therapy in Fabry's disease. *New England Journal of Medicine* **2001,** *345*, 9-16.

82. Ioannou, Y. A.; Ashton-Prolla, P.; Eng, C. M.; Desnick, R. J., Fabry disease: Biochemical, molecular and subcellular localization studies of eight alpha-Gal A missense mutations with residual activity. *American Journal of Human Genetics* **1999,** *65*, A95-A95.

83. Germain, D. P.; Waldek, S.; Banikazemi, M.; Bushinsky, D. A.; Charrow, J.; Desnick, R. J.; Lee, P.; Loew, T.; Vedder, A. C.; Abichandani, R.; Wilcox, W. R.; Guffon, N., Sustained, long-term renal stabilization after 54 months of agalsidase beta therapy in patients with Fabry disease. *Journal of the American Society of Nephrology* **2007,** *18*, 1547-1557.

84. Marshall, J.; Ashe, K. M.; Bangari, D.; McEachern, K.; Chuang, W. L.; Pacheco, J.; Copeland, D. P.; Desnick, R. J.; Shayman, J. A.; Scheule, R. K.; Cheng, S. H., Substrate reduction augments the efficacy of enzyme therapy in a mouse model of fabry disease. *Plos One* **2010,** *5*.

85. Marshall, J.; Ashe, K.; Bangari, D.; Chuang, W. L.; Wang, B.; Nietupski, J.; Desnick, R.; Leonard, J.; Scheule, R.; Cheng, S., Glucosylceramide synthase inhibition reduces gb3 and lyso-gb3 in a mouse model of Fabry disease. *Molecular Genetics and Metabolism* **2012,** *105*, S45-S45.

86. Germain, D. P.; Hughes, D. A.; Nicholls, K.; Bichet, D. G.; Giugliani, R.; Wilcox, W. R.; Feliciani, C.; Shankar, S. P.; Ezgu, F.; Amartino, H.; Bratkovic, D.; Feldt-Rasmussen, U.; Nedd, K.; El Din, U. S.; Lourenco, C. M.; Banikazemi, M.; Charrow, J.; Dasouki, M.; Finegold, D.; Giraldo, P.; Goker-Alpan, O.; Longo, N.; Scott, C. R.; Torra, R.; Tuffaha, A.; Jovanovic, A.; Waldek, S.; Packman, S.; Ludington, E.; Viereck, C.; Kirk, J.; Yu, J.; Benjamin, E. R.; Johnson, F.; Lockhart, D. J.; Skuban, N.; Castelli, J.; Barth, J.; Barlow, C.; Schiffmann, R., Treatment of Fabry's disease with the pharmacologic chaperone migalastat. *New England Journal of Medicine* **2016,** *375*, 545-555.

87. Giugliani, R.; Waldek, S.; Germain, D. P.; Nicholls, K.; Bichet, D. G.; Simosky, J. K.; Bragat, A. C.; Castelli, J. P.; Benjamin, E. R.; Boudes, P. F., A Phase 2 study of migalastat hydrochloride in females with Fabry disease: Selection of population, safety and pharmacodynamic effects. *Molecular Genetics and Metabolism* **2013,** *109*, 86-92.

88. Fan, J. Q.; Ishii, S.; Asano, N.; Suzuki, Y., Accelerated transport and maturation of lysosomal alpha-galactosidase A in Fabry lymphoblasts by an enzyme inhibitor. *Nature Medicine* **1999,** *5*, 112-115.

89. Martin, O. R.; Xie, F.; Liu, L., Synthesis of alpha-homogalactostatin and of its 1,n-anhydro derivative. *Tetrahedron Letters* **1995,** *36*, 4027-4030.

90. Martin, O. R.; Compain, P.; Kizu, H.; Asano, N., Revised structure of a homonojirimycin isomer from Aglaonema treubii: First example of a naturally occurring alpha-homoallonojirimycin. *Bioorganic & Medicinal Chemistry Letters* **1999,** *9*, 3171-3174.

91. Ikeda, K.; Takahashi, M.; Nishida, M.; Miyauchi, M.; Kizu, H.; Kameda, Y.; Arisawa, M.; Watson, A. A.; Nash, R. J.; Fleet, G. W. J.; Asano, N., Homonojirimycin analogues and their glucosides from Lobelia sessilifolia and Adenophora spp. (Campanulaceae). *Carbohydrate Research* **2000,** *323*, 73-80.

92. Asano, N.; Ishii, S.; Kizu, H.; Ikeda, K.; Yasuda, K.; Kato, A.; Martin, O. R.; Fan, J. Q., In vitro inhibition and intracellular enhancement of lysosomal alpha-galactosidase A activity in Fabry lymphoblasts by 1-deoxygalactonojirimycin and its derivatives. *European Journal of Biochemistry* **2000,** *267*, 4179-4186.

93. Sunder-Plassmann, G.; Schiffmann, R.; Nicholls, K., Migalastat for the treatment of Fabry disease. *Expert Opinion on Orphan Drugs* **2018,** *6*, 301-309.

94. Maksimainen, M. M.; Lampio, A.; Mertanen, M.; Turunen, O.; Rouvinen, J., The crystal structure of acidic beta-galactosidase from Aspergillus oryzae. *International Journal of Biological Macromolecules* **2013,** *60*, 109-115.

95. Juers, D. H.; Heightman, T. D.; Vasella, A.; McCarter, J. D.; Mackenzie, L.; Withers, S. G.; Matthews, B. W., A structural view of the action of Escherichia coli (lacZ) beta-galactosidase. *Biochemistry* **2001,** *40*, 14781-14794.

96. Vogel, A. I., *A text-book of practical organic chemistry : incl. qualitative organic analysis*. Longmans: London, 1974.

97. France, R. R.; Compton, R. G.; Davis, B. G.; Fairbanks, A. J.; Rees, N. V.; Wadhawan, J. D., Selective electrochemical glycosylation by reactivity tuning. *Organic & Biomolecular Chemistry* **2004,** *2*, 2195-2202.

98. Ye, X. S.; Sun, F.; Liu, M.; Li, Q.; Wang, Y. H.; Zhang, G. S.; Zhang, L. H.; Zhang, X. L., Synthetic iminosugar derivatives as new potential immunosuppressive agents. *Journal of Medicinal Chemistry* **2005,** *48*, 3688-3691.

99. Overkleeft, H. S.; Vanwiltenburg, J.; Pandit, U. K., A facile transformation of sugar lactones to azasugars. *Tetrahedron* **1994,** *50*, 4215-4224.

100. Overkleeft, H. S.; Vanwiltenburg, J.; Pandit, U. K., An expedient stereoselective synthesis of gluconolactam. *Tetrahedron Letters* **1993,** *34*, 2527-2528.

101. Sugiyama, T.; Iwasawa, H.; Hashizume, T., Synthesis of deuterated *N*6-(ortho-hydroxybenzyl)adenosine-D3. *Agricultural and Biological Chemistry* **1980,** *44*, 1057-1060.

102. Liu, C.; Rao, X. F.; Zhang, Y. X.; Li, X. M.; Qiu, J. S.; Jin, Z. L., An aerobic and very fast pd/c-catalyzed ligand-free and aqueous suzuki reaction under mild conditions. *European Journal of Organic Chemistry* **2013,** *2013*, 4345-4350.

103. Nikiforov, P. O.; Surade, S.; Blaszczyk, M.; Delorme, V.; Brodin, P.; Baulard, A. R.; Blundell, T. L.; Abell, C., A fragment merging approach towards the development of small molecule inhibitors of *Mycobacterium tuberculosis* EthR for use as ethionamide boosters. *Organic & Biomolecular Chemistry* **2016,** *14*, 2318-2326.

104. Scribner, A. W.; Haroutounian, S. A.; Carlson, K. E.; Katzenellenbogen, J. A., 1-aryl-2-pyridyl-3,4-dihydronaphthalenes: Photofluorogenic ligands for the estrogen receptor. *Journal of Organic Chemistry* **1997,** *62*, 1043-1057.

105. Micali, E.; Chehade, K. A. H.; Isaacs, R. J.; Andres, D. A.; Spielmann, H. P., Protein farnesyltransferase isoprenoid substrate discrimination is dependent on isoprene double bonds and branched methyl groups. *Biochemistry* **2001,** *40*, 12254-12265.

106. Johansson, H.; Cailly, T.; Thomsen, A. R. B.; Brauner-Osborne, H.; Pedersen, D. S., Synthesis of the calcilytic ligand NPS 2143. *Beilstein Journal of Organic Chemistry* **2013,** *9*, 1383-1387.

107. Mery, J.; Calas, B., Tryptophan reduction and histidine racemization during deprotection by catalytic transfer hydrogenation of an analog of the luteinizing-hormone releasing-factor. *International Journal of Peptide and Protein Research* **1988,** *31*, 412-419.

108. Chouhan, M.; Kumar, K.; Sharma, R.; Grover, V.; Nair, V. A., $NiCl_2$ center dot $6H_2O$/NaBH4 in methanol: a mild and efficient strategy for chemoselective deallylation/debenzylation of aryl ethers. *Tetrahedron Letters* **2013,** *54*, 4540-4543.

109. Ercole, F.; Mansfeld, F. M.; Kavallaris, M.; Whittaker, M. R.; Quinn, J. F.; Halls, M. L.; Davis, T. P., Macromolecular hydrogen sulfide donors trigger spatiotemporally confined changes in cell signaling. *Biomacromolecules* **2016,** *17*, 371-383.

110. Sajiki, H.; Hirota, K., A novel type of Pd/C-catalyzed hydrogenation using a catalyst poison: Chemoselective inhibition of the hydrogenolysis for *O*-benzyl protective group by the addition of a nitrogen-containing base. *Tetrahedron* **1998,** *54*, 13981-13996.

111. Berman, H. M.; Westbrook, J.; Feng, Z.; Gilliland, G.; Bhat, T. N.; Weissig, H.; Shindyalov, I. N.; Bourne, P. E., The Protein Data Bank. *Nucleic Acids Research* **2000,** *28*, 235-242.

112. Schrodinger, LLC *The PyMOL Molecular Graphics System, Version 1.8*, 1.8; 2015.

113. Morris, G. M.; Huey, R.; Lindstrom, W.; Sanner, M. F.; Belew, R. K.; Goodsell, D. S.; Olson, A. J., AutoDock4 and AutoDockTools4: Automated Docking with Selective Receptor Flexibility. *Journal of Computational Chemistry* **2009,** *30*, 2785-2791.